Characterization of the Endogenous Axin-based Complexes and Regulation in the Wnt Pathway

By

Xiaoyong LIU

Department of Biology

McGill University, Montreal

January, 2014

A thesis submitted to McGill University in partial fulfillment of the requirements of the degree of Doctor of Philosophy

To My Dearest Family and Friends.

Table of Contents

Abstract

Wnt-β-catenin signaling is a major pathway controlling gene transcription, cell cycle and cell fate determination. Deregulated Wnt signaling has been implicated in many human diseases, particularly cancers. The key step in the pathway seems to be the switch from constitutive degradation of β-catenin to its stabilization and transport into the nucleus. Axin is a scaffold protein that recruits many components to build what has been called the β-catenin destruction complex. Wnt activation appears to inhibit the function of the complex, but despite intensive investigation, the actual regulatory mechanism remains unclear.

Our lab has established a new cell fractionation method that can precisely separate multiple subcellular compartments and a kinase assay that can detect for the first time the specific endogenous phosphorylation activities toward β-catenin. By combining these and other biochemical tools, we have identified multiple endogenous Axin-based complexes, which we have characterized in terms of composition, subcellular localization and activity. We have also determined the changes induced by Wnt stimulation. This represents the first comprehensive analysis of the Wnt pathway under endogenous conditions. Our results invalidate some of the previously proposed hypothesis, while they reconcile other models, each of them representing part of a more complex mechanism. Based on our data, we proposed a model that multiple Axin-complexes could present simultaneously in the cells, which are differentially regulated by Wnt.

Résumé

La voie Wnt-β-caténine est l'une des principales voies de signalisation cellulaire, qui contrôle la transcription, le cycle cellulaire et la détermination du destin cellulaire. La dérégulation de la voie Wnt est impliquée dans de nombreuses maladies et plus particulièrement dans certains cancers. L'équilibre entre la dégradation de la β-caténine et sa stabilisation ainsi que son transport vers le noyau cellulaire semble être le mécanisme essentiel dans le fonctionnement de cette voie. L'Axin est une protéine chaperonne chargée de recruter un grand nombre de composants afin de former le complexe de destruction β-caténine. L'activation de la voie de signalisation Wnt semble inhiber les fonctions de ce complexe, pourtant à jour, les mécanismes de cette régulation reste à identifier.

Notre laboratoire a mis au point une nouvelle méthode de fractionnement cellulaire, qui permet la séparation de multiples compartiments subcellulaires, ainsi qu'un essai Kinase permettant pour la première fois de suivre l'activité endogène de phosphorylation via la β-caténine. En combinant des deux approches ainsi que la biochimie, nous avons identifié différents complexes endogènes basés sur la présence de l'Axin, dont nous avons ensuite caractérisé la composition, la localisation subcellulaire ainsi que leur activité. Nous avons aussi analysé les changements induits lors de l'activation de la voie Wnt. Ce travail represente la première fois une analyse compréhensive de la voie de signalisation Wnt dans des condition endogène. Nos résultats invalident certaines des précédentes hypothèses tout en réconciliant d'autres modèles, chacun d'entre eux ne représentant qu'une partie d'un mécanisme bien plus complexe. D'après l'ensemble de nos résultats, nous proposons un modèle selon lequel différents complexes composé d'Axin seraient présents simultanément dans la cellule et différentiellement régulés par la voir Wnt.

Acknowledgements

First and foremost, I would like to thank my supervisor, Dr. François FAGOTTO, for giving me the opportunity to be involved in a project that held my curiosity and interest from the beginning until the end. I am very appreciative of his help and ideas with project direction, and indispensable guidance on how to communicate the story of Axin complexes and Wnt signaling pathway so that others may find it as interesting as I do. I am grateful also for all his endless support, friendship, and instilling his tireless love and passion for science.

I have to thank my PhD committee members, Drs. Louise Larose, Arnim Pause. They have been incredibly supportive and I have appreciated their advice and guidance throughout my Ph.D. training. I would also thank Drs. Nathalie Lamarche-Vane, Jean-François CÔTÉ for their valuable expertise, comments and kindness on the FLCO meetings.

I am indebted to many of both previous and present colleagues in the lab: Ekaterina GUSEV, Laura CANTY, Nadim MAGHZAL, Nazanin ROHANI, Anne-Sophie TOURET, Lili WANG, Wen ZHOU, Yeo Jin LEE, Joel SPRATT, Icten MERAS, Zoe Joly-LOPEZ, Vanessa SUNG, Youssef TAWIL, Renu HEIR, Renée WANG, Brian SIU for countless guidance, expertise, technical tips and entertainment on a daily basis. I would also thank Drs. Richard ROY lab and Frieder SCHÖCK lab members for giving me the wonderful memories.

I appreciate all the contributions of time, assistance and knowledge from Department of Biology: Drs. Elke KÜSTER-SCHÖCK, Guillaume LESAGE, Laura NILSON, Frieder SCHÖCK, Richard ROY, Gregory BROWN, Monique ZETKA, Gary BROUHARD and Susan BOCTI, Ancil GITTENS, Susan GABE, Anna MCNICOLL, Joe IANTOMASI, Frank SCOPELETTI, Kathy HEWITT to make my Ph.D experience productive and rewarding.

On a personal note, I would also appreciate the amazing support of my family and friends. I am especially grateful for my parents Hong and Bangzhi LIU for their

support and endless love throughout my life. Special thanks to my supportive and encouraging wife, Boluan for her faithful support and especially her cares for our beloved baby during the final stages of my thesis. They have sacrificed so much for my well-being, and provided me a better life.

Thank you to everyone who made this thesis possible.

Contributions

Chapter I is a comprehensive review of the literature pertinent to my area of research. I researched and wrote this chapter with guidance of my thesis supervisor, Prof. Dr. Francois Fagotto.

Chapter II was published in Science Signaling: **X. Liu**, F. Fagotto, A method to separate nuclear, cytosolic, and membrane-associated signaling molecules in cultured cells. Science Signaling 4, pl2 (2011). X.L. and F.F. conceived and designed the experiments. X.L. performed all experiments. X.L. and F.F. interpreted the results and wrote the paper.

Chapter III is a manuscript in preparation: **Liu, X.**, Gusev, E., Siu, B., Wang, L. and F. Fagotto. Characterization of the endogenous Axin complexes: properties, activity and Wnt regulation. L. Wang helped to establish the *in vitro* kinase assay. E. Gusev did most kinase assay and sucrose gradient analysis. B. Siu did the floatation experiment and some sucrose gradient analysis More specifically, E. Gusev contributed to Figure 3B, 5A, 6D, 6E, 7, S1A, S3A, S3B and S4A; B. Siu contributed to Figure F4A, S3. F. Fagotto contributed to the experimental design, data analysis, results interpretation and writing. I designed, performed, analyzed most experiments and wrote the paper under the guidance from F. Fagotto. More specifically, I contributed to Figure 1, 2, 3, 4B, 4C, 5D, 6A, 6B, 6C, 7, 8, 9, 10A, S1, S2A, S2B, S2C, S3, S4A, S4B, S5, S8 and S9.

Chapter IV is a general discussion and comments of the work in this thesis. I wrote this chapter with guidance of my thesis supervisor, Prof. Dr. Francois Fagotto.

Abbreviations

APC	Adenomatous polyposis coli
ATP	Adenosine-5'-triphosphate
Axin	Axis Inhibitor
BNGE/BN	Blue Native Gel Electrophoresis
BSA	Bovine Serum Albumin
CK1	Casein Kinase 1
CRD	Cysteine-Rich Domain
DEP	Dishevelled, Egl-10 and Pleckstrin domain
DIX	Dishevelled and Axin Domain
Dsh/Dvl	Dishevelled
ER	Endoplasmic Reticulum
Fz	Frizzled
GBP	GSK3 Binding Protein
GSK3	Glycogen Synthase Kinase 3
I2	PP1 inhibitor 2
Int-1	Integration -1gene
JNK	c-Jun N-terminal kinases
LEF	Lymphoid enhancer-binding factor
LRP5/6	Low-density lipoprotein Receptor-related Protein 5/6
MEKK	MAP Kinase Kinase Kinase
Min	Minute(s)
OA	Okadaic Acid
PDZ	Post synaptic density protein (PSD95)+ Drosophila disc large tumor suppressor (Dlg1)+ and Zonula occludens-1 protein (zo-1) domain
PKC	Protein Kinase C

pLRP6	Phospho-LRP6
PP1	Protein Phosphatase 1
PP2A	Protein Phosphatase 2 A
pSer-45/p45	Phospho-Serine 45
pSer-33/Ser-37/ Thr41 /p33/37/41	Phospho-Serine 33, Serine 37, Threonine 41
RGS	Regulation of G-protein Signaling domain
S45D	Serine 45 changed to Aspartate
SG	Sucrose Gradient
TCF	T-Cell Factor
Wg	Wingless
Wls	Wntless
Wnt	Wingless + Int-1
wt	Weight

CHAPTER I

Literature Review and Thesis Objectives

Introduction

Wnts are a family of extracellular cell-cell signaling molecules that mediate intercellular communication throughout animal development to determine the fate of both embryos and adult tissues. The Wnt signaling pathway is highly conserved across various species and plays important regulatory roles in many developmental processes; including the initial formation of the embryonic axes, regulation of cell shape, movement, adhesion, proliferation and differentiation (Logan and Nusse 2004). Currently there are 19 known human Wnt proteins. The name Wnt derives from the *Drosophila* gene *Wingless*, and the related mammalian oncogene *Int-1* (now Wnt1, Cadigan and Peifer 2009). Wnts are secreted lipid-modified glycoproteins (Willert 2003) found in all metozoans examined to date. Wnt proteins activate several different downstream pathways that are divided into either the canonical Wnt pathway or non-canonical Wnt pathways, where the latter includes the Wnt/ Ca^{2+} signaling and the planar cell polarity (PCP) pathways (Figure 1). Currently, the actual mechanism regulating these pathways is not understood. This chapter will focus on the canonical Wnt/β-catenin pathway and introduce their major components and discuss prevailing models of the Wnt/β-catenin pathway.

1. General Features of Wnt Signaling

1.1 Canonical Wnt/β-catenin pathway

Wnt signaling pathways can be classified into two categories: canonical and noncanonical. They differ in that the canonical pathway involves the protein β-catenin while a noncanonical pathway operates independently of it.

Many Wnts, such as Wnt1, Wnt3a and Wnt8, tend to activate in a β-catenin-dependent signaling pathway by stabilizing and regulating the subcellular localization of β-catenin (Logan and Nusse, 2004). This so-called “canonical” Wnt/β-catenin pathway is known to play important roles in many biological processes,

including cell fate determination, cell proliferation, and stem cell maintenance. The dysregulation of the pathway in adult tissues results in a large variety of cancers (Cadigan and Peifer 2009).

A series of molecular events occur in the canonical Wnt pathway where Wnt proteins bind to cell-surface receptors, cause a change in the amount of β-catenin that enters the nucleus, and subsequently affects its ability to interact with transcription factors to promote gene expression. The current model of Wnt-β-catenin regulation is a two-state model. In the absence of Wnt, free β-catenin is recruited by the scaffold protein Axin, to the β-catenin destruction complex. This cytoplasmic protein complex is comprised of Axin, casein kinase I (CK1), glycogen synthase kinase 3 (GSK3), and adenomatous polyposis coli (APC). In the destruction complex, β-catenin is first primed and phosphorylated by CK1 at Ser 45 and then phosphorylated by GSK3 at Ser33, Ser 37 and Thr 41. Ubiquitin ligase β-TrCP recognizes and ubiquitinates the phosphorylated form of β-catenin for degradation by the proteasome. These events maintain the free cytosolic β-catenin at extremely low levels and results in low nuclear transcription activity in non-stimulated cells. In the second state, Wnt stimulation induces stabilization of soluble β-catenin, resulting in the accumulation of β-catenin in the cytoplasm and its subsequent import into the nucleus for the activation of gene transcription (Figure 2). It is also important to note that there is a Wnt-independent pool of β-catenin found in cadherin complexes at the plasma membrane (Cadigan and Peifer 2009). Although the general sequence of events is known, the actual mechanism regulating these events remains unclear.

1.2 Non-canonical Wnt pathways

Some Wnt proteins, like Wnt 5a and Wnt11, preferentially activate through Frizzled receptors in pathways independent of β-catenin (Figure 1). These non-canonical pathways have also been characterized as the Wnt/Ca^{2+} and the Wnt/planar cell polarity pathway (PCP) in vertebrates and *Drosophila* (Veeman, Axelrod *et al.,* 2003). Activation of the Wnt/Ca^{2+} pathway involves Wnt binding to a Frizzled receptor, resulting in the release of intracellular calcium and the activation of enzymes

such as CamKII and PKC (Kohn and Moon 2005). Wnt/Ca^{2+} signaling can function as a tumor suppressor by antagonizing the Wnt/β-catenin signaling under certain conditions (Seifert and Mlodzik 2007).

The PCP pathway has been studied mainly in *Drosophila*, where it is involved in planar cell polarity during development. The mechanism of how this pathway functions is still unclear, but it has been reported that Frizzled receptors activate a cascade that involves the small GTPases Rac1 and RhoA, as well as JUN-N-terminal kinase (JNK) (Veeman, Axelrod *et al.,* 2003). The downstream signaling results in changes in Actin remodeling and planar cell polarity through small GTPases and/or transcriptional activation of JNK-dependent transcription factors (Niehrs 2012). It has also been reported that the noncanonical Wnt family members, like Wnt4, 5a and 11 could activate the downstream signaling in a RAR-related orphan receptors (Ror) and Tyrosine-protein kinase (Ryk) mediated way other than Frizzled (Minami *et al* 2013).

Unlike the Wnt/β-catenin signaling, the molecular mechanisms underlying the activation of noncanonical Wnt pathways remain unclear. Noncanonical Wnt pathways have been shown to regulate many processes in embryo development, tissue development and homeostasis, e.g., polarized cell movements and planar polarity of epithelial cells. Furthermore, noncanonical Wnt signaling has also been linked to cancers. The noncanonical Wnt pathways could promote tumor cell migration and invasiveness.

I will mainly focus on reviewing the components and prevailing models of this canonical pathway as the regulation of Wnt/β-catenin signaling is my interest.

2. Major Components of the Wnt/β-catenin Pathway

I will briefly introduce the main components of the Wnt/β-catenin pathway in this section and will discuss the models regulated by these components in the following sections.

2.1 Wnts as secreted ligands

Wnt proteins are highly conserved across species from vertebrates to invertebrates. . (Moon, Kohn *et al.,* 2004, Nusse, Fuerer *et al.,* 2008). Currently there are 19 known Wnt proteins in humans, 7 in *Drosophila* and 5 in *C. elegans*.

All Wnt proteins show a conserved general structure: they have an N-terminal signal peptide, one or more N-linked glycosylation sites, and 23 conserved cysteine residues, most of which form disulfide linkages that function to maintain a globular secondary structure. In addition, most Wnt proteins are acylated, by the acyltransferase Porcupine (Porc), in the endoplasmic reticulum (ER) and then transported to the Golgi. Wntless (Wls), an integral membrane protein, appears to be involved in Wnts secretion. Wls guides Wnts from the Golgi to the cell surface where they are then released outside of the cell (Figure 3, Blitzer and Nusse 2006).

2.2 Receptors at the membrane

The binding of Wnt proteins to its cell-surface co-receptors, namely the Frizzled family and LRP5/6, members of the LDL-receptor-related protein family results in the reception and transduction of canonical Wnt signals. I will first briefly describe the general features before discussing in detail the regulatory mechanisms.

Frizzled

A subfamily of seven-transmembrane G protein-coupled receptor proteins (GPCRs), Frizzled (Fz) receptors are specific for Wnt. They are involved in both canonical and non-canonical Wnt pathways. All Fzs share a cysteine-rich ligand-binding domain (CRD), which binds directly Wnt proteins (Figure 4A, Logan and Nusse 2004) and differ in their C-terminal tail. How Fzs function in the transmission of Wnt signaling remains unclear. One effect is to promote the phosphorylation of Dishevelled (Dvl), which is involved in activating canonical Wnt/β-catenin signaling (Gonzalez-Sancho *et al.,* 2004); however, the phosphoacceptor sites on Dvl required for activation have not yet been identified (Yang-Snyder, Miller *et al.,* 1996, Hsieh, Kodjabachian *et al.,* 1999, Dann, Hsieh *et al.,* 2001). Fzs can also interact and signal through G proteins, although the mechanism is yet unknown (Gunnar Schulte, Vitezslav Bryja, 2007).

LRP5/6

LDL receptor related proteins 5 and 6 (LRP5/6) and their *Drosophila* homolog, Arrow, are single span transmembrane proteins (Figure 4A). They function as co-receptors with Fz to bind Wnts and initiate the β-catenin dependent signaling (Tamai 2000, Wehrli 2000). There are several models on how Wnt can activate the downstream cascade via LRP5/6 and Fz (See part 3 for more details). In a word, GSK3 phosphorylates the PPPSP motifs on the intracellular domain of LRP6, which primes for xS phosphorylation by CK1s (Davidson, Wu *et al.,* 2005, Zeng, Tamai *et al.,* 2005). I will not address here the role for CK1 in the phosphorylation of LRP6, since it is still not well understood and not the main object of my study.

2.3 Intracellular components of the Wnt pathway

Axin

Axin was first characterized as a product of the mouse *fused* locus. It was found that mice with mutant Fused alleles developed axial duplications, suggesting Axin as a negative regulator of an axis-inducing signal (**Ax**is-**In**hibitor). Indeed, injection of Axin mRNA into *Xenopus* embryos resulted in the inhibition of the formation of the dorsal axis via interference with the Wnt pathway (Zeng, Fagotto *et al.,* 1997). The Axin gene is conserved in vertebrates, *Drosophila* and *C. elegans* (PRY-1, a homologue of Axin) (Zeng, Fagotto *et al.,* 1997, Ikeda 1998, Hamada 1999, Korswagen 2002, Luo and Lin 2004). There are 2 closely related vertebrate Axin genes and both act as negative regulators of Wnt signaling. Axin1 (refered to here as Axin) is constitutively expressed in all tissues. On the other hand, Axin2 (also known as Conductin, or Axil) is induced by active Wnt signaling as a transcriptional target of β-catenin, and therefore acts in a negative feedback loop.

Axin contains many interactor-binding sites consistent with a role as scaffold protein (Figure 4C, Zeng, Fagotto *et al.,* 1997, Kishida 1998, Ikeda 1998, Fagotto 1999, Kishida 1999, Cliffe, Hamada *et al.,* 2003, Luo, Peterson *et al.,* 2007, Zeng, Huang *et al.,* 2008). The N-terminus of Axin contains an RGS domain (named for the

regulators of G-protein signaling protein family) within the N-terminus, which binds APC and G protein, and the C-terminus contains a DIX domain, which is a conserved 85-residue module of unclear structure and biological function in both Dvl and Axin (Zeng, Fagotto *et al.,* 1997).

Axin works by docking other regulators, allowing for efficient phosphorylation of β-catenin and APC (Figure 4). This allows Axin to serve as a control point for β-catenin destruction, making it a central platform of the Wnt/β-catenin pathway. GSK3 and β-catenin-binding sites are essential for Axin function (Ikeda 1998, Kishida 1998, Fagotto 1999, Kishida 1999, Kishida 2001) and deletion of the Axin RGS domain in both vertebrates and *Drosophila* compromises β-catenin destruction *in vivo* (Fagotto 1999, Peterson-Nedry, Erdeniz *et al.,* 2008) demonstrating the importance of the Axin-APC interaction. Furthermore, G proteins like Goα, through a currently unknown mechanism, are also thought to function as signal transducers in transmitting Wnt signals from Fz to downstream regulators (Luo, Zou *et al.,* 2005).

The DIX domain is responsible for both Axin-Dvl oligomerization and Axin-Axin interactions (Kishida 1998, Fagotto 1999, Kishida 1999, Cliffe, Hamada *et al.,* 2003). Binding to Dvl may inhibit β-catenin phosphorylation (Gao, Virshup 2002, Hino 2003), while Axin homo-oligomerization seems to be required for Axin-mediated JNK regulation, but not for β-catenin regulation (Zhang 2000, Neo 2000, Zhang 2004). It has also been demonstrated that Axin could mediate cytoskeleton rearrangement via the DIX domain (Cowan 2001).

In addition, Axin contains numerous interacting regions for MEKK-1/4, CK1, GSK, β-catenin, PP2A, LRP6, Smad-3 etc (Zhang 1999, Luo 2003, Furuhashi 2001, Luo and Lin 2004).

While the domains and interactors of Axin have been studied extensively, the localization, composition and function of endogenous Axin complexes are not well characterized. Under certain conditions, Axin has been detected in the nucleus (Cong and Varmus 2004, Wiechens, Heinle *et al.,* 2004). In general, Axin has been shown to have a disperse, subcellular localization pattern, while myc-tagged Axin is observed

as intracellular spots and at the plasma membrane (Fagotto 1999, Cliffe, Bienz 2003).

Measurements in *Xenopus* egg extracts show Axin concentration (0.02 nM) to be roughly 2000x lower than that of β-catenin and 5000x lower than that of APC (Salic, Lee *et al.,* 2000, Lee, Salic *et al.,* 2003) indicating Axin to be the limiting factor for the formation of the complex. However, Axin is present at much higher concentrations in mammalian cells (20–150 nM) (Tan, Gardiner *et al.,* 2012). The significance of the disparity of Axin concentration between cell types is not known, but the comparison warns us against translating directly published Axin-mediated degradation kinetics to all model systems.

Axin can be stabilized by GSK3-mediated phosphorylation (Yamamoto 1999, Willert 1999). Wnt induces dephosphorylation and sequentially destabilization of Axin. The dephosphorylated Axin binds β-catenin less efficiently than its phosphorylated form. I will discuss in more detail how Axin regulates the Wnt pathway in the "models" section.

Tankyrase has been shown to promote Axin PARsylation and degradation (Huang, Mishina *et al.,* 2009) in a Wnt-independent process.

Axin has been suggested to participate in many signaling pathways other than the Wnt/β-catenin pathway. For example, it interacts with MEKK to activate the JNK pathway (Luo, Ng *et al.,* 2003, Luo and Lin 2004), and functions as an adaptor for Smad3, facilitating its activation by TGF-β receptors (Guo, Ramirez *et al.,* 2008).

Casein Kinase I (CK1)

CK1 represents a group of related and ubiquitously expressed serine/threonine protein kinases found in all eukaryotes (Gross and Anderson 1998, Knippschild, Gocht *et al.,* 2005). The CK1 isoforms are highly conserved within their kinase domains, but differ in their length and primary structures of their N-terminal and C-terminal non-catalytic domains (Hanks and Hunter 1995). The CK1 family has a preference for "primed", pre-phosphorylated or acidic substrates (Cheong and Virshup 2011). Various CK1

isoforms have been implicated as both positive and negative regulators of Wnt signaling.

CK1ε was first reported as a positive regulator. Injection of CK1ε mRNA can mimic the Wnt-induced second axis formation in *Xenopus* embryos, and activate expression of the Wnt target genes (Peters *et al.,* 1999). The same effect is seen with CK1α/δ isoform (Sakanaka, Leong *et al.,* 1999, McKay, Peters *et al.,* 2001). A possible molecular mechanism could be that CK1ε-mediated phosphorylation of Dvl acts to enhance the interaction between Dvl, GSK3 and Frat, thereby inhibiting GSK3 activity and stabilizing β-catenin. CK1ε can also bind and phosphorylate TCF3, which results in an increase in TCF-β-catenin interaction (Yost, Farr *et al.,* 1998, Li, Yuan *et al.,* 1999, Salic, Lee *et al.,* 2000, Lee, Salic *et al.,* 2001). It also has been reported that the phosphatase PP2A could reduce the autophosphorylation of CK1ε, which has been shown to activate CK1ε *in vitro* (Gietzen and Virshup 1999).

However, CK1α and CK1ε also play a negative role in the pathway. Both CK1α and CK1ε have been reported to interact with Axin and CK1δ can phosphorylate β-catenin *in vitro* (Amit 2002). There exists evidence suggesting that CK1α is the actual β-catenin kinase. Overexpression of CK1α, but not CK1ε, leads to the phosphorylation of S45 *in vivo* (Liu 2002). Injection of CK1α RNA in *Drosophila* embryos results in a naked cuticle phenotype and the expansion of the stripes of *wg* and *engrailed* expression (Liu 2002, Yanagawa 2002, Lum 2003, Price 2006). Biochemical assays have reported both Axin and APC to be CK1 substrates as well (Kishida, Hino *et al.,* 2001, Rubinfeld, Tice *et al.,* 2001, Cheong and Virshup 2011).

CK1γ was reported to phosphorylate LRP6 on sites primed by GSK3, where phosphorylated form of LRP6 has a higher affinity for Axin (Davidson 2005, Zeng 2005). Furthermore, in *Drosophila* SL2 cells, Gilgamesh (the *Drosophila* CK1γ) synergizes with Arrow (the *Drosophila* LRP5/6) to activate a Wg transcriptional reporter. In a reporter assay, dominant-negative forms of CK1γ inhibit Wnt signaling (Davidson 2005).

Many functions of CK1 isoforms in the Wnt pathway have been discovered

recently. However, there still exist many open questions concerning the details that require answers before these molecular puzzles can be turned into persuasive models.

Glycogen Synthase Kinase 3 (GSK3)

The serine/threonine kinase glycogen synthase kinase 3 (GSK3) is involved in numerous cellular processes, ranging from glycogen metabolism to microtubule dynamics, and from the modulation of transcription factors to axis development (Plyte, Hughes *et al.,* 1992, Woodgett 1992, Doble and Woodgett 2003, Patel, Doble *et al.,* 2004). Many GSK3 substrates require a "priming phosphate" (Ser/Thr residues) located C-terminally from the site. Negatively charged residues can replace the function of the priming site in some substrates lacking the priming sites (Fiol 1987, Fiol 1989, Fiol 1990).

GSK3 was initially isolated in *Drosophila*, also named Shaggy or Zest-white-3, where it acts as an enzyme that could phosphorylate and inactivate glycogen synthase. In *Xenopus* embryos, the dominant negative form of GSK3 induced the formation of a double axis, implicating it in the Wnt/β-catenin pathway. Subsequently, β-catenin was identified as a GSK3 substrate. Post priming by CK1 at Ser45, GSK3 phosphorylates three consecutive N-terminal residues of β-catenin (Ser33, Ser37, Thr41) (Figure 5). This GSK-phosphorylation promotes β-catenin ubiquitination and destabilization (Aberle *et al.,* 1997).

Drosophila has only one gene for GSK3, named Shaggy or Zest-white-3. Vertebrates express two GSK3 isoforms, α and β. They are virtually identical within their catalytic domains, except for an N-terminal extension present only in GSK3α. In the Wnt/β-catenin pathway, these two isoforms appear to be interchangeable in carrying out the function of β-catenin phosphorylation (Wu and Pan 2010).

It has been proposed that Wnt stimulation would act by inhibiting more or less directly GSK3. GSK3 inhibition not only affects β-catenin phosphorylation, but it also can affect the phosphorylation of Axin. Wnt may recruit GSK3 inhibitory proteins such as GSK3-binding protein (GBP, also named FRAT) to compete with Axin for

binding to GSK3 (Hinoi, Yamamoto *et al.,* 2000), which results in the dephosphorylation and destabilization of Axin. Subsequently, a reduction in Axin level leads to β-catenin stabilization.

The activity of GSK3 is directly inhibited by the PPPSP motifs on the cytoplasmic tail of phospho-LRP6 (Bilic 2007, Wu, Huang *et al.,* 2009). The PPPSP motifs are required for Axin-LRP6 interaction, and in this model, GSK3 might phosphorylate the Ser1490 of the PPPSP motifs to mediate the recruitment of Axin to LRP6. However, it is not yet known how Axin interacts with LRP6.

There are other reports showing that Wnt may regulate GSK3 via G proteins (Liu, Rubin *et al.,* 2005, Chen 2009) and a specific cadherin-dependent β-catenin destruction complex (Maher, Flozak *et al.,* 2009). Unfortunately, the evidence underlying these reports remains too unclear to form an acceptable model. Taken it all together, the prevailing view could be that Wnt might inhibit several GSK3 pools to regulate the pathway: one via the Axin-associated GSK3 pool, (most likely by the LRP6 signalosome), and others via some unidentified Axin-independent GSK3 pools (Wu and Pan 2010).

β-catenin

β-catenin is a multi-functional protein that plays essential roles both in cell-cell adhesion and in Wnt signaling (Peifer, Orsulic *et al.,* 1993). β-catenin has a central region composed of 12 "armadillo repeats" (Figure 4E), an N-terminal region and a C-terminal region. The central domain binds to most β-catenin binding partners, including cadherin, LEF/TCF, Axin and APC; the N-terminal region contains the binding site for α-catenin as well as the GSK3 and CKI phosphorylation sites and the C-terminal region that interacts with the LEF/TCF transcription factors (Kimelman and Xu 2006). Other sequences in the protein also contribute to the transcriptional regulation (Huber *et al* 1996, Cox *et al* 1999). Some of the bindings are mutually exclusive (e.g. APC/Cadherin) and in other cases completion contributes to regulation (e.g. Phospho-APC/Axin, more details will be discussed later).

Current model of WNT/β-catenin signaling

It is generally admitted that the phosphorylation of β-catenin is the central event that regulates Wnt signaling. Under basal conditions, free cytoplasmic β-catenin is captured in a "so-called" destruction complex, where it is first primed and phosphorylated by CK1 at Ser 45 and then phosphorylated by GSK3 at Ser33, Ser 37 and Thr 41 (Figure 5). Once phosphorylated, these four amino acids constitute the binding sites for β-TrCP and target β-catenin for proteasome-mediated degradation. Upon stabilization by Wnt stimulation, free β-catenin translocates to the nucleus where it binds to TCF and transiently displaces the Groucho transcriptional repressor, thus converting TCF into a transcriptional activator (Cavallo 1998, Roose 1998, Lee, Swarup *et al.,* 2009, Hikasa, Ezan *et al.,* 2010).

β-catenin and cell adhesion

In addition to transcription, β-catenin is also required for cell-cell adhesion in a Wnt-independent manner. In fact, β-catenin was originally isolated as a protein associated with the cytoplasmic region of cadherin, a transmembrane protein involved in homotypic cell-cell contacts. Cadherins only exhibit normal adhesive function when they are associated with β-catenin (Gumbiner 2005, Halbleib and Nelson 2006).

Nuclear-cytoplasmic shuttling of β-catenin

β-catenin does not contain any nuclear localization sequences or nuclear signal export sequences. However, the subcellular localization of β-catenin is essential to perform its signaling function, and so there are several models suggesting the nuclear-cytoplasmic shuttling of β-catenin (Fagotto 2013).

It has been shown that β-catenin can enter the nucleus in pre-permeabilized cells depleted of transport factors such as RanGTPase and importins (Fagotto, Gluck *et al.,* 1998, Yokoya, Imamoto *et al.,* 1999). The structure of the β-catenin armadillo repeats is related to importin-β HEAT repeats (Fagotto 2013). Also, β-catenin can compete with importin-β for docking to components of the nuclear pore complex. These facts suggested that β-catenin can directly interact with nuclear pore components, in an

importin/karyopherin-independent fashion to enter the nucleus (Fagotto, Gluck *et al.,* 1998, Yokoya, Imamoto *et al.,* 1999, Sharma, Henderson *et al.,* 2012). Recently, Henderson and colleagues (Sharma, Jamieson *et al.,* 2012) showed that the specific interactions between Arm repeats and the nucleoporin Nup family such as Nup62, Nup153, and Ran binding protein 2 (RanBP2)/Nup358 are required for the import and export of β-catenin. Another discovery has shown that JNK2 phosphorylates β-catenin at Ser191 and Ser605 in response to Rac1 activation, and that this phosphorylation at the serine residues controls the nuclear translocation of β-catenin (Chen, Yang *et al.,* 2008, Wu, Tu *et al.,* 2008).

It is thought that the interaction of β-catenin with its binding partners helps it exit the nucleus; however, how other factors regulate its export is still a contentious issue. It was initially proposed that APC directly interacts with Axin, which actively exports β-catenin from the nucleus (Henderson 2000, Neufeld, Zhang *et al.,* 2000, Rosin-Arbesfeld, Townsley *et al.,* 2000). It was then clarified that APC is not required to accelerate nuclear export of β-catenin (Krieghoff *et al* 2006, Wang *et al.,* 2014). An alternate model suggests that Axin and APC do not participate in shuttling, but rather acts as a cytoplasmic "anchors", a function similar to that of cadherins (Townsley, Cliffe *et al.,* 2004), while the nuclear factors, such as TCF-4 function as nuclear "anchors" (Tolwinski and Wieschaus 2001, Krieghoff *et al.,* 2006, Sharma, Jamieson *et al.,* 2012, Fagotto 2013). It's also proposed that β-catenin export is stimulated by direct interaction with RanBP3 (Henderson and Fagotto 2002, Cong and Varmus 2004, Hendriksen, Fagotto *et al.,* 2005).

Adenomatous polyposis coli (APC)

APC is a very large (>300kDa) tumor suppressor protein frequently mutated in colorectal cancer. Both *Drosophila* and mammals have two APC family members, APC1 and APC2. APC acts as a scaffold protein, containing several regions that bind to specific partners (Figure 4D): the N-terminus of APC contains a dimerization domain in vertebrates (Jimbo, Kawasaki *et al.,* 2002, Day and Alber 2000) and an armadillo repeat (arm) domain, which interacts with cytoskeletal regulators

(Kawasaki 2000, Jimbo, Kawasaki *et al.,* 2002), PP2A (Seeling, Miller *et al.,* 1999) and indirectly with Axin (Roberts, Pronobis *et al.,* 2011); the central region of APC contains a 15- and 20-amino-acid repeats important for binding to β-catenin and a SAMP (Ser-Ala-Met-Pro) repeat motif that bind directly to Axin and a B domain, also called β-catenin inhibitory domain, which is involved in regulating the activity of the destruction complex (Roberts *et al.,* 2012, Figure 6); the C-terminal region of APC contains basic domains required for interactions with microtubule, but this region is not required for Wnt signaling, since the *Drosophila* APC2 lacking them can still regulate the pathway. Most cancer-linked APC mutations are found in a central region, named the mutation cluster region (MCR), which results in C-terminal truncations of APC. There are also several NES and NLS identified within the N terminal and central regions, respectively, regulating the cellular distributions of APC (Stamos and Weis 2013).

Initially, APC was initially considered as the scaffold for the β-catenin destruction complex (Rubinfeld, Albert *et al.,* 1996), but it is now clear that Axin plays that role, although APC may also cooperate (Hinoi, Yamamoto *et al.,* 2000, Ha, Tonozuka *et al.,* 2004, Xing, Clements *et al.,* 2004). How APC contributes to the function of the destruction complex is still controversial. What is known is that both Axin and APC compete for β-catenin binding. Normally, Axin has higher affinity than APC, however, when 20 aa repeats are phosphorylated by CK1 and GSK3, this leads APC to possess a higher affinity than Axin for β-catenin binding. Several hypotheses have been proposed based on the switchable binding abilities (Hinoi *et al.,* 2000; Xing *et al.,* 2003).

The first model proposes that APC stimulates the phosphorylation of β-catenin in the destruction complex by removing the catalytic product, the phosphorylated β-catenin, from the active site, thus allowing Axin to recruit the next β-catenin (Kimelman, *et al.,* 2006). In this model, APC is phosphorylates with β-catenin in the complex causing APC to bind tightly to β-catenin, displacing Axin from β-catenin. Then, APC and phosphorylated β-catenin may be released from the destruction

complex while remaining tightly bound to each other and do not separate until β-catenin is degraded by the proteasome. APC may also protect β-catenin from dephosphorylation before its transfer to β-TrCP (Su, Fu *et al.,* 2008). In this model, the higher affinity binding sites (phosphorylated 20R3) play the essential role in transferring β-catenin to β-TrCP, whereas, the lower affinity binding sites (both 15Rs and non-phosphorylated 20Rs) serve as docking sites for the transfer of β-catenin to Axin .(Ha *et al.,*2004, Xing *et al.,* Choi *et al.,* 2006, Liu *et al.,*2006, Robert *et al.,* 2011).

The second model addresses more the distinct roles of both high and low-affinity sites on APC in regulating cytoplasmic levels of β-catenin under different Wnt conditions (Ha *et al.,* 2004). High affinity β-catenin-binding sites produced by APC phosphorylation targets free β-catenin for degradation and thus maintains a low level of β-catenin in the absence of Wnt. Low affinity binding sites captures β-catenin when present of higher concentration (due to Wnt stimulation) and thus reduces free β-catenin levels to turn off the pathway rapidly after Wnt ligands are no longer present.

Recently, Robert *et al.* suggested an adaption of these two models based on their data; they proposed that APC regulates both β-catenin phosphorylation and its subsequent release from the complex (Robert *et al.,* 2011, Stamos *et al.,* 2013, Figure 6 A, B). Thus, constitutively high levels of β-catenin in APC-mutant cancer cells can be linked to the fact that truncated APC proteins lack of this protective function (Figure 6C).

A related debate is whether APC is essential to phosphorylate β-catenin. Some claim that APC truncations that delete the Axin-binding SAMP repeats do not prevent β-catenin phosphorylation (Yang, Zhang *et al.,* 2006), indicating that APC does not enhance Axin-mediated phosphorylation of β-catenin. Consistently, Axin was reported to rescue β-catenin degradation in SW480 cells (Behier, 1998). However, in other studies, Axin failed to compensate for APC truncation, supporting the models in which APC plays a specific role in the complex (Xing, Clements *et al.,* 2003, Ha,

Tonozuka *et al.,* 2004, Roberts, Pronobis *et al.,* 2011, Roberts, Pronobis *et al.,* 2012). Our data (Wang *et al.,* 2014) confirmed that APC is necessary for both CK1/GSK3-mediated β-catenin phosphorylation.

Another study suggested that APC is broadly required for GSK3 activity in various pathways. Wnt would induce APC dissociation from the Axin–GSK3 complex, thus inhibiting the activities of GSK3 (Valvezan, Zhang *et al.,* 2012).

Protein Phosphatase 2A (PP2A)

PP2A is an intracellular serine/threonine protein phosphatase implicated in a large number of cellular processes, including the Wnt signaling pathway. PP2A is composed of three protein subunits: a structural subunit (A), a variable regulatory subunit (B) which determines the substrate specificity, and a conserved catalytic subunit (C). The subunits A and C form a dimeric core complex that associates with the subunit B. Distinct PP2A heterodimers dephosphorylate different substrates or different sites on the same substrate (Li, Yost *et al.,* 2001).

Depending on the associated regulatory subunit, PP2A can either influence the Wnt pathway in a positive or negative manner (Creyghton, Roel *et al.,* 2005, Creyghton, Roel *et al.,* 2006). First, the phosphatase inhibitor okadaic acid stabilizes β-catenin, while this stabilization may be unrelated to Wnt signaling (Patturajan, Nomoto *et al.,* 2002). Moreover, it also has been shown that upon Wnt induction, phosphorylated β-catenin can be dephosphorylated by PP2A (Figure 5). Second, PP2A binds to Dvl (Yang, Wu *et al.,* 2003), Axin (Li, Yost *et al.,* 2001, Yamamoto, Hinoi *et al.,* 2001) and APC (Seeling, Miller *et al.,* 1999). PP2A is able to dephosphorylate the GSK3-mediated phosphorylation of Axin and APC, thereby disrupting the destruction complex and facilitating β-catenin activation. Conversely, it has been implied that PP2A could regulate GSK3 activity by changing its phosphorylation status resulting in a decrease in β-catenin activation (Janssens and Goris 2001, Kimelman and Xu 2006). Third, PP2A can also directly stabilize β-catenin in the membranal E-cadherin complex. Depletion of the PP2A from the complex leads to a redistribution of

β-catenin to the cytoplasm where it is rapidly degraded by the proteasome (Gotz, Probst *et al.,* 2000).

Ubiquitin-proteasome system (UPS) and E3 ligase β-TrCP

Many signaling pathways are controlled by the selective proteolysis of proteins via the ubiquitin-proteasome system (UPS), where the majority of intracellular protein degradation occurs via the 26S proteasome. This process involves the covalent transfer of ubiquitin to one or more lysine residues of the target protein in a three-enzyme cascade involving an E1 activating enzyme, an E2 conjugating enzyme and an E3 ubiquitin ligase. Specificity is achieved by E3s, which function to link the target substrates to cognate E2s. Ubiquitination of proteins is reversible (Tauriello and Maurice 2010).

It has been shown that multiple E3 Ligases influence the Wnt pathway by targeting core proteins like β-catenin (Aberle, Bauer *et al.,* 1997), APC (Takacs, Baird *et al.,* 2008), Axin (Lui, Lacroix *et al.,* 2011), Dvl (Angers 2006), LRP5/6 (Abrami, Kunz *et al.,* 2008) etc, for ubiquitin-mediated degradation. In this part, I will only introduce briefly one of the E3 ligases, β-TrCP, and the β-TrCP-mediated modification of β-catenin.

β-TrCP is a component of the multiprotein Skp1-Cullin-F-box (SCF) RING-type E3 ligase, which is responsible for recognizing, like many other proteins, phosphorylated β-catenin (Aberle, Bauer *et al.,* 1997). β-TrCP binds to a substrate recognition motif (DSG(X)2+nS) in β-catenin in a phosphorylation-dependent manner. Then, polyubiquitin chains are transferred from the β-TrCP-associated SCF complex to the lysine residues at the N-terminus of β-catenin, targeting the protein for proteasomal degradation (Winston, Strack *et al.,* 1999, Staal, Noort Mv *et al.,* 2002, Wu, Xu *et al.,* 2003, Li, Kumar *et al.,* 2004). Wnt inhibits phosphorylation of β-catenin, which prevents the β-TrCP-mediated degradation of β-catenin (Figure 5, Staal, Noort Mv *et al.,* 2002). There are several E3 ligases that also induce β-catenin degradation in a phosphorylation-independent manner (Liu, Stevens *et al.,* 2001,

Chitalia, Foy *et al.,* 2008, Stamos and Weis 2013), but they will not discussed here since they are less related to the Wnt signaling pathway.

Dishevelled (Dvl)

The *Drosophila* protein Dishevelled and its three homologues in Vertebrates (Dvl1-3) were genetically shown to be required for the Wnt/β-catenin and Wnt/PCP pathways (Cong, Schweizer *et al.,* 2004, Gao and Chen 2010). Dvl is composed of three domains, PDZ, DEP and DIX (Figure 4B). It can directly interact with Fzs (Wong 2003), and can also bind to casein kinases 1 (Graff, Thies *et al.,* 1994), GSK-binding protein (van Amerongen, Mikels *et al.,* 2008), as well as the Axin DIX domain (Kishida 1999, Li, Yuan *et al.,* 1999, Itoh, Antipova *et al.,* 2000). While genetic data clearly demonstrated that Dvl is essential for the activation of the Wnt pathway, its molecular function is not completely understood and several mechanisms have been proposed.

The interaction between Axin and Dvl involves the DIX domains of both proteins. 1. Dvl polymerization may promote the formation of the Wnt-LRP-Fz signalosomes, resulting in the phosphorylation of LRP6 by GSK3 and CK1 (Cliffe, Hamada *et al.,* 2003, Cong, Schweizer *et al.,* 2004, Bilic 2007). 2. Trimeric G proteins (α, β, γ subunits) probably are required for Fz function to recruit Dvl to the plasma membrane (Angers 2006, Junge 2009, Koval, Purvanov *et al.,* 2011). 3. Wnt can induce Dvl to bind to and activate PtdIns 4-kinase type II (PI4KIIa) and PtdIns-4-phosphate 5-kinase type I (PIP5KI) to form a complex with phosphatidylinositol 4,5-bisphosphate (PIP2), where PIP2 is required for the phosphorylation of LRP6 (Pan 2008). 4. Dvl and phosphorylated LRP6 recruit can Axin to the plasma membrane (Bilic 2007).

The functions of Dvl are still mysterious. For example, upon Wnt stimulation, the hyperphosphorylated forms of Dvl have been detected (Wharton Jr 2003). But, the precise role of Dvl phosphorylation is still unknown. Also, within C-terminal domain of Dvl, a nuclear export sequence (NES) and a nuclear localization sequence (NLS)

have been identified (Itoh, Brott *et al.,* 2005) and several reports show that Dvl is able to shuttle between the cytoplasm and nucleus (Fanto, Weber *et al.,* 2000, Wharton Jr 2003, Habas and Dawid 2005).

2.3 The evolutionary origin of Wnt and other signaling pathways

Wnt signaling and its components is found in all animals from primitive metazoan forms to vertebrates (Holstein, Watanabe *et al.,* 2011). The slime mold Dictyostelium has no Wnt, but does have a β-catenin-like gene (called aardvark) and GSK3 (Pires-daSilva and Sommer 2003, Holstein 2012). GSK3is a highly conserved protein which can be found in plants. Proteins with armadillo repeats are also found in plants and yeast (Pan and Goldfarb 1998, Amador, Monte *et al.,* 2001). By analogy to structurally similar Arm proteins, these proteins play roles in nuclear import and structuring the actin cytoskeleton. However, no evidence for a Wnt itself has been obtained in any of these organisms (Martin and Kimelman 2009). It is possible, therefore, that an ancient β-catenin based mechanism was present prior to the evolution of animals. Upon the addition of Wnt and Frizzled, β-catenin activity became subject to control from other cells, as it's an essential aspect of organized multicellular life.

3. Models of the Wnt/β-catenin Pathway Regulation

A fundamental question in Wnt signaling is how the binding of ligand to its receptors regulates the activity of the β-catenin/Axin destruction complex. It is generally accepted that Wnt stimulation inhibits the activity of the complex, and stabilization of β-catenin is in turn the cause of signal transmission (Figure 1). At this point, it is unclear whether the Wnt signal leads to the disassembly of the Axin/β-catenin destruction complex or if it controls its activity through a change in and/or composition. There are several models describing this inactivation step.

3.1 Regulation at the membrane

LRP5/6 is well known to promote the canonical Wnt signaling pathway. It is commonly accepted that Wnt-induced phosphorylation of PPPSPxS motifs in the cytoplasmic tail of LRP6 is an important step in the transmembrane transduction of Wnt signals, which initiates the downstream cascade that inactivates the Axin destruction complex and stabilizes β-catenin (MacDonald and He 2012).

The first model is an initiation–amplification model, which proposed two phases of LRP6 phosphorylation (Figure 7A, Zeng 2008, MacDonald, Tamai *et al.,* 2009, MacDonald and He 2012). In the initiation phase, Wnt induces an LRP6-Fz complex, which recruits the Axin-GSK3 complex through Fz-bound Dvl to initiate LRP phosphorylation. In the amplification phase, phosphorylated LRP6 initially serves as high affinity docking site for more Axin–GSK3, so that GSK3 acts *in cis* (among five PPPSPxS motifs within an LRP6 molecule) and possibly in trans (among PPPSPxS motifs of different LRP6 molecules if LRP6 forms higher orders of oligomers), to phosphorylate LRP6 (Zeng, Huang *et al.,* 2008). According to this model, the phosphorylated LRP6-Axin-GSK3 complex forms a positive feedback loop to phosphorylate LRP6 and inhibit GSK3 to amplify Wnt signaling.

In the second model Wnt induces cytoplasmic Axin to colocalize with LRP6 into ribosome-sized signalosomes (Figure 7B, Bilic *et al.,* 2007). These signalosomes maybe mainly composed of LRP6, Fz, Dvl, GSK3and Axin (Bilic *et al.,* 2007). According to this model, polymerization of the scaffold proteins Dvl and Axin plays an essential role in LRP6 phosphorylation. Wnt would induce Dvl polymerization and interaction with the membrane receptors. Thereafter Dvl would recruit the Axin complex via the DIX domain to phosphorylate LRP6 (Schwarz-Romond 2007). Phospholipids and lipid kinases are thought to be required for the signalosome formation (Pan 2008). Wnt induces phosphatidyl-4-phosphate 5-kinase type 1 (PIP5K1) activation through Fz and Dvl, which in turn produces phosphatidylinositol 4, 5-bisphosphate [PtdIns (4,5)P2 or PIP2] to promote LRP6 phosphorylation through an unknown mechanism (Figure 7C).

Another model suggested that phosphorylation of LRP6 happens in lipid rafts and

that the caveolin-depedent endocytosis is required to recruit Axin (Yamamoto, Komekado *et al.,* 2006, Yamamoto, Sakane *et al.,* 2008). Bilic *et al.* (2007) also found that caveolin binds to LRP6 signalosomes upon Wnt stimulation, and suggested that this model is complementary to the signalosome model. In addition, the role of phospholipids and lipid kinases in LRP6 phosphorylation provides support to this "endosomal signaling" model (MacDonald and He 2012).

Fz is also thought to induce phosphorylation of Dvl, mediated via trimeric G proteins in a poorly understood mechanism (Malbon 2004). Phosphorylated Dvl may then inhibit the Axin-GSK3, perhaps through one of the mechanisms presented above.

Taken together, these models predicet a similar general state of receptor-complex activation. The net result of LRP6 complexes formation is the relocation of Axin by phosphorylated LRP6, which leads to inhibition of the complex, as explained in the next setion.

3.2 Axin/β-catenin Complex Inhibition

I will summarize here the major hypotheses proposed to explain how the complex can be inhibited. Some of them propose that the complex is disassembled; others state that the activity is directly inhibited without necessarily dissociation of the complex (Figure 8). Note that the two types of mechanisms may not be mutually exclusive.

Axin-GSK3 Complex Disassembly Models

Early studies suggested that GSK3 binding protein (GBP/Frat) and Dishevelled (Dvl) cooperatively inhibit β-catenin phosphorylation by the destruction complex. Upon Wnt activation, Dvl and Axin can form a complex via their DIX domain (Figure 8A). The recruitment of GBP to the destruction complex by Dvl would allow GBP to disrupt the ability of GSK3 to phosphorylate β-catenin (Yost, Farr *et al.,* 1998, Farr, Ferkey *et al.,* 2000). Insight into the mechanism of GBP function comes from data showing that GBP antagonizes GSK3-dependent phosphorylation of Tau both *in vitro* and *in vivo*. This suggests that GBP stabilizes by inhibiting GSK3 activity. Although

the lack of requirement for GBP in Wnt signaling in *Drosophila* and mice makes this GBP-based model suspicious (van Amerongen and Berns 2005, van Amerongen, Nawijn *et al.,* 2005), the data of the complex disruption in this model remains a fundamental concept to understand the pathway.

Another early model suggested that Wnt induces the disruption of the Axin complex mediated by Dvl (Figure 8B, Kimelman and Xu 2006, MacDonald and He 2012). It has been shown that after Wnt stimulation, Axin is less associated with β-catenin and GSK3 (Ikeda, Kishida *et al.,* 1998, Kishida 1999, Willert, Shibamoto *et al.,* 1999, Yamamoto, Kishida *et al.,* 1999, Luo and Lin 2004). This model was further developed when data showed a direct inhibition of GSK3 by the phosphorylated PPPSPxS motifs of LRP6 (Figure 8C, please refer to the previous LRP6 signalosomes model for details).

Wnt-induced phosphorylation and destabilization of Axin

Axin can highly regulate itself through phosphorylation. It has been demonstrated that Wnt induces degradation of Axin (Willert 1999), while GSK3 stabilizes Axin by inducing its phosphorylation (Yamamoto 1999), and phospho-Axin binds more effectively to LRP6 (Figure 8D, Mao 2001, Tolwinski, Wehrli *et al.,* 2003). The phosphatases PP1 have also been suggested to positively regulate the pathway by reducing CK1-mediated Axin phosphorylation, possibly leading to disruption of the Axin-GSK3 complex (Figure 8D, Luo, Peterson *et al.,* 2007). Furthermore, it has been reported that Wnt-induced Axin dephosphorylation results in the decreased ability of β-catenin to prevent the complex formation (Jho 1999, Willert 1999).

Models of Inhibition of the Axin-GSK3 Complex

Several studies have suggested that Wnt activates the downstream pathway by inhibiting the intact complex instead of disrupting it. One model proposes that Wnt stimulation induces the sequestration of GSK3/Axin-Wnt receptor complexes from the cytosol into the intraluminal vesicles (ILVs) of multivesicular bodies (MVBs), resulting in a decrease in the available cytosolic pool of GSK3 and separates GSK3

from its cytosolic substrates (Figure 8E, Taelman 2010). Note that in this model, some β-catenin colocalizes with the GSK3/Axin-Wnt receptor complexes in the ILVs of MVBs. After cytoplasmic GSK3 is sequestered in MVBs, it is the β-catenin that is released from the plasma membrane and newly synthesized β-catenin that may translocate to the nucleus to activate transcription. The same group also suggested that GSK3 can be a global regulator of protein half-life, which would also imply a global function in the cellular regulation for the Wnt signaling pathway (Kim *et al* 2009, Taelman 2010).

Clevers and colleagues provided a contrasting model. From analysis of the endogenous Axin complex (Figure 8F, Li, Ng *et al.,* 2012), they claimed that neither the reduction of β-catenin phosphorylation by GSK3 in the Axin complex nor the sequestration of GSK3 in MVBs was observed upon Wnt stimulation, at least not before a noticeable decrease in the levels of Axin. They suggested a new model where Wnt does not change the composition of the Axin destruction complex nor its activity, but rather, the ubiquitination of β-catenin. Wnt stimulation would saturate the Axin complex with phosphorylated β-catenin by inducing the dissociation of β-TrCP.

However, recent research on the kinetic responses of β-catenin upon Wnt stimulation by quantitative measurements stands against the latter model. The results indicated that Wnt stimulation results in the inhibition of β-catenin phosphorylation by dissociation/inactivation of the destruction complex. (Hernández, Klein *et al.,* 2012, Saito-Diaz, Chen *et al.,* 2013).

Recently, He and colleagues proposed an "Axin inactivation" model where in the absence of Wnt, Axin is associated with and activated by GSK3 phosphorylation to be "Open" for β-catenin binding (Figure 8G). While Wnt induced phosphorylation of LRP6 recruits the active Axin complex to relocate into the signalosomes and switches Axin complex from "Open" to "Closed" via dephosphorylating Axin, leading to the disassembly of the destruction complex and release from the signalosomes (Kim, Huang *et al.,* 2013). This model can be considered as a consequence and an "amplification" step of the direct inhibition of GSK3 by LRP6 model.

Taken together, more studies are required to support the opinion that the complex is inhibited as a whole, as opposed to the complex disassembly models.

3.3 General Comments on Current Models

This review of the current models shows how confusing the state of our knowledge still is. Possible causes of the confusion are the use of overexpression systems or the inference of activity based on the observation of steady state levels, rather than direct measurements of the endogenous kinase activity. *In vitro* data are controversial, some even contradictory. For instance, it has been shown that purified GSK3 could phosphorylate β-catenin without CK1 priming and APC/Axin scaffolding (Yost *et al.,* 1996, Hinoi *et al.,* 2000). Without sufficient knowledge of the actual concentrations, activities, compositions and localization of the endogenous components, it is impossible to translate this *in vitro* data directly to the *in vivo* environment. This raises the following questions: How many complexes exist *in vivo*? What is the composition of these endogenous complex(es)? Do different complexes play different roles? This emphasizes the need for a more thorough investigation of the nature, activity and regulation of the endogenous destruction complex, and is the subject of my thesis.

4. Thesis Objectives

For this project, I investigated the regulation of the Wnt pathway, with focus on the endogenous Axin based-complexes. As previously published methods were not adequate to achieve this goal, I had to establish a new protocol to separate clearly various subcellular compartments and that comprised the first part of my thesis. I used this protocol and a series of other methods developed by myself and fellow lab members, to address the following questions:

1. Where is the β-catenin and Axin distributed within the cell? The major pool for Axin-based complex(es) is found in which cellular compartment?

2. The characterization of the endogenous Axin-based complex(es), in terms

of subcellular localization, stability, composition and activity? (Chapter III)

3. What is the effect of Wnt regulation on the Axin-based complex(es)?

I will interpret data obtained by a precise cell fractionation method, an *in vitro* kinase assay and other biochemical approaches to present our distinct model.

Figures

Figure 1. Outline of the different Wnt signaling pathways.

The Wnt/β-catenin, PCP and Wnt/Ca^{2+} pathways are shown. All three require Frizzled-family members. Dishevelled is required for both the β-catenin and PCP pathways; its role in Wnt/Ca^{2+} signaling is less clear. LRP5/6 is thought to be specific for Wnt/β-catenin signaling.

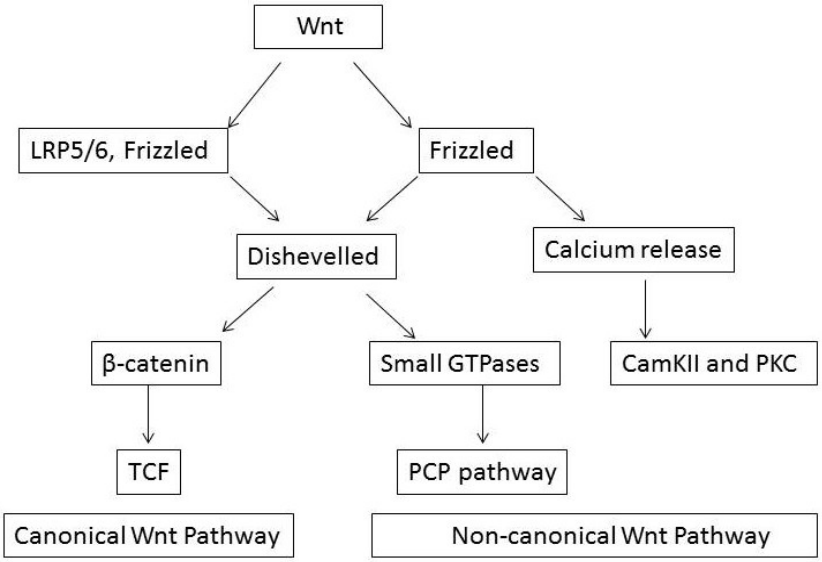
Wnt
LRP5/6, Frizzled
Frizzled
Dishevelled
Calcium release
β-catenin
Small GTPases
CamKII and PKC
TCF
PCP pathway
Canonical Wnt Pathway
Non-canonical Wnt Pathway

Figure 2. Current model of WNT/β-catenin signaling.

The current model of Wnt-β-catenin regulation is a two-state model:

A. In the absence of Wnt, β-catenin is phosphorylated by a destruction complex that contains the two scaffolding proteins Axin and adenomatous polyposis coli (APC), casein kinase 1 (CK1), and glycogen synthase kinase 3 (GSK3). Phosphorylated β-catenin is then ubiquitinated by the ubiquitin ligase β-TrCP and targeted for proteasomal degradation.

B. Wnt binding to the receptors Frizzled (Fz) and LRP6 at the plasma membrane initiates the pathway. The signal is then relayed through Dishevelled (Dvl) and leads to the inhibition of the Axin destruction complex. Thus, dephosphorylated β-catenin can accumulate in the cytoplasm and enter into the nucleus where it will interact with transcription factors TCF/LEF to activate transcription.

In cadherin-expressing cells, there is another pool of β-catenin at the plasma membrane complexed with cadherins.

Note that only one molecule is drawn in the complex for clarity. The same applies to the following diagrams.

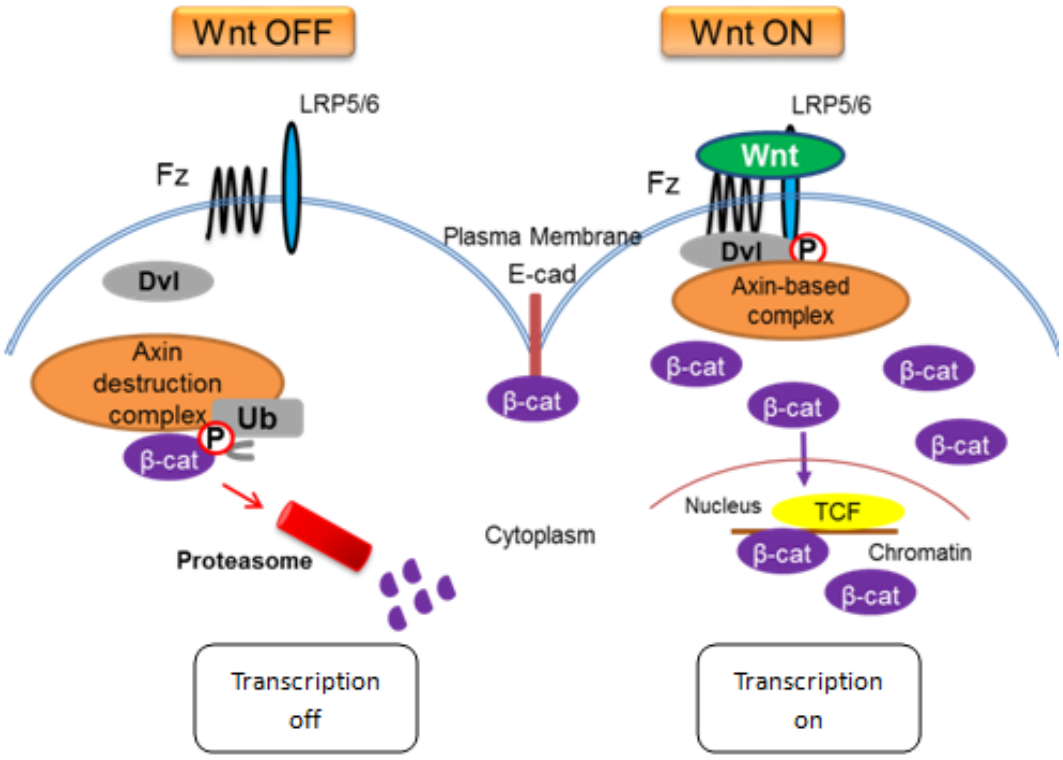
Wnt OFF
Wnt ON
LRP5/6
Fz
Dvl
Axin
destruction
complex
Ub
P
β-cat
Proteasome
Plasma Membrane
E-cad
β-cat
Cytoplasm
Transcription
off
LRP5/6
Wnt
Fz
Dvl
P
Axin-based
complex
β-cat
β-cat
β-cat
β-cat
Nucleus
TCF
β-cat
Chromatin
β-cat
Transcription
on

Figure 3. The Wnt Secretion Machinery.

Wnt proteins undergo lipid modifications in the endoplasmic reticulum by the Porcupine (Porc) enzyme. Their transport from the Golgi apparatus to the cell surface involves the association with the Wntless (Wls) multiple pass transmembrane protein. Efficient secretion of Wnts requires the recycling of Wls via the endosomal retromer complex.

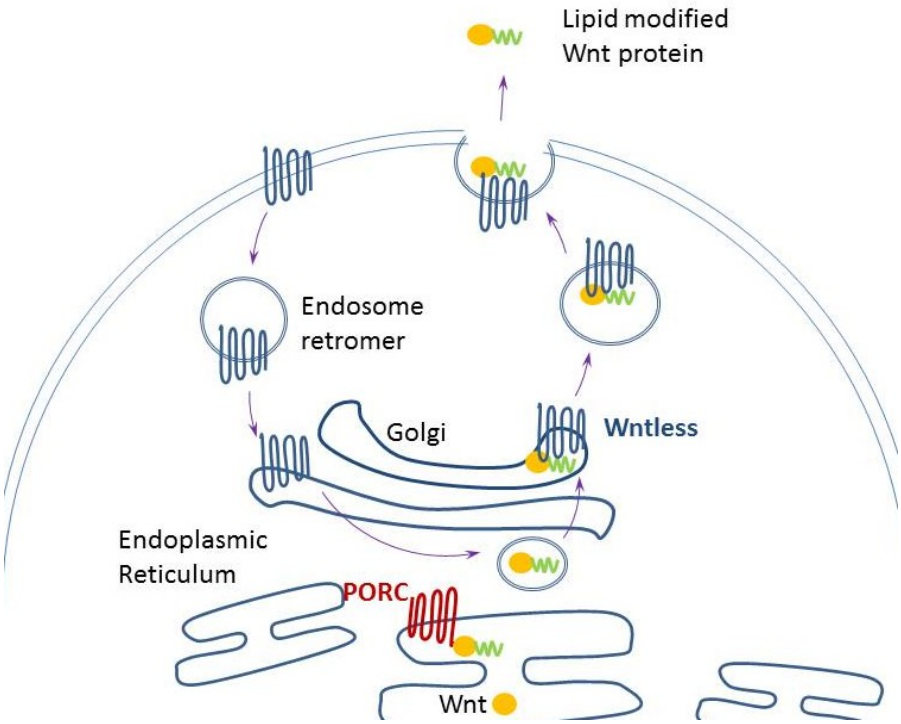
Lipid modified
Wnt protein
Endosome
retromer
Golgi
Wntless
Endoplasmic
Reticulum
PORC
Wnt

Figure 4. Diagram of the major scaffolds and β-catenin in the Wnt signaling pathway.

A. The intracellular tail of LRP5/6 contains five PPPSP motifs for GSK3/CK1 phosphorylation.

B-D. Among components of the Wnt pathway, Dvl, Axin, APC are multi-domain proteins, which provide a binding platform for a wide array of proteins. They contain many interactor-binding sites.

E. β-catenin is the major substrate of GSK3 and CK1, and binds to many pathway components via the Armadillo repeats.

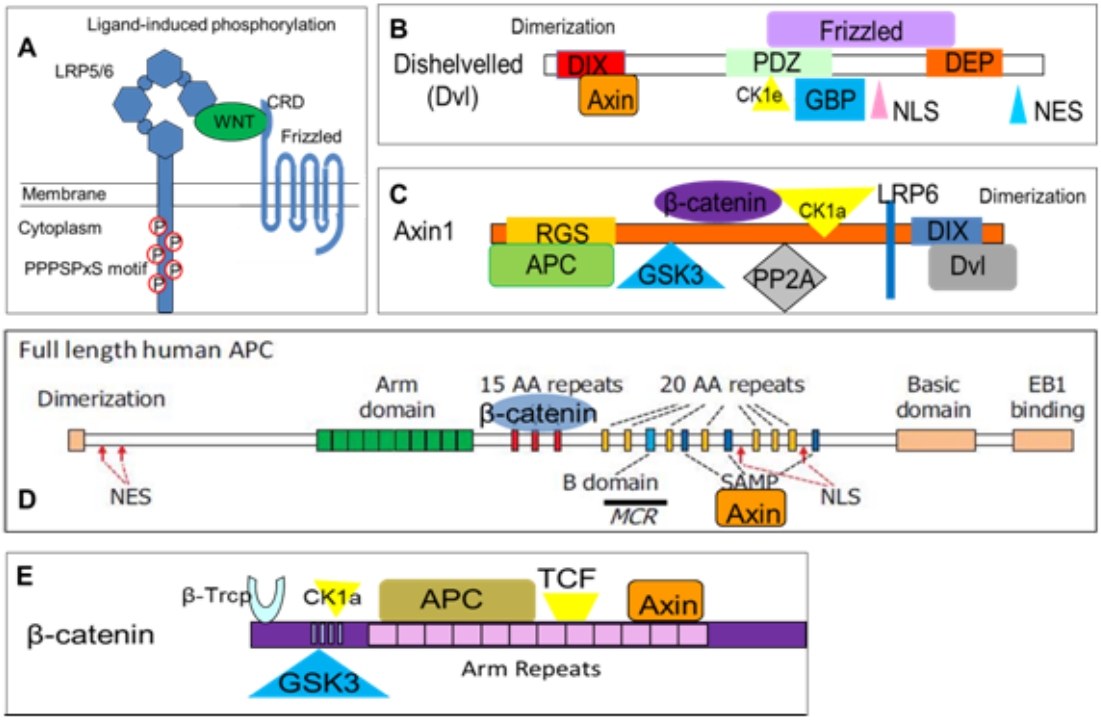
A
Ligand-induced phosphorylation
LRP5/6
WNT
CRD
Frizzled
Membrane
Cytoplasm
PPPSPxS motif
B
Dimerization
Frizzled
Dishelvelled
(Dvl)
DIX
PDZ
DEP
Axin
CK1e
GBP
NLS
NES
C
Axin1
β-catenin
CK1a
LRP6
Dimerization
RGS
APC
GSK3
PP2A
DIX
Dvl
D
Full length human APC
Dimerization
Arm
domain
15 AA repeats
β-catenin
20 AA repeats
Basic
domain
EB1
binding
NES
B domain
MCR
SAMP
Axin
NLS
E
β-Trcp
CK1a
APC
TCF
Axin
β-catenin
GSK3
Arm Repeats

Figure 5. Regulation of the Axin/β-catenin complex assembly for β-catenin degradation.

A. In the absence of Wnt, β-catenin is captured by two scaffold proteins, Axin and APC. In addition to phosphorylating β-catenin, GSK3 (yellow) and CK1 (blue) also phosphorylate Axin and APC. This enhances Axin stability and APC binding to β-catenin. The core components of the Axin complex (Axin, APC, GSK3 and CK1) collectively promote β-catenin phosphorylation. The phosphorylated-β-catenin is then ubiquitinated by β-TrCP, leading to its degradation by proteasome. Phosphorylated-β-catenin can be dephosphorylated by PP2A, which can be experimentally inhibited by the phosphatase inhibitor okadaic acid.

B. The N-terminus of β-catenin is first phosphorylated by CK1 at Ser 45, which serves as priming for subsequent phosphorylation by GSK3 at Ser 33, Ser 37 and Thr 41 (Modified from Gusev, 2012).

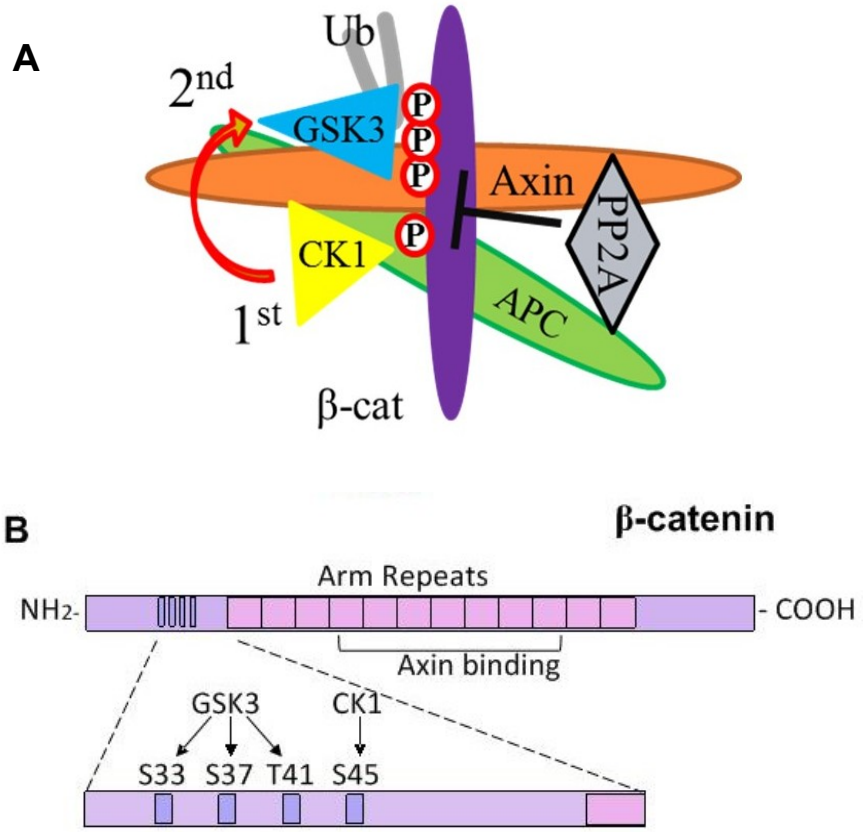
A
Ub
2nd
GSK3
P
P
P
Axin
PP2A
CK1
P
APC
1st
β-cat
B
β-catenin
Arm Repeats
NH2-
- COOH
Axin binding
GSK3
CK1
S33 S37 T41 S45

Figure 6. Models for APC-mediated Axin Complex Dynamics.

A. Sequence B and 20R2 on APC promote a cyclic assembly/ disassembly of Axin–APC complexes.

B. Truncated or mutant APC can no longer be released from the destruction complex for β-catenin degradation.

C. APC can regulate the pathway by retaining cytoplasmic β-catenin. In the presence of a completely functional destruction complex, β-catenin protein levels are greatly decreased. APC binds any β-catenin and retains it in the cytoplasm and the transcription is fully turned off. While in human cancer cells harbouring truncated APCs and *Drosophila* embryos with APC1/2 mutant, mutated APC can inactivate the destruction complex, thereafter, increasing β-catenin protein levels. Mutated APC can only bind and retain partial β-catenin and the transcription is on (Modified from Roberts *et al* 2011).

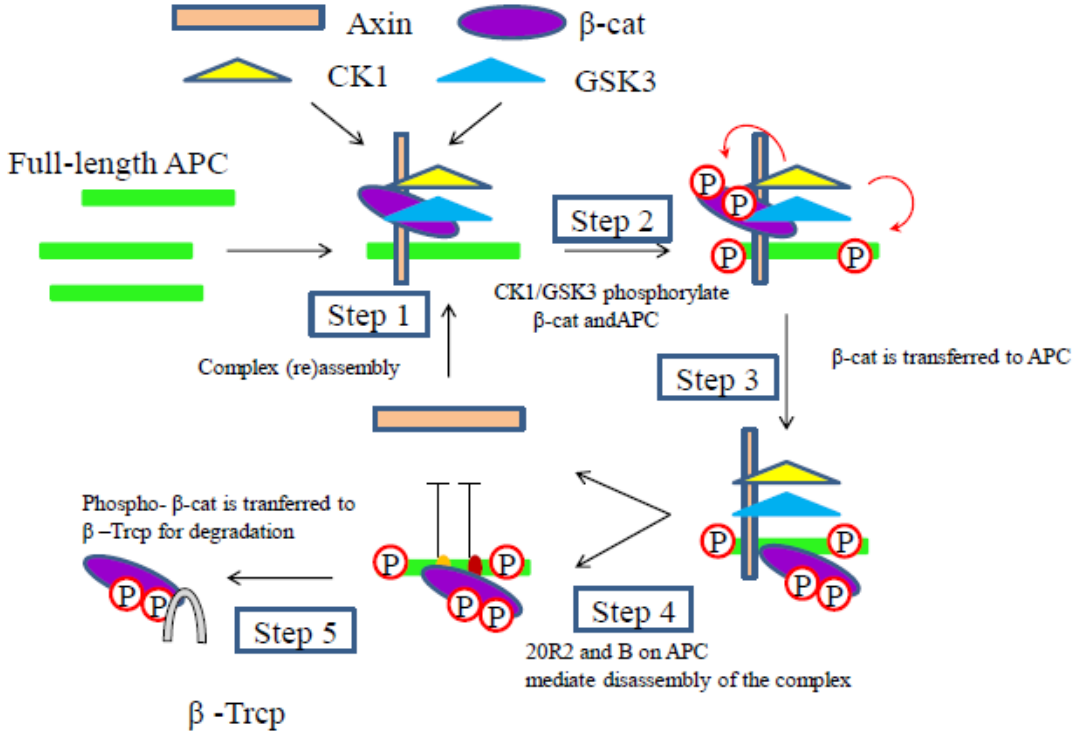

A. APC mediates disassembly of the destruction complex.

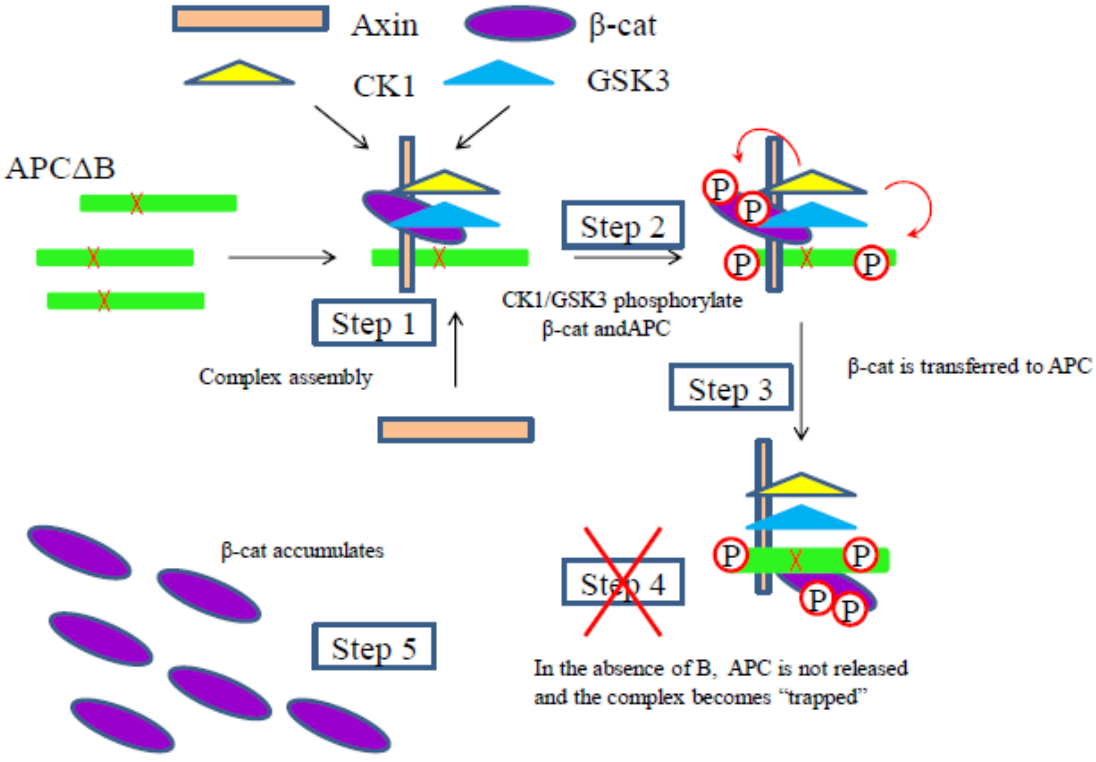

B. Truncated or mutant APC locks up the destruction complex.

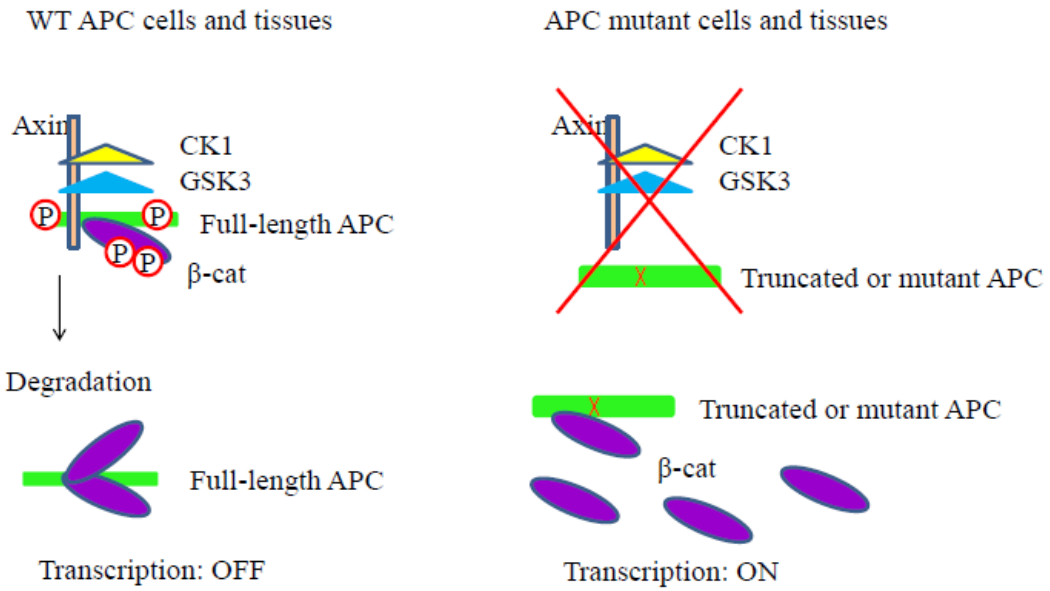

C. Cytoplasmic retention of β-cat by APC regulates the pathway.

Figure 7. Models for LRP6 activation.

A. Initiation-amplification model.

B. LRP6-Axin Signalosome model. Normally, Each LRP6 molecule could bind several Axin and Dvl molecules. The diagrams are simplified, showing only one Axin/Dvl molecule per complex.

C. Dvl/PIP5K1-mediated PIP2 production model.

These models describe the same receptor activation events. The net result of the formation of LRP6 complexes is the relocation and inhibition of Axin-GSK3 by phosphorylated LRP6, which stabilizes β-catenin.

Color codes for the components: APC (green), Axin (orange), β-catenin (purple), CK1 (yellow), GSK3 (blue), Dvl (grey), DIX domains (red dots on Dvl and Axin).
See explanations in the text.

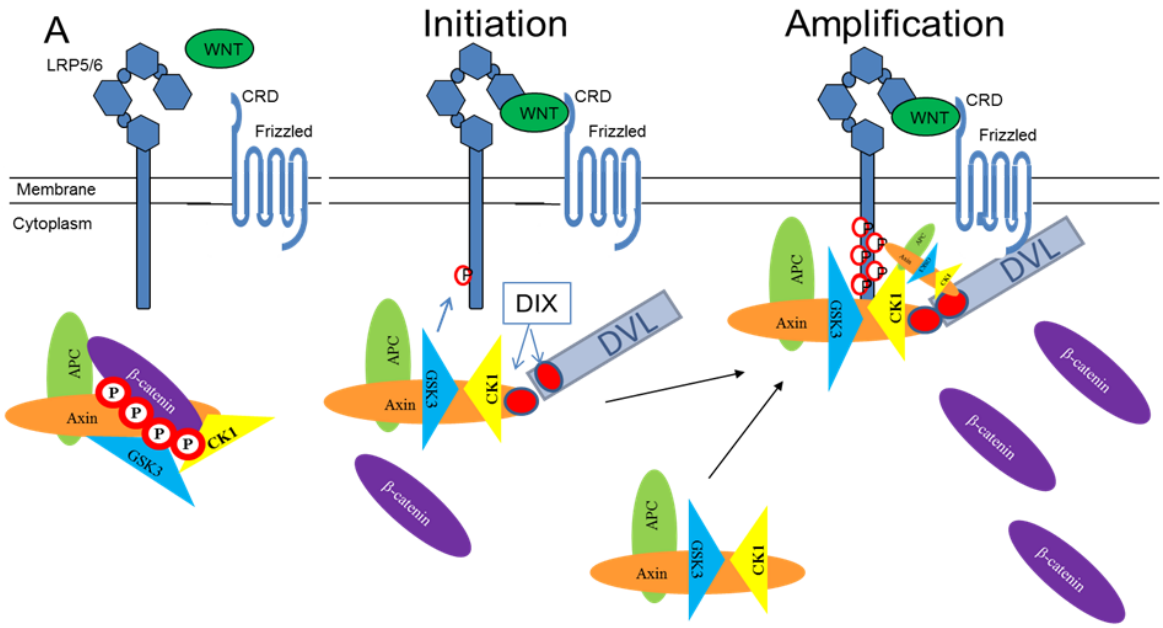
A
Initiation
Amplification
WNT
LRP5/6
CRD
Frizzled
Membrane
Cytoplasm
DIX
DVL
APC
Axin
GSK3
CK1
β-catenin
P

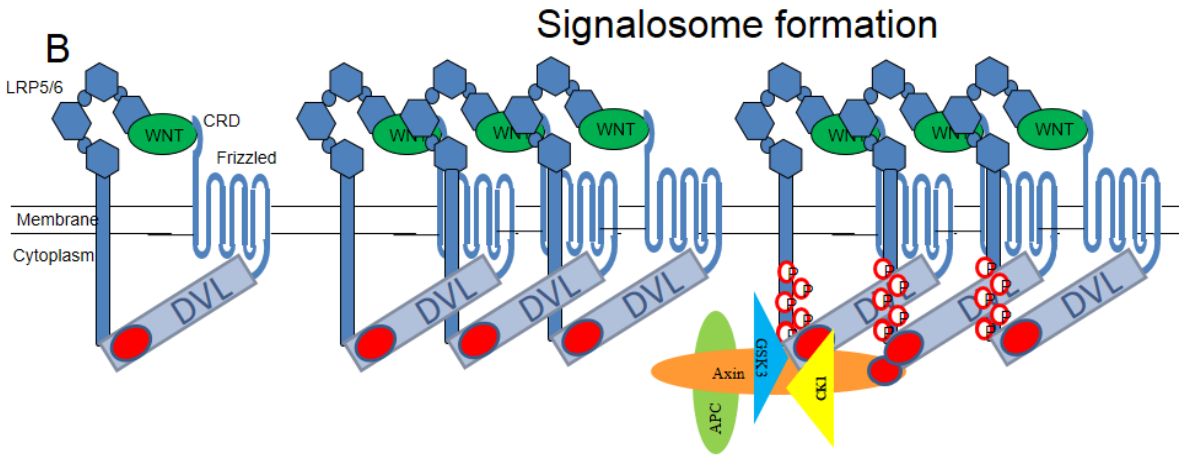
B
Signalosome formation
LRP5/6
WNT
CRD
Frizzled
Membrane
Cytoplasm
DVL
Axin
GSK3
CK1
APC

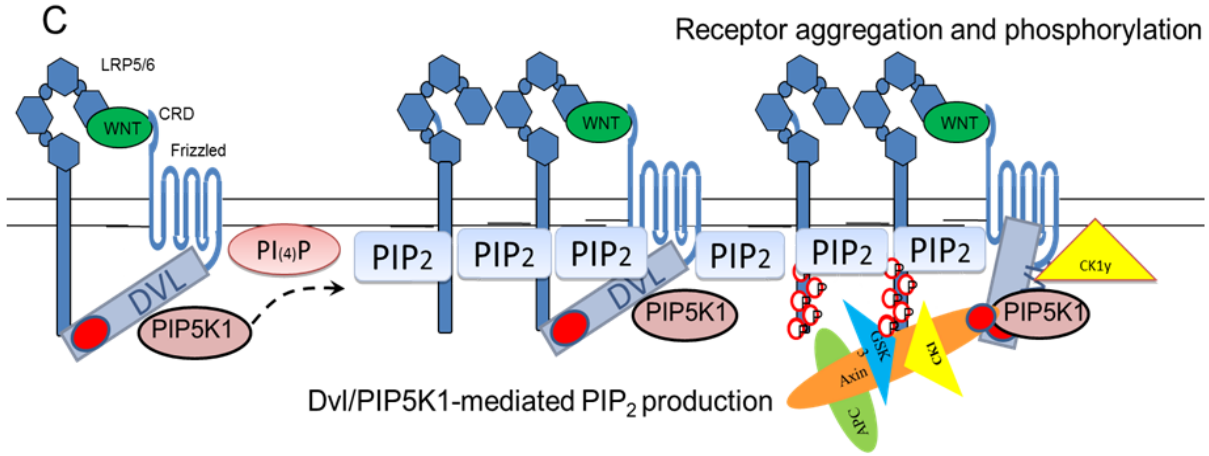
C
Receptor aggregation and phosphorylation
LRP5/6
WNT
CRD
Frizzled
PI(4)P
PIP2
PIP5K1
DVL
CK1γ
Dvl/PIP5K1-mediated PIP2 production

Figure 8. Models for Wnt-induced disassembly/inhibition of the Axin complex and stabilization of β-catenin.

A. GBP replaces GSK3 in the complex via Wnt-induced Dvl recruitment.

B. Wnt induces Axin complex disassembly via Dvl.

C. Phosphorylated PPPSPxS motifs inhibit GSK3 directly.

D. Wnt induces the PP1-mediated dephosphorylation and degradation of Axin.

E. Wnt induces the inhibition of the Axin complex by including GSK3 into the multivesicular bodies (MVB) (Modified from Taelman, *et al.,* 2010).

F. Wnt induces the association of the intact complex with phospho- LRP6. Then the existing complexes are trapped by removing β-TrCP. Newly synthesized β-catenin accumulates in cytoplasm (Modified from Li *et al.,* 2012).

G. Wnt induces the activated Axin complex from "Open" state to "Closed" for inactivation, thus releasing phospho-LRP6 for next rounds of recruitment of the complexes (Modified from Kim *et al.,* 2013).

A GBP is recruited by Dvl to displace GSK3 in the Axin complex.

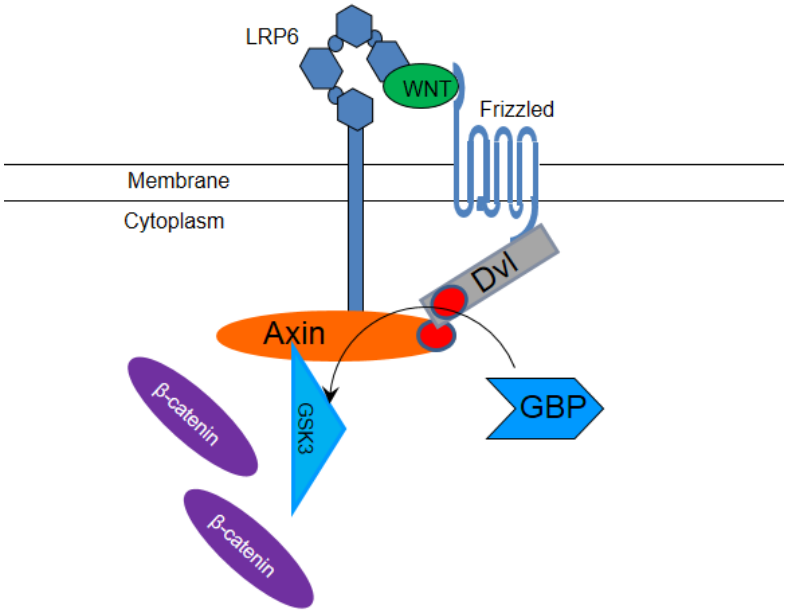

B Wnt induces Axin complex disassembly via Dvl.

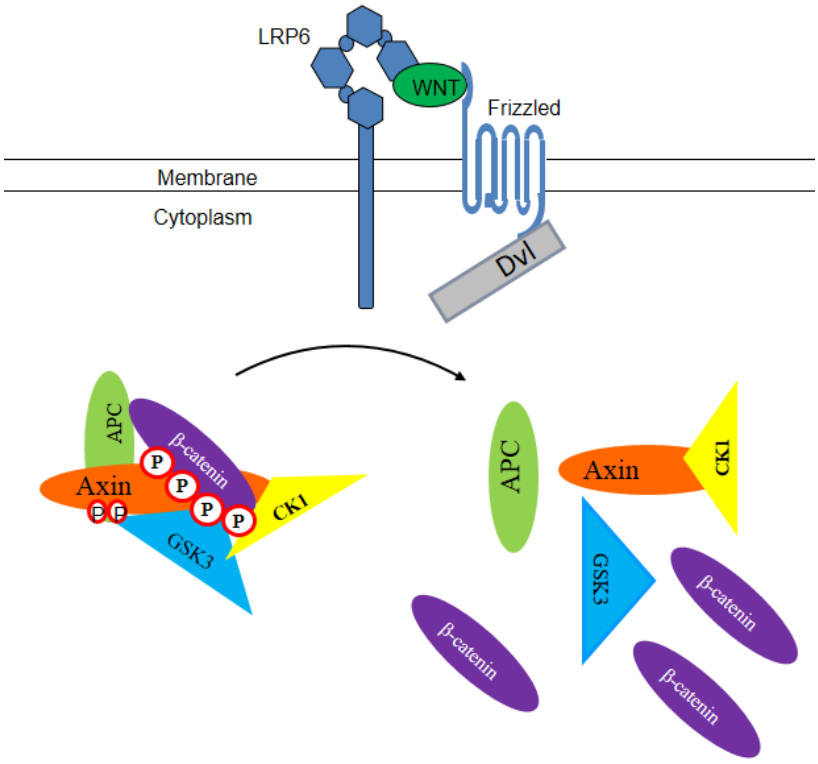

C Direct inhibition of GSK3 through pLRP6

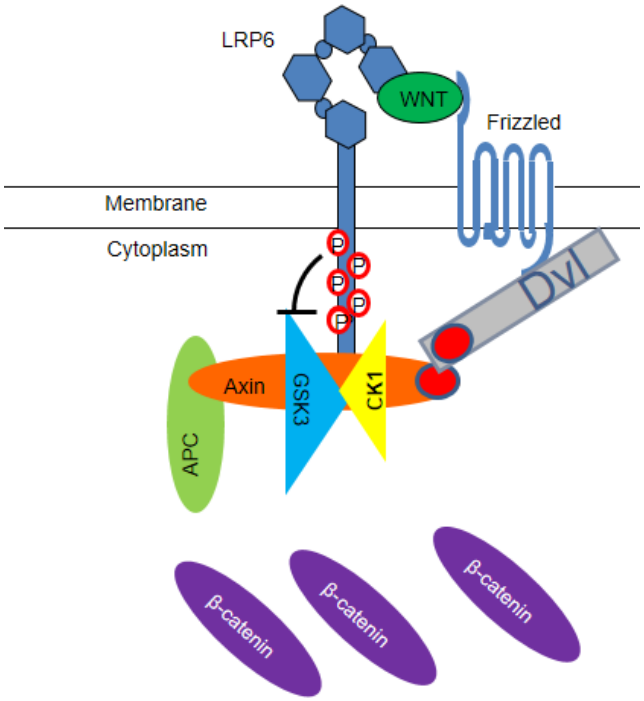

D Wnt-induced Axin degradation

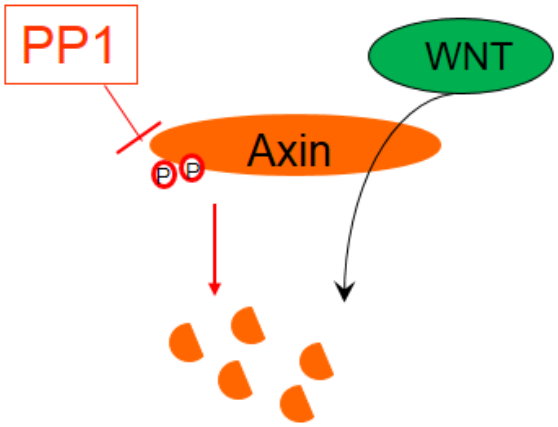

E Wnt induces internalisation of GSK3 intomultivesicular bodies.

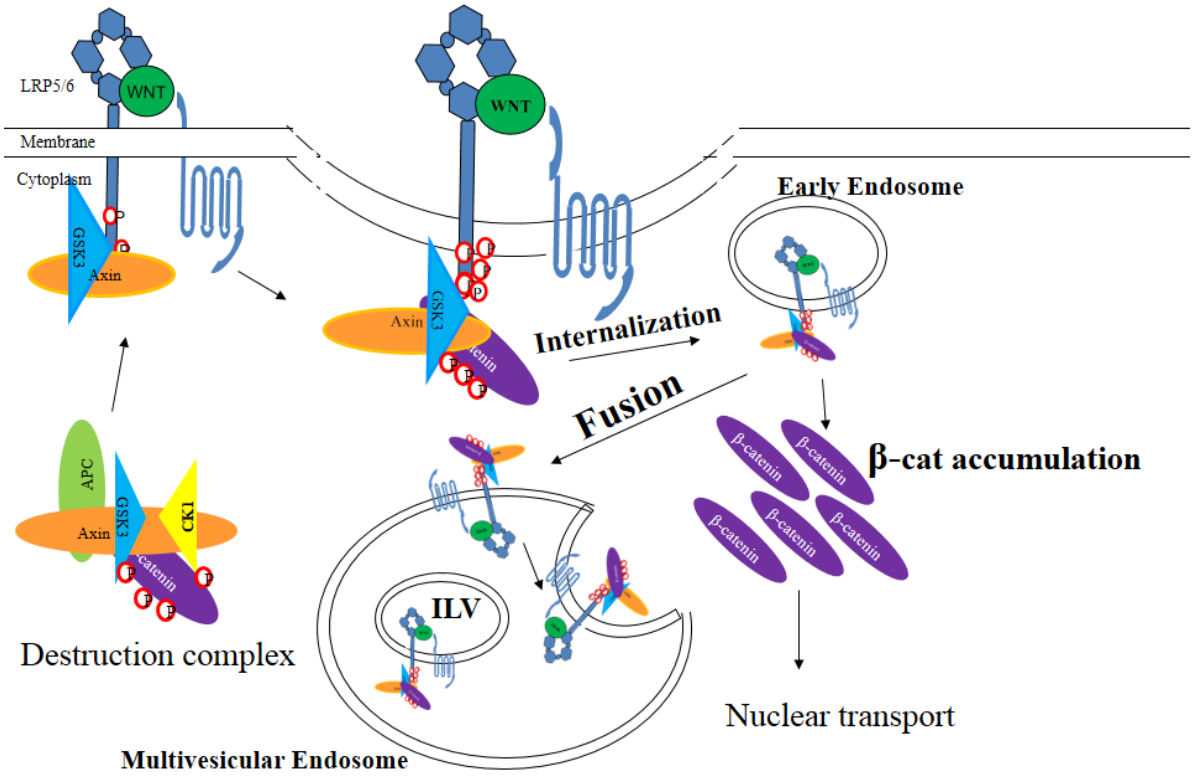

F Wnt induces saturation of the Axin complex with phosphorylated β-catenin by removing β-TrCP.

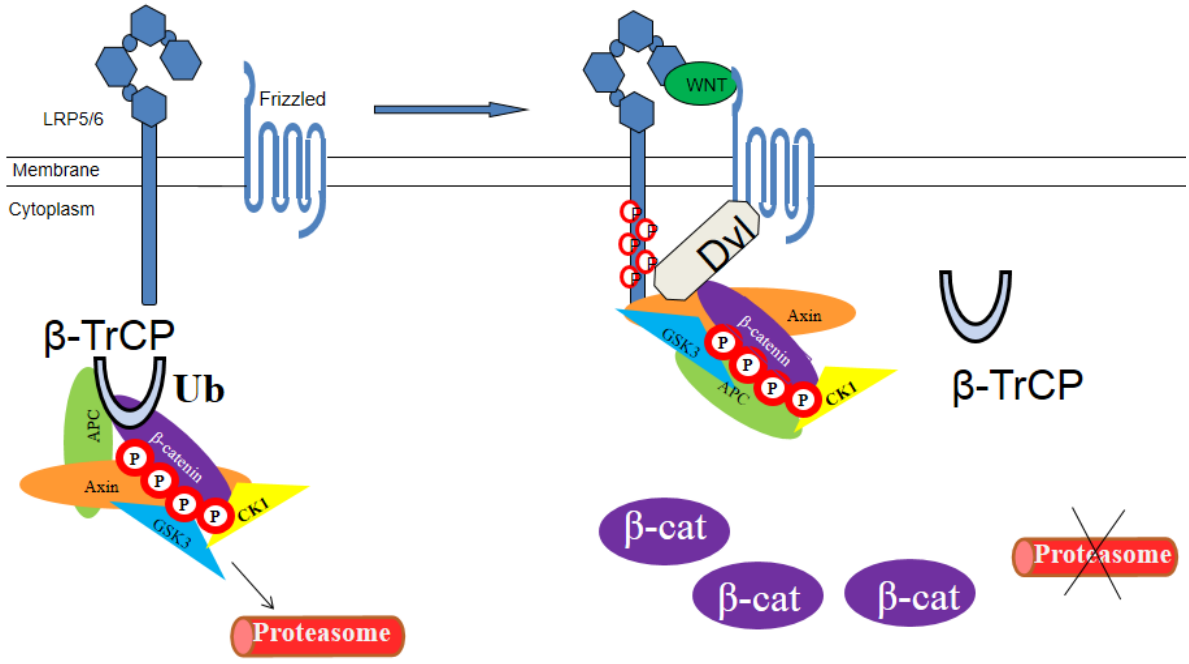

G PP1 mediated dephosphorylation of Axin makes it from "Open" state to "Closed" for inactivation.

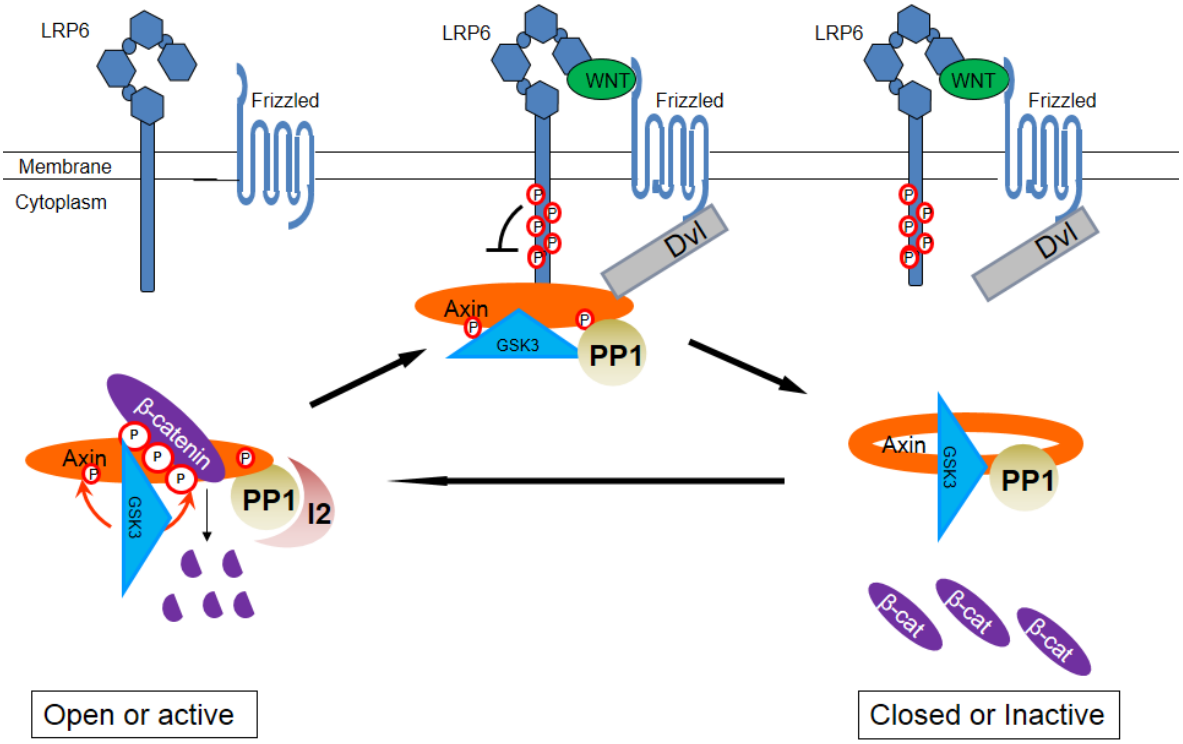

References

Aberle, H., *et al.,* (1997). "beta-catenin is a target for the ubiquitin-proteasome pathway." EMBO J **16**: 3797-3804.

Abrami, L., *et al.,* (2008). "Palmitoylation and ubiquitination regulate exit of the Wnt signaling protein LRP6 from the endoplasmic reticulum." Proc Natl Acad Sci U S A **105**(14): 5384-5389.

Amador, V., *et al.,* (2001). "Gibberellins signal nuclear import of PHOR1, a photoperiod-responsive protein with homology to *Drosophila* armadillo." Cell **106**(3): 343-354.

Angers, S. (2006). "The KLHL12-cullin-3 ubiquitin ligase negatively regulates the Wnt-[beta]-catenin pathway by targeting Dishevelled for degradation." Nature Cell Biol. **8**: 348-357.

Bienz, M. (2005). "beta-Catenin: a pivot between cell adhesion and Wnt signalling." Curr Biol **15**(2): R64-67.

Bilic, J. (2007). "Wnt induces LRP6 signalosomes and promotes dishevelled-dependent LRP6 phosphorylation." Science **316**: 1619-1622.

Blitzer, J. T. and R. Nusse (2006). "A critical role for endocytosis in Wnt signaling." BMC Cell Biol. **7**: 28.

Cadigan, K. M. and M. Peifer (2009). "Wnt signaling from development to disease: insights from model systems." Cold Spring Harb Perspect Biol **1**: a002881.

Cavallo, R. A. (1998). "*Drosophila* Tcf and Groucho interact to repress Wingless signalling activity." Nature **395**: 604-608.

Chen, M. (2009). "G protein-coupled receptor kinases phosphorylate LRP6 in the Wnt pathway." J. Biol. Chem. **284**: 35040-35048.

Chen, X., *et al.,* (2008). "Wnt signaling: the good and the bad." Acta Biochimica et Biophysica Sinica **40**(7): 577-594.

Cheong, J. K. and D. M. Virshup (2011). Int J Biochem Cell Biol **43**: 465-469.

Chitalia, V. C., *et al.,* (2008). "Jade-1 inhibits Wnt signalling by ubiquitylating

beta-catenin and mediates Wnt pathway inhibition by pVHL." Nat Cell Biol **10**: 1208-1216.

Cliffe, A., *et al.,* (2003). "A role of Dishevelled in relocating Axin to the plasma membrane during Wingless signaling." Curr Biol **13**: 960-966.

Cong, F., *et al.,* (2004). "Casein kinase Iepsilon modulates the signaling specificities of dishevelled." Mol Cell Biol **24**(5): 2000-2011.

Cong, F. and H. Varmus (2004). "Nuclear-cytoplasmic shuttling of Axin regulates subcellular localization of beta-catenin." Proc Natl Acad Sci USA **101**: 2882-2887.

Cox RT, Pai LM, Kirkpatrick C, Stein J, Peifer M. Roles of the C terminus of Armadillo in Wingless signaling in Drosophila. Genetics. 1999;153:319–332.

Creyghton, M. P., *et al.,* (2005). "PR72, a novel regulator of Wnt signaling required for Naked cuticle function." Genes Dev 19: 376-386.

Creyghton, M. P., *et al.,* (2006). "PR130 is a modulator of the Wnt-signaling cascade that counters repression of the antagonist Naked cuticle." Proc Natl Acad Sci USA **103**: 5397-5402.

Dann, C. E., *et al.,* (2001). "Insights into Wnt binding and signalling from the structures of two Frizzled cysteine-rich domains." Nature **412**: 86-90.

Davidson, G., *et al.,* (2005). "Casein kinase 1 gamma couples Wnt receptor activation to cytoplasmic signal transduction." Nature **438**: 867-872.

Day, C. L. and T. Alber (2000). "Crystal structure of the amino-terminal coiled-coil domain of the APC tumor suppressor." J Mol Biol **301**(1): 147-156.

Doble, B. W. and J. R. Woodgett (2003). "GSK-3: tricks of the trade for a multi-tasking kinase." J Cell Sci **116**: 1175-1186.

Fagotto, F. (1999). "Domains of axin involved in protein-protein interactions, wnt pathway inhibition, and intracellular localization." J. Cell Biol. **145**: 741-756.

Fagotto, F. (2013). "Looking beyond the Wnt pathway for the deep nature of [beta]-catenin." EMBO Rep **14**(5): 422-433.

Fagotto, F., *et al.,* (1998). "Nuclear localization signal-independent and importin/karyopherin-independent nuclear import of [beta]-catenin." Curr. Biol. **8**: 181-190.

Fanto, M., *et al.,* (2000). "Nuclear signaling by Rac and Rho GTPases is required in the establishment of epithelial planar polarity in the *Drosophila* eye." Curr Biol **10**(16): 979-988.

Farr, I. G., *et al.,* (2000). "Interaction among GSK-3, GBP, Axin, and APC in *Xenopus* axis specification." J Cell Biol **148**: 691-702.

González-Sancho JM, Brennan KR, Castelo-Soccio LA, Brown AM. Wnt proteins induce dishevelled phosphorylation via an LRP5/6- independent mechanism, irrespective of their ability to stabilize beta-catenin. Mol Cell Biol. 2004 Jun;24(11):4757-68.

Gottardi, C.J., B.M. Gumbiner. 2004a. Distinct molecular forms of β-catenin are targeted to adhesive or transcriptional complexes. J. Cell Biol. 167:339–349

Gotz, J., *et al.,* (2000). "Distinct role of protein phosphatase 2A subunit Calpha in the regulation of E-cadherin and beta-catenin during development." Mech Dev **93**(1-2): 83-93.

Graff, J. M., *et al.,* (1994). "Studies with a *Xenopus* BMP receptor suggest that ventral mesoderm-inducing signals override dorsal signals *in vivo*." Cell **79**(1): 169-179.

Gross, S. D. and R. A. Anderson (1998). "Casein kinase I: spatial organization and positioning of a multifunctional protein kinase family." Cell Signal **10**(10): 699-711.

Guo, X., *et al.,* (2008). "Axin and GSK3- control Smad3 protein stability and modulate TGF- signaling." Genes Dev **22**(1): 106-120.

Ha, N. C., *et al.,* (2004). "Mechanism of phosphorylation-dependent binding of APC to [beta]-catenin and its role in [beta]-catenin degradation." Mol Cell **15**: 511-521.

Habas, R. and I. B. Dawid (2005). "Dishevelled and Wnt signaling: is the nucleus the final frontier?" J Biol **4**(1): 2.

Hanks, S. K. and T. Hunter (1995). "Protein kinases 6. The eukaryotic protein kinase superfamily: kinase (catalytic) domain structure and classification." FASEB J **9**(8): 576-596.

Henderson, B. R. (2000). "Nuclear-cytoplasmic shuttling of APC regulates beta-catenin subcellular localization and turnover." Nat Cell Biol **2**: 653-660.

Henderson, B. R. and F. Fagotto (2002). "The ins and outs of APC and beta-catenin nuclear transport." EMBO Rep **3**: 834-839.

Hendriksen, J., *et al.,* (2005). "RanBP3 enhances nuclear export of active (beta)-catenin independently of CRM1." J Cell Biol **171**: 785-797.

Hendriksen, J., *et al.,* (2008). "Plasma membrane recruitment of dephosphorylated beta-catenin upon activation of the Wnt pathway." J Cell Sci **121**: 1793-1802.

Hernández, A. R., *et al.,* (2012). "Kinetic Responses of β-catenin Specify the Sites of Wnt Control." Science **338**(6112): 1337-1340.

Hikasa, H., *et al.,* (2010). "Regulation of TCF3 by Wnt-dependent phosphorylation during vertebrate axis specification." Dev Cell **19**: 521-532.

Hinoi, T., *et al.,* (2000). "Complex formation of adenomatous polyposis coli gene product and axin facilitates glycogen synthase kinase-3 beta-dependent phosphorylation of beta-catenin and down-regulates beta-catenin." J Biol Chem **275**(44): 34399-34406.

Holstein, T. (2012). "The evolution of the Wnt pathway." Cold Spring Harb Perspect Biol.

Holstein, T. W., *et al.,* (2011). "Signaling pathways and axis formation in the lower metazoa." Curr Top Dev Biol **97**: 137-177.

Hsieh, J. C., *et al.,* (1999). "A new secreted protein that binds to Wnt proteins and inhibits their activities." Nature **398**: 431-436.

Huang, S. M., *et al.,* (2009). "Tankyrase inhibition stabilizes axin and antagonizes Wnt signalling." Nature **461**(7264): 614-620.

Huber O., Korn R., McLaughlin J., Ohsugi M., Herrmann B.G., Kemler R. (1996) Nuclear localization of beta-catenin by interaction with transcription factor LEF-1. Mech. Dev. **59**:3–10.

Ikeda, S., *et al.,* (1998). "Axin, a negative regulator of the Wnt signaling pathway, forms a complex with GSK-3beta and beta-catenin and promotes GSK-3beta-dependent phosphorylation of beta-catenin." EMBO J **17**: 1371-1384.

Itoh, K., *et al.,* (2000). "Interaction of dishevelled and *Xenopus* axin-related protein is required for wnt signal transduction." Mol Cell Biol **20**: 2228-2238.

Itoh, K., *et al.,* (2005). "Nuclear localization is required for dishevelled function in Wnt//beta-catenin signaling." J Biol **4**: 3.

Janssens, V. and J. Goris (2001). "Protein phosphatase 2A: a highly regulated family of serine/threonine phosphatases implicated in cell growth and signalling." Biochem. J. **353**: 417-439.

Jimbo, T., *et al.,* (2002). "Identification of a link between the tumour suppressor APC and the kinesin superfamily." Nat Cell Biol **4**(4): 323-327.

Junge, H. J. (2009). "TSPAN12 regulates retinal vascular development by promoting Norrin- but not Wnt-induced FZD4/[beta]-catenin signaling." Cell **139**: 299-311.

Kawasaki, Y. (2000). "Asef, a link between the tumor suppressor APC and G-protein signaling." Science 289: 1194-1197.

N.G. Kim, C. Xu, B.M. Gumbiner. (2009). Identification of targets of the Wnt pathway destruction complex in addition to β-catenin. Proc. Natl. Acad. Sci. USA, 106, pp. 5165–5170.

Kim Sung-Eun, *et al.,* (2013). ” Wnt Stabilization of β-catenin Reveals Principles for Morphogen Receptor-Scaffold Assemblies.” Science 340 (6134), 867.

Kimelman, D. and W. Xu (2006). "Beta-catenin destruction complex: insights and questions from a structural perspective." Oncogene **25**: 7482-7491.

Kishida, M., *et al.,* (2001). "Synergistic activation of the Wnt signaling pathway by Dvl and casein kinase Iepsilon." J Biol Chem **276**(35): 33147-33155.

Kishida, S. (1999). "DIX domains of Dvl and axin are necessary for protein interactions and their ability to regulate [beta]-catenin stability." Mol. Cell. Biol. **19**: 4414-4422.

Knippschild, U., *et al.,* (2005). "The casein kinase 1 family: participation in multiple cellular processes in eukaryotes." Cell Signal **17**(6): 675-689.

Kohn, A. D. and R. T. Moon (2005). "Wnt and calcium signaling: beta-catenin-independent pathways." Cell Calcium **38**: 439-446.

Koval, A., *et al.,* (2011). "Yellow submarine of the Wnt/Frizzled signaling: submerging from the G protein harbor to the targets." Biochem. Pharmacol. **82**: 1311-1319.

Krieghoff, E., Behrens, J., and Mayr, B. (2006). Nucleo-cytoplasmic distribution of beta-catenin is regulated by retention. J. Cell Sci. 119, 1453–1463.

Lee, E., *et al.,* (2001). "Physiological regulation of [beta]-catenin stability by Tcf3

and CK1εpsilon." J Cell Biol **154**(5): 983-993.

Lee, E., *et al.,* (2003). "The roles of APC and Axin derived from experimental and theoretical analysis of the Wnt pathway." PLoS Biol **1**: E10.

Lee, W., *et al.,* (2009). "Homeodomain-interacting protein kinases (Hipks) promote Wnt/Wg signaling through stabilization of beta-catenin/Arm and stimulation of target gene expression." Development **136**: 241-251.

Li, L., *et al.,* (1999). "Axin and Frat-1 interact with Dvl and GSK, bridging Dvl to GSK in Wnt-mediated regulation of LEF-1." EMBO J **18**: 4233-4240.

Li, V., *et al.,* (2012). "Wnt signaling inhibits proteasomal [beta]-catenin degradation within a compositionally intact Axin1 complex." Cell.

Li, X., *et al.,* (2001). "Protein phosphatase 2A and its B56 regulatory subunit inhibit Wnt signaling in *Xenopus*." EMBO J **20**: 4122-4131.

Li, Y., *et al.,* (2004). "Negative regulation of prolactin receptor stability and signaling mediated by SCF[beta]-TrC E3 ubiquitin ligase." Mol. Cell. Biol. **24**: 4038-4048.

Liu, C. (2002). "Control of [beta]-catenin phosphorylation/degradation by a dual-kinase mechanism." Cell **108**: 837-847.

Liu, J., *et al.,* (2001). "Siah-1 mediates a novel [beta]-catenin degradation pathway linking p53 to the adenomatous polyposis coli protein." Mol Cell **7**: 927-936.

Liu, X., *et al.,* (2005). "Rapid, Wnt-induced changes in GSK3[beta] associations that regulate [beta]-catenin stabilization are mediated by G[alpha] proteins." Curr. Biol. **15**: 1989-1997.

Liu X., Fagotto F. (2011). A method to separate nuclear, cytosolic, and membrane-associated signaling molecules in cultured cells. Sci Signal 4: pl2

Logan, C. Y. and R. Nusse (2004). "The Wnt signaling pathway in development and disease." Annu. Rev. Cell Dev. Biol. **20**: 781-810.

Lui, T. T., *et al.,* (2011). "The ubiquitin-specific protease USP34 regulates axin stability and Wnt/beta-catenin signaling." Mol Cell Biol **31**(10): 2053-2065.

Luo, W. and S. C. Lin (2004). "Axin: a master scaffold for multiple signaling pathways." Neurosignals **13**(3): 99-113.

Luo, W., *et al.,* (2003). "Axin utilizes distinct regions for competitive MEKK1 and

MEKK4 binding and JNK activation." J Biol Chem **278**(39): 37451-37458.

Luo, W., *et al.,* (2007). "Protein phosphatase 1 regulates assembly and function of the beta-catenin degradation complex." EMBO J **26**(6): 1511-1521.

Luo, W., *et al.,* (2005). "Axin contains three separable domains that confer intramolecular, homodimeric, and heterodimeric interactions involved in distinct functions." J Biol Chem **280**(6): 5054-5060.

MacDonald, B. T. and X. He (2012). "Frizzled and LRP5/6 Receptors for Wnt/β-catenin Signaling." Cold Spring Harbor Perspectives in Biology **4**(12).

MacDonald, B. T., *et al.,* (2009). "Wnt/beta-catenin signaling: components, mechanisms, and diseases." Dev Cell **17**: 9-26.

Maher, M. T., *et al.,* (2009). "Activity of the beta-catenin phosphodestruction complex at cell-cell contacts is enhanced by cadherin-based adhesion." J Cell Biol **186**(2): 219-228.

Malbon, C. C. (2004). "Frizzleds: new members of the superfamily of G-protein-coupled receptors." Front Biosci **9**: 1048-1058.

Mao, J. (2001). "Low-density lipoprotein receptor-related protein-5 binds to Axin and regulates the canonical Wnt signaling pathway." Mol. Cell **7**: 801-809.

Martin, B. L. and D. Kimelman (2009). "Wnt signaling and the evolution of embryonic posterior development." Curr Biol **19**: R215-R219.

McKay, R. M., *et al.,* (2001). "The casein kinase I family in Wnt signalling." Dev. Biol. **235**: 388-396.

Minami, Y., Oishi, I., Endo, M. and Nishita, M. (2009) Ror-family receptor tyrosine kinases in noncanonical Wnt signaling: Their implications in developmental morphogenesis and human diseases. Dev. Dyn. **239**, 1-15

Moon, R. T., *et al.,* (2004). "WNT and [beta]-catenin signalling: diseases and therapies." Nature Rev. Genet. **5**: 691-701.

Nathke IS, Adams CL, Polakis P, Sellin JH, Nelson WJ. The adenomatous polyposis coli tumor suppressor protein localizes to plasma membrane sites involved in active cell migration. J Cell Biol. 1996;134:165–179.

Neufeld, K. L., *et al.,* (2000). "APC-mediated downregulation of [beta]-catenin

activity involves nuclear sequestration and nuclear export." EMBO Rep. **1**: 519-523.

Niehrs C. The complex world of WNT receptor signalling. Nat Rev Mol Cell Biol (2012) **13**:767–79.

Nusse, R., *et al.,* (2008). "Wnt signaling and stem cell control." Cold Spring Harb Symp Quant Biol **73**: 59-66.

Pan, W. (2008). "Wnt3a-mediated formation of phosphatidylinositol 4,5-bisphosphate regulates LRP6 phosphorylation." Science **321**: 1350-1353.

Pan, X. and D. S. Goldfarb (1998). "YEB3/VAC8 encodes a myristylated armadillo protein of the Saccharomyces cerevisiae vacuolar membrane that functions in vacuole fusion and inheritance." J Cell Sci **111 (Pt 15)**: 2137-2147.

Patel, S., *et al.,* (2004). "Glycogen synthase kinase-3 in insulin and Wnt signalling: a double-edged sword?" Biochem Soc Trans **32**: 803-808.

Patturajan, M., *et al.,* (2002). "DeltaNp63 induces beta-catenin nuclear accumulation and signaling." Cancer Cell **1**(4): 369-379.

Peifer, M., *et al.,* (1993). "A model system for cell adhesion and signal transduction in *Drosophila*." Development **Suppl**: 163-176.

Peterson-Nedry, W., *et al.,* (2008). "Unexpectedly robust assembly of the Axin destruction complex regulates Wnt/Wg signaling in *Drosophila* as revealed by analysis *in vivo*." Dev Biol **320**(1): 226-241.

Pires-daSilva, A. and R. J. Sommer (2003). "The evolution of signalling pathways in animal development." Nat Rev Genet **4**(1): 39-49.

Plyte, S. E., *et al.,* (1992). "Glycogen synthase kinase-3: functions in oncogenesis and development." Biochim Biophys Acta **1114**(2-3): 147-162.

Reinacher-Schick A, Gumbiner BM. Apical membrane localization of the adenomatous polyposis coli tumor suppressor protein and subcellular distribution of the beta-catenin destruction complex in polarized epithelial cells. J Cell Biol.2001;152:491–502.

Rivers, A., *et al.,* (1998). "Regulation of casein kinase I epsilon and casein kinase I delta by an *in vivo* futile phosphorylation cycle." J Biol Chem **273**(26): 15980-15984.

Roberts, D. M., *et al.,* (2012). "Defining components of the [beta]-catenin destruction complex and exploring its regulation and mechanisms of action during development."

PLoS ONE **7**: e31284.

Roberts, D. M., *et al.,* (2012). "Regulation of Wnt signaling by the tumor suppressor adenomatous polyposis coli does not require the ability to enter the nucleus or a particular cytoplasmic localization." Mol Biol Cell **23**(11): 2041-2056.

Roberts, D. M., *et al.,* (2011). "Deconstructing the sscatenin destruction complex: mechanistic roles for the tumor suppressor APC in regulating Wnt signaling." Mol Biol Cell **22**(11): 1845-1863.

Roose, J. (1998). "The *Xenopus* Wnt effector XTcf-3 interacts with Groucho-related transcriptional repressors." Nature **395**: 608-612.

Rosin-Arbesfeld, R., *et al.,* (2000). "The APC tumour suppressor has a nuclear export function." Nature **406**: 1009-1012.

Rubinfeld, B., *et al.,* (1996). "Binding of GSK3beta to the APC-beta-catenin complex and regulation of complex assembly." Science (New York, NY) **272**: 1023-1026.

Rubinfeld, B., *et al.,* (2001). "Axin-dependent phosphorylation of the adenomatous polyposis coli protein mediated by casein kinase 1[epsiv]." J. Biol. Chem. **276**: 39037-39045.

Saito-Diaz, K., *et al.,* (2013). "The way Wnt works: components and mechanism." Growth Factors **31**(1): 1-31.

Sakanaka, C., *et al.,* (1999). "Casein kinase [epsiv] in the wnt pathway: regulation of [beta]-catenin function." Proc. Natl Acad. Sci. USA **96**: 12548-12552.

Salic, A., *et al.,* (2000). "Control of [beta]-catenin stability: reconstitution of the cytoplasmic steps of the wnt pathway in *Xenopus* egg extracts." Mol. Cell **5**: 523-532.

Schwarz-Romond, T. (2007). "The DIX domain of Dishevelled confers Wnt signaling by dynamic polymerization." Nature Struct. Mol. Biol. **14**: 484-492.

Seeling, J. M., *et al.,* (1999). "Regulation of [beta]-catenin signaling by the B56 subunit of protein phosphatase 2A." Science **283**: 2089-2091.

Seifert, J. R. and M. Mlodzik (2007). "Frizzled/PCP signalling: a conserved mechanism regulating cell polarity and directed motility." Nat Rev Genet **8**(2): 126-138.

Sharma, M., *et al.,* (2012). "Specific armadillo repeat sequences facilitate [beta]-catenin nuclear transport in live cells via direct binding to nucleoporins Nup62,

Nup153, and RanBP2/Nup358." J Biol Chem **287**: 819-831.

Simcha, I., *et al.,* (2001). "Cadherin sequences that inhibit beta-catenin signaling: a study in yeast and mammalian cells." Mol Biol Cell **12**(4): 1177-1188.

Staal, F. J., *et al.,* (2002). "Wnt signals are transmitted through N-terminally dephosphorylated beta-catenin." EMBO R **3**: 63-68.

Stamos, J. L. and W. I. Weis (2013). "The β-catenin Destruction Complex." Cold Spring Harbor Perspectives in Biology **5**(1).

Su, Y., *et al.,* (2008). "APC is essential for targeting phosphorylated beta-catenin to the SCFbeta-TrCP ubiquitin ligase." Mol Cell **32**: 652-661.

Taelman, V. F. (2010). "Wnt signaling requires sequestration of glycogen synthase kinase 3 inside multivesicular endosomes." Cell **143**: 1136-1148.

Takacs, C. M., *et al.,* (2008). "Dual positive and negative regulation of wingless signaling by adenomatous polyposis coli." Science **319**(5861): 333-336.

Tamai, K. (2000). "LDL-receptor-related proteins in Wnt signal transduction." Nature **407**: 530-535.

Tan, C. W., *et al.,* (2012). "Wnt signalling pathway parameters for mammalian cells." PLoS ONE **7**(2): e31882.

Tauriello, D. V. and M. M. Maurice (2010). "The various roles of ubiquitin in Wnt pathway regulation." Cell Cycle **9**(18): 3700-3709.

Tolwinski, N. S., *et al.,* (2003). "Wg/Wnt signal can be transmitted through arrow/LRP5,6 and Axin independently of Zw3/GSK3beta activity." Dev Cell **4**(3): 407-418.

Tolwinski, N. S. and E. Wieschaus (2001). "Armadillo nuclear import is regulated by cytoplasmic anchor Axin and nuclear anchor dTCF/Pan." Development **128**(11): 2107-2117.

Townsley, F. M., *et al.,* (2004). "Pygopus and Legless target Armadillo/[beta]-catenin to the nucleus to enable its transcriptional co-activator function." Nature Cell Biol. **6**: 626-633.

Tran, H. and P. Polakis (2012). "Reversible modification of adenomatous polyposis coli (APC) with K63-linked polyubiquitin regulates the assembly and activity of the beta-catenin destruction complex." J Biol Chem **287**(34): 28552-28563.

Valvezan, A. J., *et al.,* (2012). "Adenomatous polyposis coli (APC) regulates multiple signaling pathways by enhancing glycogen synthase kinase-3 (GSK-3) activity." J Biol Chem **287**(6): 3823-3832.

van Amerongen, R. and A. Berns (2005). "Re-evaluating the role of Frat in Wnt-signal transduction." Cell Cycle **4**: 1065-1072.

van Amerongen, R., *et al.,* (2008). "Alternative wnt signaling is initiated by distinct receptors." Sci. Signal. **1**: re9.

van Amerongen, R., *et al.,* (2005). "Frat is dispensable for canonical Wnt signaling in mammals." Genes Dev **19**: 425-430.

Veeman, M. T., *et al.,* (2003). "A second canon. Functions and mechanisms of [beta]-catenin-independent Wnt signaling." Dev. Cell **5**: 367-377.

Wang L., Liu X., Gusev E., Wang C., Fagotto F. (2014). Regulation of β-catenin phosphorylation and nuclear/cytoplasmic transport by APC and its cancer-related truncated form. In process.

Wehrli, M. (2000). "Arrow encodes an LDL-receptor-related protein essential for Wingless signalling." Nature **407**: 527-530.

Wharton Jr, K. A. (2003). "Runnin' with the Dvl: proteins that associate with Dsh//Dvl and their significance to Wnt signal transduction." Dev Biol **253**: 1-17.

Wiechens, N., *et al.,* (2004). "Nucleo-cytoplasmic shuttling of Axin, a negative regulator of the Wnt-beta-catenin pathway." J Biol Chem **279**: 5263-5267.

Willert, K. (2003). "Wnt proteins are lipid-modified and can act as stem cell growth factors." Nature **423**: 448-452.

Willert, K., *et al.,* (1999). "Wnt-induced dephosphorylation of axin releases [beta]-catenin from the axin complex." Genes Dev. **13**: 1768-1773.

Winston, J. T., *et al.,* (1999). "The SCF[beta]-TRCP-ubiquitin ligase complex associates specifically with phosphorylated destruction motifs in I[kappa]B[alpha] and [beta]-catenin and stimulates I[kappa]B[alpha] ubiquitination *in vitro*." Genes Dev **13**: 270-283.

Wong, H. C. (2003). "Direct binding of the PDZ domain of Dishevelled to a conserved internal sequence in the C-terminal region of Frizzled." Mol. Cell **12**: 1251-1260.

Woodgett, J. R. (1992). "Finding the stepping stones downstream of Ras." Curr Biol **2**(7): 357-358.

Wu, D. and W. Pan (2010). "GSK3: a multifaceted kinase in Wnt signaling." Trends Biochem. Sci. **35**: 161-168.

Wu, G., *et al.,* (2009). "Inhibition of GSK3 phosphorylation of β-catenin via phosphorylated PPPSPXS motifs of Wnt coreceptor LRP6." PLoS ONE **4**: e4926.

Wu, G., *et al.,* (2003). "Structure of a beta-TrCP1-Skp1-beta-catenin complex: destruction motif binding and lysine specificity of the SCF(beta-TrCP1) ubiquitin ligase." Mol Cell **11**: 1445-1456.

Wu, X., *et al.,* (2008). "Rac1 activation controls nuclear localization of beta-catenin during canonical Wnt signaling." Cell **133**: 340-353.

Xing, Y., *et al.,* (2003). "Crystal structure of a [beta]-catenin//Axin complex suggests a mechanism for the [beta]-catenin Destruction complex." Genes Dev **17**: 2753-2764.

Xing, Y., *et al.,* (2004). "Crystal structure of a [beta]-catenin//APC complex reveals a critical role for APC phosphorylation in APC function." Mol Cell **15**: 523-533.

Yamamoto, H., *et al.,* (2001). "Inhibition of the Wnt signaling pathway by the PR61 subunit of protein phosphatase 2A." J Biol Chem **276**(29): 26875-26882.

Yamamoto, H., *et al.,* (1999). "Phosphorylation of axin, a Wnt signal negative regulator, by glycogen synthase kinase-3beta regulates its stability." J Biol Chem **274**: 10681-10684.

Yamamoto, H., *et al.,* (2006). "Caveolin is necessary for Wnt-3a-dependent internalization of LRP6 and accumulation of [beta]-catenin." Dev. Cell **11**: 213-223.

Yamamoto, H., *et al.,* (2008). "Wnt3a and Dkk1 regulate distinct internalization pathways of LRP6 to tune the activation of [beta]-catenin signaling." Dev. Cell **15**: 37-48.

Yang-Snyder, J., *et al.,* (1996). "A Frizzled homolog functions in a vertebrate Wnt signaling pathway." Curr. Biol. **6**: 1302-1306.

Yang, J., *et al.,* (2003). "PP2A:B56[epsiv] is required for Wnt//[beta]-catenin signaling during embryonic development." Development **130**: 5569-5578.

Yang, J., *et al.,* (2006). "Adenomatous Polyposis Coli (APC) differentially regulates

[beta]-catenin phosphorylation and ubiquitination in colon cancer cells." J Biol Chem **281**: 17751-17757.

Yokoya, F., *et al.,* (1999). "Beta-catenin can be transported into the nucleus in a Ran-unassisted manner." Mol Biol Cell **10**: 1119-1131.

Yost, C., *et al.,* (1998). "GBP, an inhibitor of GSK-3, is implicated in *Xenopus* development and oncogenesis." Cell **93**: 1031-1041.

Zeng, L., *et al.,* (1997). "The mouse Fused locus encodes Axin, an inhibitor of the Wnt signaling pathway that regulates embryonic axis formation." Cell **90**: 181-192.

Zeng, X. (2008). "Initiation of Wnt signaling: control of Wnt coreceptor Lrp6 phosphorylation/activation via Frizzled, Dishevelled and Axin functions." Development **135**: 367-375.

Zeng, X., *et al.,* (2005). "A dual-kinase mechanism for Wnt co-receptor phosphorylation and activation." Nature **438**: 873-877.

Bridge to Chapter II

Our lab has started to separate subcellular β-catenin/ Axin pools by cell fractionation (Sucrose gradient, more details will be discussed in Chapter III). Several pools of Axin/β-catenin were detected, but each of them corresponded to mixtures of several cellular compartments, in particular, the heaviest fractions which could be nuclear Axin/β-catenin cosedimented with receptor LRP6. The sedimentation of LRP6 may represent a pool of membranes associated with cytoskeleton—which we called "Heavy plasma membranes". However, the association between Axin/ β-catenin and membranes or nuclei in the pellet became ambiguous, and I found none of the existing protocols could separate these pools satisfactorily. To analyze the Axin/ β-catenin pools, we have to establish another protocol to separate nuclei from the "heavy membranes". With this protocol, we should be able to isolate relevant Axin/β-catenin pools, analyze their biochemical nature and their interacting partners.

In Chapter II, I describe the new protocol that provides rapid separation of cytosolic, nucleosolic, nuclear insoluble and membrane components in a variety of mammalian cell lines. It is suitable for parallel analysis and quantitative comparison of multiple experimental conditions. Chapter II is a reproduction of the following published article: **X. Liu**, F. Fagotto, A method to separate nuclear, cytosolic, and membrane -associated signaling molecules in cultured cells. Science Signaling 4, pl2 (2011).

CHAPTER II

A Method to Separate Nuclear, Cytosolic, and Membrane-Associated Signaling Molecules in Cultured Cells

Abstract

Direct comparison of protein distribution between the nucleus, the cytoplasm, and the plasma membrane is important for understanding cellular processes and, in particular, signal transduction, where cascades generated at the cell surface regulate functions in other cellular compartments, such as the nucleus. Yet, many commonly used methods fail to effectively separate the plasma membrane and the cytoskeleton from the nucleus, and the cytosol from the nucleosol. This problem has led to confounding results in the study of signaling pathways due to incorrect assignment of cellular localization to signaling molecules and presents challenges in the biochemical study of soluble proteins that shuttle between the cytoplasm and the nucleus. We present a simple method, based on partial membrane permeabilization with detergent followed by density gradient centrifugation, which provides rapid separation of cytosolic, nucleosolic, nuclear insoluble, and membrane components in various mammalian cell lines.

Introduction

Much of the knowledge regarding the composition and function of cellular structures and organelles has resulted from the development of cell fractionation protocols. The most sophisticated methods can yield pure subcompartments of these organelles (1-3). Coupled to proteomics, they enable a full description of organellar protein composition (4-6). These "specialized" protocols typically focus on one or a few compartments at a time (5, 7, 8).

Cruder fractionation protocols, however, are also routinely used to study the subcellular distribution of components of interest, to compare the abundance and properties of the molecules in various locations, to monitor shifts from one compartment to another, or to assess both of these attributes. These questions are especially pertinent to the field of signal transduction, where intra- or extracellular

stimuli trigger complex cascades that propagate through the cell, often leading to translocation of downstream effectors into the nucleus [for example, the transcriptional regulators β-catenin (9, 10), STAT (11), and Smads (12), or the kinase ERK (13)].

Studies of subcellular localization by fractionation are often plagued by insufficient characterization of the cellular fractions. For example, nuclear fractions are frequently only checked for the absence of cytosolic markers and not for contamination by plasma membranes or for other insoluble components (14-16). Evaluation of cytoskeletal elements is particularly problematic: Tubulin, used often as a general "cytoplasmic marker", is inappropriate to monitor the cytoskeleton in cell homogenates, because microtubules depolymerize in the cold (17). Actin can also be found in the nucleus (18). Analysis of the nuclear components is similarly incomplete: The standard nuclear markers, histones and lamins, only represent the insoluble nuclear material (chromatin and nuclear lamina), and the nucleosol is virtually never monitored (19-21).

We tested five common fractionation methods and found that all of these protocols resulted in nuclear fractions that were contaminated with plasma membrane components, and that the nucleosolic components were lost from the nuclear fraction and were instead detected in the cytosolic fraction. Therefore, we developed a method to effectively separate the cytosol and the nucleosol and separate nuclei from membrane and cytoskeletal components. To validate our protocol, we used a large number of markers representing the major cellular components.

The aim of this protocol is to separate membranes, nuclei, and cytosol, with minimal loss from each fraction, in order to obtain a global view of subcellular distribution. To circumvent the "leakiness" of the nuclei during mechanical homogenization and obtain a bona fide nucleosolic fraction, the cytosol is extracted before performing cellular disruption. For this purpose, we use a well-established method in which the plasma membrane is semipermeabilized with digitonin (16, 22-24), a steroid glycoside that interacts specifically with 3β-hydroxysterols. Internal

membranes, which are poor in cholesterol, are left intact, and nuclear membranes remain functional for selective nuclear transport (22). Once the cytosol has been extracted, we release the nucleosol from the nuclei through mechanical homogenization and then recover the nucleosol by centrifugation as a soluble fraction that is free of cytosolic contaminants.

The remaining insoluble fraction contains the nucleosol-depleted nuclei, all the cellular membranes, and the cytoskeleton. A major problem in isolation of plasma membranes is its dispersion into fragments of variable size and density after homogenization with standard fractionation methods, and this cannot be overcome solely through detergent solubilization. Our method maintains plasma membranes in a single sedimentable fraction after digitonin treatment and mechanical homogenization; the membranes do not burst, because the cells are already permeabilized. We then add detergent to separate the nuclei from other membrane components during the subsequent density gradient centrifugation, using conditions under which membrane proteins, irrespective of their solubility in the detergent Triton X-100, remain clustered in the gradient and are recovered well separated from the insoluble nuclear components.

In summary, our strategy involves semipermeabilization of intact cells to extract the cytosol, cell homogenization and nucleosolic extraction, and flotation of the insoluble fraction to separate insoluble nuclear components from membranes and cytoskeletal elements (Fig. 1). Although the protocol was originally established for mouse fibroblast L cells, we have achieved effective cellular fractionation with multiple cell lines, including human embryonic kidney (HEK) 293 cells, HeLa cells, breast cancer MCF-7 cells, and intestinal Caco-2 cells.

Materials

Reagents

Aprotinin (A-1153, Sigma)

Benzamidine (B6506, Sigma)

Digitonin (300410, Calbiochem)

Dithiothreitol (DTT, 15508-013, Invitrogen)

Immobilon Western reagent (WBKLS0500, Millipore).

Iodacetamide (I1149, Sigma)

Leupeptin (L2884, Sigma)

Nitrocellulose membranes (0.45-µm pores, 162-0097, Bio-Rad)

Percoll (17-0891-02, GE Healthcare).

PBS: Dulbecco's phosphate-buffered saline, 1x with Ca^{2+} and Mg^{2+} (14040, Gibco)

Phenylmethanesulfonyl fluoride (PMSF, P-7626, Sigma)

Soybean trypsin inhibitor (T-9003, Sigma)

Nα-Tosyl-L-lysine chloromethyl ketone hydrochloride (TLCK, 90182, Sigma)

Triton X-100 (BP151, Fisher)

Western Blot Blocking Buffer (10x stock, B6429, Sigma)

All other chemicals are standard and can be obtained from any of the major suppliers.

Antibodies

Mouse anti-actin (AC-15, Sigma)

Mouse anti-α-actinin (AG6070, Biomol)

Mouse anti-Pan-cadherin (CH-19, C1821, Sigma)

Mouse anti-Calnexin (270-390-2, Developmental Studies Hybridoma Bank, Iowa City, IA)

Rabbit anti-Caveolin-1 (N-20, sc-894, Santa Cruz Biotechnology)

Rabbit anti-EEA1 (ab2900, Abcam)

Mouse anti-ERK2 (610103, BD Biosciences)

Mouse anti-phospho-ERK (ERK1+ERK2, phospho T183+Y185, ab50011, Abcam)

Rabbit anti-Flotillin (3253S, Cell Signaling Technology)

Mouse anti-GAPDH (6C5, AM4300, Applied Biosystems)

Mouse anti-Golgin97 (A-21270, Invitrogen).

Rabbit anti-Histone H4 (ab10158, Abcam)

Rabbit anti-Lamin B1(ab16048, Abcam)

Mouse anti-Lamp1 (1D4B, Developmental Studies Hybridoma Bank, Iowa City, IA)

Mouse anti-LRP6 (C-10, sc-25317, Santa Cruz Biotechnology)

Rabbit anti-phospho-LRP6 (Ser1490, ab76417, Cell Signaling Technology)

Mouse anti-RanBP3 (612050, BD Biosciences)

Rabbit anti-TCF4 (H125, sc-13027, Santa Cruz Biotechnology)

Rabbit anti-Tom20 (a gift from G. C. Shore, McGill University)

Goat anti-γ-Tubulin (C-20, sc-7396, Santa Cruz Biotechnology)

Horse radish peroxidase (HRP)-conjugated secondary antibodies: donkey anti-mouse (715-035-150), donkey anti-rabbit (711-035-152), donkey anti-goat (705-035-147) (Jackson ImmunoResearch)

Cell Lines

Caco-2 (human epithelial colorectal adenocarcinoma) cells

HEK293 (human embryonic kidney) cells

HeLa cells

Mouse fibroblast L cells

Note: The above cell lines were obtained from American Type Culture Collection, were maintained in Dulbecco's modified Eagle's medium (DMEM, 11965, Gibco) supplemented with 10% fetal bovine serum (FBS, 12483, Gibco), and were grown just to confluence.

MCF-7 (mammalian breast cancer) cells

Note: These cells (a gift from N. Lamarche-Vane, McGill University) were maintained in DMEM supplemented with 10% FBS and were grown just to confluence.

Equipment

Tight-fitted Dounce homogenizer (06-434, Fisher).

Standard fixed angle tabletop centrifuge (either refrigerated or placed in a 4 ℃ room or cabinet)

Refrigerated clinical centrifuge (equipped with swing-out rotor and adaptors for 10- to 15-ml tubes)

Sonicator (Sonic Dismembrator Model 500, Fisher) with a 0.125 microtip.

Beckman Optima tabletop ultracentrifuge with the following rotors: MLS50 (swing-out) and TLA100.1 and TLA100.3 (both fixed angle) and the appropriate adaptors for 1.5-ml tubes (MLS50 and TLA100.3) or 0.5-ml tubes (TLA100.1)

Note: An ultracentrifuge is only required to obtain clean nucleosol and for Percoll removal, which are optional steps, depending on the cellular fractions desired.

1.5-ml microfuge tubes

Note: All tubes should be made of low protein binding material (polypropylene, polyallomer, or polycarbonate). Unless otherwise stated (that is, for ultracentrifugation), standard polypropylene microfuge tubes are used.

1.5-ml ultracentrifuge microfuge tube [polyallomer 1.5-ml tubes (357448, Beckman Coulter)]

0.5-ml ultracentrifuge tubes [thick-walled, polycarbonate, 0.5-ml tubes (353776, Beckman Coulter)]

10- to 15-ml centrifuge tubes with a 13- to 16-mm diameter (Sarstedt 13-ml polypropylene tubes)

Recipes

Recipe 1: Protease Inhibitor Cocktail 1 (500x)

Prepare a 50 mM PMSF, 0.1 mg/ml TLCK solution in isopropanol.

Note: Store at -20 ℃. PMSF is unstable in water (half-life 30 min) and should be added to the buffers just before use.

Recipe 2: Protease Inhibitor Cocktail 2 (500x)

Prepare a 1 mg/ml leupeptin, 2 mg/ml aprotinin, 0.2 M benzamidine, 0.5 mg/ml soybean trypsin inhibitor, 0.25 M iodacetamide solution in double-distilled H_2O.

Note: Store at -20 ℃. May be substituted with commercially available ready-to-use protease inhibitor mixes.

Recipe 3: 0.5 M EDTA

Prepare EDTA as a 0.5 M stock solution titrated to pH 8.0 with NaOH.

Note: EDTA is not soluble at such concentration at lower pH.

Recipe 4: 10x NEH Buffer

Prepare a solution of 1500 mM NaCl, 2 mM EDTA, 200 mM Hepes-NaOH at pH 7.4. Dilute with distilled H2O to make 1x NEH.

Recipe 5: Digitonin Solution

Prepare a solution of 42 μg/ml digitonin, 2 mM DTT, 2 mM $MgCl_2$ in 1x NEH buffer (Recipe 4). Always prepare freshly just before use.

Note: Commercial digitonin powder is impure and should be purified by recrystallization in ethanol according to supplier's instructions. Crystallized, dried digitonin can be stored in sealed tubes at room temperature. We obtained similar results with digitonin solutions ranging from 35 to 45 µg /ml digitonin.

Recipe 6: Low Salt Homogenization Buffer

Prepare a solution of 20 mM Hepes-NaOH (pH 7.4), 0.2 mM EDTA (Recipe 3). Add Protease Inhibitor Cocktails 1 and 2 (Recipe 1 and 2) just before use.

Recipe 7: High Salt Homogenization Buffer

Prepare a solution of 300 mM NaCl, 200 mM Hepes-NaOH (pH 7.4), 0.2 mM EDTA (Recipe 3). Add 1 mM DTT and Protease Inhibitor Cocktails 1 and 2 (Recipe 1 and 2) just before use.

Recipe 8: Percoll Gradient Solutions

Prepare 35, 55, 70, 80, and 85% (vol/vol) Percoll solutions by combining pure Percoll with 1x NEH supplemented with 0.6% (wt/vol) Triton X-100. For example, for 35% Percoll, mix 3.5 parts of 100% Percoll with 6.2 parts of 1x NEH and 0.3 parts of 20% (wt/vol) Triton X-100.

Note: This is an unorthodox way to prepare Percoll solutions and will produce a Percoll gradient with an opposite gradient of salt: high NaCl in the light fractions, low NaCl in the heavy fractions. These special salt conditions are crucial for successful separation. When a high salt concentration (150 mM NaCl) is used all along the gradient, nuclei do not float and overlap with membranes. When a low salt concentration is used throughout the gradient, nuclei float to the very top of the gradient (fraction 1), but γ-tubulin is then not restricted to the heaviest fraction 11 (fraction "X") and partially overlaps with the membrane fraction.

Recipe 8: 4x Laemmli Sample Buffer

Prepare a solution of 0.2 M Tris-HCl (pH 6.8), 8% SDS, 40% glycerol, 0.004% bromphenol blue, and 40 mM DTT.

Recipe 9: HRP Inactivation Solution

Prepare a solution of 0.02 to 0.05% sodium azide in PBS. Store at room temperature.

Instructions

Data from a representative experiment with L cells show the presence of subcellular compartment markers in the various fractions (Fig. 2). The amounts and volumes listed are for processing a 10-cm (diameter) dish of confluent adherent cells. One should avoid using overconfluent cells, because not only can their physiology be affected, but also they may not be optimally permeabilized. The protocol can be further scaled up with a proportionate increase of reagents and buffers. However, it is then important to maintain for all centrifugation steps the same length of the sedimentation path (and thus the height of the liquid column). Thus, to process larger volumes of sample, we recommend using wider centrifuge tubes of the same length as those used here, or splitting the samples in several tubes and centrifuging them in parallel. Otherwise, centrifugation times must be adjusted for tubes of a different length.

Additionally, a minimal volume of Digitonin Solution (Recipe 5) is required to ensure that the amount of digitonin does not become limiting relative to the amount of membranes. We have experimentally determined that the ratio between the volume of the Digitonin Solution and the surface area of the cell culture dish must be maintained above 2 ml per 55 cm^2 of confluent cells (100-mm-diameter dish or ~5 x 10^6 cells). Some cell lines may require higher ratios of Digitonin Solution to cells.

All steps up to addition of sample buffer for SDS polyacrylamide gel electrophoresis (PAGE) should be performed at 4 ℃. Solutions, tubes, and homogenizer should be precooled to 4 ℃.

Digitonin Semipermeabilization

1. Remove the medium and quickly wash cells with 5 to 10 ml of ice-cold PBS, thoroughly removing the PBS.

2. Add 3 ml of Digitonin Solution (Recipe 5) to the dish and gently shake it at 100 rpm for 10 min on an orbital shaker at 4 ℃.

Note: It is essential to perform the permeabilization at 4 ℃. Substantial amounts of membrane materials may be extracted at higher temperatures.

3. Remove the digitonin-solubilized material and save it in a 15-ml polypropylene tube as sample D (Fig. 2), the "cytosolic fraction."

4. Quickly wash the remaining cellular material with 5 to 10 ml of cold PBS, thoroughly removing and discarding the PBS.

Note: This wash removes residual traces of cytosol.

Harvesting and Homogenization

1. Add 150 to 250 µl of Low Salt Homogenization Buffer (Recipe 6), scrape, and collect in a 1.5-ml microfuge tube.

2. Add another 150 to 250 µl of Low Salt Homogenization Buffer (Recipe 6) to the dish, scrape again, and pool with the first fraction.

3. Incubate on ice for 5 min, and then pass 50 strokes with a tight-fitted Dounce homogenizer.

Note: For some cell types (such as epithelial cells), more strokes may be needed to release the nucleosol. Alternatively, give a short pulse (5 to 10 s) of mild sonication before Dounce homogenization.

4. Add an equal volume (~300 to 500 µl) of High Salt Homogenization Buffer (Recipe 7) in the homogenizer, followed by 50 additional strokes.

5. Reserve 90 µl of the cell homogenate in one tube as sample T (Fig. 2), the "total" fraction, for later analysis.

6. Transfer the remaining cell homogenate to a 1.5-ml microfuge tube.

7. Centrifuge the cell homogenate at 1000g for 10 min (regular tabletop centrifuge).

Note: The pellet is processed in the section called "Separation of Nuclei and Membranes by Flotation" and the supernatant is processed in the next section, "Preparation of Nucleosolic Fraction."

Preparation of Nucleosolic Fraction

1. Reserve 90 µl of the supernatant (from step 7 in the previous section) in a 1.5-ml microfuge tube as sample s1 (Fig. 2), the "1000g supernatant" fraction.

2. Collect the remaining supernatant into a 1.5-ml polyallomer ultracentrifuge microfuge tube.

3. Centrifuge at 80,000g for 30 min in a fixed-angle rotor, Beckman TLA100.3.

4. Collect the supernatant in a 1.5-ml microfuge tube as sample s2 (Fig. 2), the "80,000g supernatant", which is the nucleosolic fraction.

5. Resuspend the pellet in a volume equal to the supernatant (~750 µl) of 1xNEH Buffer (Recipe 4) as sample p2 (Fig. 2), the "80,000g pellet" fraction.

Note: This fraction contains mainly small amounts of various membrane markers.

Separation of Nuclei and Membranes by Flotation

1. Resuspend the pellet of the 1000g centrifugation with 1 ml of 85% Percoll (Recipe 8). Note: This is the pellet from step 7 of the section "Harvesting and Homogenization."

2. Reserve 90 µl in another 1.5-ml microfuge tube as sample p1 (Fig. 2), the "1000g pellet" fraction.

3. Transfer the remaining resuspended pellet (~900 µl) to a 10- to 15-ml centrifuge tube.

4. Prepare a discontinuous gradient on top of this fraction by successively laying four 900-µl layers of Percoll of the following decreasing concentrations: 80, 70, 55, and 35%.

5. Centrifuge the gradient in a swing-out rotor for 2 hours at 1000g.

6. Collect ten 450-µl fractions from the top by carefully pipetting out each fraction successively and placing each fraction in a 1.5-ml microfuge tube. These fractions represent samples 2 through 10 in Fig. 2.

Note: Fraction 1 is discarded, as it does not contain any detectable trace of markers. The pellet in the bottom of the tube should not be disturbed as the 10 fractions are removed.

7. Resuspend the pellet in 450 µl of 1x NEH (Recipe 6) as sample 11 (Fig. 2), "fraction X."

Percoll Removal

We routinely remove the Percoll from these fractions by ultracentrifugation. If an ultracentrifuge is not available and fractions will only be used for analysis by Western blot, it is also possible to process the samples without removing the Percoll.

1. Transfer the Percoll gradient fractions to 0.5- to 1.5-ml ultracentrifuge tubes and centrifuge in a swing-out rotor at 100,000g for 2 hours or in a fixed-angle rotor at 100,000g for 90 min.

Note: The Percoll will form a stone-hard pellet. The soluble biological material will be recovered in the supernatant, and the insoluble material will form a thin visible layer just on top of the Percoll pellet.

2. Resuspend the insoluble material by gently pipetting with a 200- µl pipette tip. Transfer the whole biological material (soluble + insoluble) of each fraction to a fresh 1.5-ml microfuge tube.

3. Pool the nuclear (fractions 2 through 5) and membrane (fractions 7 through 10) fractions.

Preparation of Samples for Western Blotting

1. Add 1:3 volume of 4x Laemmli sample buffer.

2. Boil at 95 ℃ for 3 to 5 min.

3. Centrifuge at 16,000g for 20 min.

Note: This centrifugation removes traces of Percoll. For direct gel loading, avoid pipetting the bottom of the tube, or first transfer samples to fresh tubes. Shorter centrifugation (5 min) is sufficient for cytosolic and nucleosolic fractions.

3. Sonicate the samples from Percoll gradient fractions, using a thin probe, dipped as deeply as possible without touching the bottom of the tube, with three 5-s bursts (15% amplitude) separated by 1-min periods of cooling on ice.

Note: This step is optional. However, sonication of the samples containing insoluble material before loading on the gel prevents streaking of some proteins in the gel. Sonication should be performed with the amplitude set to the highest level that does not cause foaming. Amplitude and time have to be adjusted for each model.

Western Blot

To verify the composition of each fraction, aliquots are separated by standard SDS-PAGE, transferred to a nitrocellulose membrane, and exposed to antibodies that recognize the specific markers of the various compartments (Table 1). We typically use a 10% acrylamide gel for minimal validation (GAPDH, RanBP3, lamin, cadherin, α-actinin, and γ-tubulin). Large proteins, such as LRP6, can be efficiently separated only in≤8% acrylamide gels, whereas histones can only be separated in high (>13%)

acrylamide gels. We typically cut the membrane horizontally in two pieces and simultaneously blot the piece with the high molecular weight portion for one high molecular size marker (for example, RanBP3) and the piece with the low molecular weight portion for an appropriately sized marker (for example, GAPDH).

1. Separate 20 to 40 µl of each sample by SDS-PAGE.

2. Transfer to nitrocellulose membrane.

3. Incubate the membranes for 3 to 16 hours in 1x Blocking Buffer with primary antibodies (Table 1).

4. Wash the membrane three times for 15 min in PBS with 0.1% Triton X-100.

5. Incubate the membrane with the appropriate HRP-conjugated secondary antibodies.

6. Visualize HRP activity by chemoluminescence according to the manufacturer's recommendations.

7. Inactivate HRP by incubating the membrane for 30 min or longer in HRP Inactivation Solution (Recipe 9) and reblot with another primary antibody from another species.

Note: With an appropriate sequence of antibodies and the use of secondary antibodies of donkey origin, the same membrane can be probed sequentially for three markers (for example, rabbit anti-lamin, mouse anti-GAPDH, and goat anti-γ-tubulin).

Notes and Remarks

Validation of the Semipermeabilization Step

This protocol was established by systematically titrating the digitonin concentration and volumes to determine the range that produced complete release of the detectable cytosolic content (GAPDH), while retaining all other components, in particular the nucleosolic (RanBP3) and plasma membrane proteins. Although the protocol works over a range of concentrations (35 to 45 µg/ml digitonin), the volume of Digitonin

Solution is equally important. If the volume is too small, the plasma membrane will not be sufficiently permeabilized, because at these very low volumes, the amounts (rather than the concentration) of digitonin becomes limiting relative to the amounts of membranes. Thus, the minimal volume of Digitonin Solution per surface of cells that works reproducibly for the cell lines tested is 2 ml per 55 cm^2 of confluent cells (100-mm-diameter dish or ~5 x 10^6 cells).

Considering the diversity of plasma membrane proteins and their distribution in different membrane domains with distinct biochemical properties, we evaluated the effect of digitonin treatment with various plasma membrane markers (Fig. 2). We tested a growth factor receptor (LRP6), adhesion molecules (cadherins), and markers of lipid microdomains (caveolin and flotilin). We confirmed the absence of plasma membrane protein extraction following digitonin semipermeabilization by monitoring total cell surface proteins labeled by biotinylation (Fig. 2B). We also screened markers for the following membrane-bound organelles: endoplasmic reticulum, Golgi, early endosomes, lysosomes, and mitochondria (Fig. 2A). We did not detect membrane proteins in the cytosolic fraction, indicating that the digitonin semi-permeabilization step did not extract membrane proteins. Because membrane proteins exhibit differential solubilization characteristics, we recommend that the fractions are validated for the specific proteins under investigation.

Homogenization and Nucleosol Release

Following a robust homogenization (25), the nucleosol can be readily isolated in the supernatant (s1 fraction) after low-speed centrifugation. All membrane and organelle markers sediment at this step (p1 fraction) (Fig. 2A). Some cell lines may require harsher homogenization or sonication for full release of the nucleosol. To exclude any contamination of the nucleosol by membrane components, we ultracentrifuged the low-speed supernatant and collected the resulting high-speed supernatant (s2) as the purified nucleosol. We have not detected more than trace amounts of membrane or organelle markers in either the s1 or s2 fractions. Thus, in practice, the supernatant from the first low-speed centrifugation can be used as the nucleosolic fraction.

Conditions for Separation of Nuclei from Membranes and Insoluble Cytoskeletal Proteins

Because of heterogeneity of the membranes and the overlap in size and density with nuclei, we found a very narrow range of conditions under which nuclei are well separated from all plasma membrane markers in a Percoll gradient (Fig. 2A). In addition to the gradient of Percoll, the salt concentration along the gradient, as well as the nature and concentration of the detergent, were important factors in achieving adequate separation.

The distribution of the various cellular components in the Percoll gradient is likely to result from a complex combination of multiple factors. Although many of the membrane and organelle components can be solubilized by Triton X-100, some membrane components are Triton-insoluble, either because they are associated with cytoskeletal components or because they are associated with Triton X-100-resistant lipid domains (26-28). We found that, in addition to the cytoskeleton-associated components, all membrane markers remained in the dense part of the gradient. These included caveolin and flotilin, reported to localize in lipid rafts or detergent-insoluble membranes (28, 29), which were expected to float to the top of the Percoll gradient. Although we did not observe solubilization of integral or membrane-associated proteins and their appearance in the cytosolic fraction, digitonin permeabilization may have modified the properties of the membrane--in particular, cholesterol-rich domains--which may explain the unusual behavior of markers of lipid rafts. Unlike membrane components, chromatin and nuclear lamina appear to remain associated and float in the Percoll gradient. Flotation of nuclei appeared to depend on the low salt concentration used in the bottom of the gradient. We hypothesize that under these conditions, chromatin may at least partially decondense (30), thus increasing the buoyancy of the structure.

We found that all endomembrane markers (endoplasmic reticulum, Golgi, early endosomes, and lysosomes) tested cosedimented in the same dense fractions of the Percoll gradient with the plasma membrane markers (Fig. 2A). We observed a similar

distribution for mitochondria, although a small fraction floated on the top of the gradient. Markers of the actin cytoskeleton (actin and α-actinin) were also separated from the insoluble nuclear components (chromatin and lamin) and cosedimented with membrane markers. The protocol does not separate plasma membrane components from those associated with other membranes. However, cytoskeleton-associated components remained insoluble in the Percoll fractions. An additional centrifugation step may separate them easily from most other membrane components, which are largely solubilized due to the presence of detergent.

Fraction "X"

The bottom fraction of the gradient was positive for all markers--nuclear, membrane, and cytoplasmic (Fig. 2A). We thus considered it as a "debris fraction," likely containing aggregates from various sources. However, sedimentable γ-tubulin was specifically recovered there, identifying the presence of the centrosomes. Intermediate filaments (vimentin) were also enriched in this fraction.

Example of Application for the Study of Signal Transduction

We used activation and nuclear translocation of the related kinases ERK1 and 2 (ERK1/2) both to validate the selective retention of the nucleosol and to illustrate that the fractionation protocol is useful for monitoring proteins that exhibit nucleocytoplasmic redistribution. Upon stimulation of tyrosine kinase receptors or direct activation of protein kinase C (PKC) by the phorbol ester PMA, ERK becomes phosphorylated (P-ERK) and is imported into the nucleus. We chose ERK because of its relatively small size (35 kD), which would make it likely to diffuse rapidly out of leaky nuclei, thus providing a stringent criterion for nuclear integrity. Examination of P-ERK localization by immunofluorescence typically shows an increase in nuclear P-ERK signal and a weaker signal in the cytoplasm (Fig. 3, A and C), consistent with the multiple functions of this kinase in diverse cellular processes (13, 31-33). However, determining the relative amounts in the cytosol versus nucleosol on fixed samples is impossible, because a substantial fraction of soluble cytosolic proteins may

be lost during the permeabilization step following fixation (34). Our fractionation protocol showed that the nonnuclear P-ERK was predominantly in the soluble cytoplasmic fraction with less detected in the fraction containing membranes and cytoskeleton, both under resting conditions and in response to PMA stimulation (Fig. 3E). Incubation with PMA produced a strong increase of P-ERK in most compartments, including the nucleosol (Fig. 3E). The increase in P-ERK associated with the membrane fraction was similar to that in the nucleosolic fraction. We detected very little P-ERK in the insoluble nuclear fraction, consistent with P-ERK not interacting with chromatin (35).

The amounts that we observed in the cytosolic fraction (Fig. 3E) were not evident in the immunofluorescence images (Fig. 3, A and C), and the nucleosolic P-ERK pool detected by fractionation was surprisingly small. These results could not be explained by leakage from the nuclei during digitonin treatment. Immunofluorescence analysis of cells processed with and without digitonin semipermeabilization showed a decrease in the cytoplasmic P-ERK signal and retention of the nuclear signal after PMA stimulation in the digitonin-treated cells, confirming the effectiveness of semipermeabilization (Fig. 3, A to D). Quantification of three independent experiments showed that on average, 72 ±10% of the nuclear signal remained after digitonin semipermeabilization, which is notable considering that P-ERK is small enough to potentially diffuse passively through the nucleopore of intact nuclei (36). We conclude that the weaker cytoplasmic staining by immunofluorescence provides an inaccurate picture of P-ERK distribution, a notable example of the potential caveats when using immunofluorescence to study soluble proteins.

Related Techniques

Standard cell fractionation methods all include a low-speed (500g to 1500g) centrifugation after the initial homogenization step (5, 14, 15, 37). This first pellet is traditionally categorized as “nuclei plus cell debris,” because the presence of any nonnuclear protein is usually considered the result of unbroken cells. This nuclear

pellet may also contain mitochondria that "stick" to the nuclei (6, 7). The content of this pellet is not typically analyzed unless nuclei are the subject of the study.

Plasma membranes should remain in the "postnuclear supernatant" and may be subsequently separated from the cytosol and other cellular components by flotation in a density gradient, due to their high cholesterol content and thus low density. However, we found that a large portion of plasma membrane proteins remained in this first pellet, irrespective of the harshness of cell disruption (Fig. 4, A and B). We consistently observed that a substantial proportion exhibited a high-density sedimentation pattern (Fig. 4F). The appearance of plasma membrane in a high-density fraction may be due to its association with the "cortical cytoskeleton," a structure that is important for cell shape and motility (38-41), but so far this has not received sufficient attention in cell fractionation studies on cell signaling. Another method for subcellular fractionation is the NE-PER Nuclear and Cytoplasmic Extraction kit (Pierce), which is based on detergent extraction and is supposed to produce a "nuclear" and a "cytoplasmic" fraction. We found that the nuclear fractions were contaminated with plasma membrane markers (Fig. 4, C and D). A similarly poor separation has been reported for ProteoExtract, another commercial cell fractionation kit (42). Another published method (43) also exhibited failure to separate correctly the nuclei from membranes (Fig. 4E). With all methods, massive leakage of the nucleosolic marker RanBP3 was observed (Fig. 4, A to E).

Considering the caveats of previous methods, subcellular distribution of many signaling components needs to be revisited. This protocol should facilitate this goal. In addition, the fractions contain proteins or protein complexes in a native state and, thus, are compatible with further biochemical studies, such as analysis by immunoprecipitation or proteomics. The protocol may also be further extended to include, for instance, separation of chromatin-bound molecules from other nuclear insoluble components, isolation of centrosomes, or fractionation of membranes and membrane domains. Our experiments stress the importance of using proper markers for the various compartments of interest. Although in our hands, the protocol is robust

and highly reproducible, we recommend that key control markers should be routinely included in all experiments, the method should be validated for each cell line, and additional markers should be used according to the cellular process under investigation.

Figures

Figure 1. Cell fractionation strategy.

The cytosol is first extracted through plasma membrane semipermeabilization with digitonin. Cells are then homogenized and the nucleosol, which has leaked from the nuclei, is recovered by centrifugation. Insoluble nuclear components (chromatin and lamina) are then separated from membrane components and cytoskeletal elements by flotation on a density gradient after addition of Triton X-100. Fractions correspond to those in **Fig. 2**.

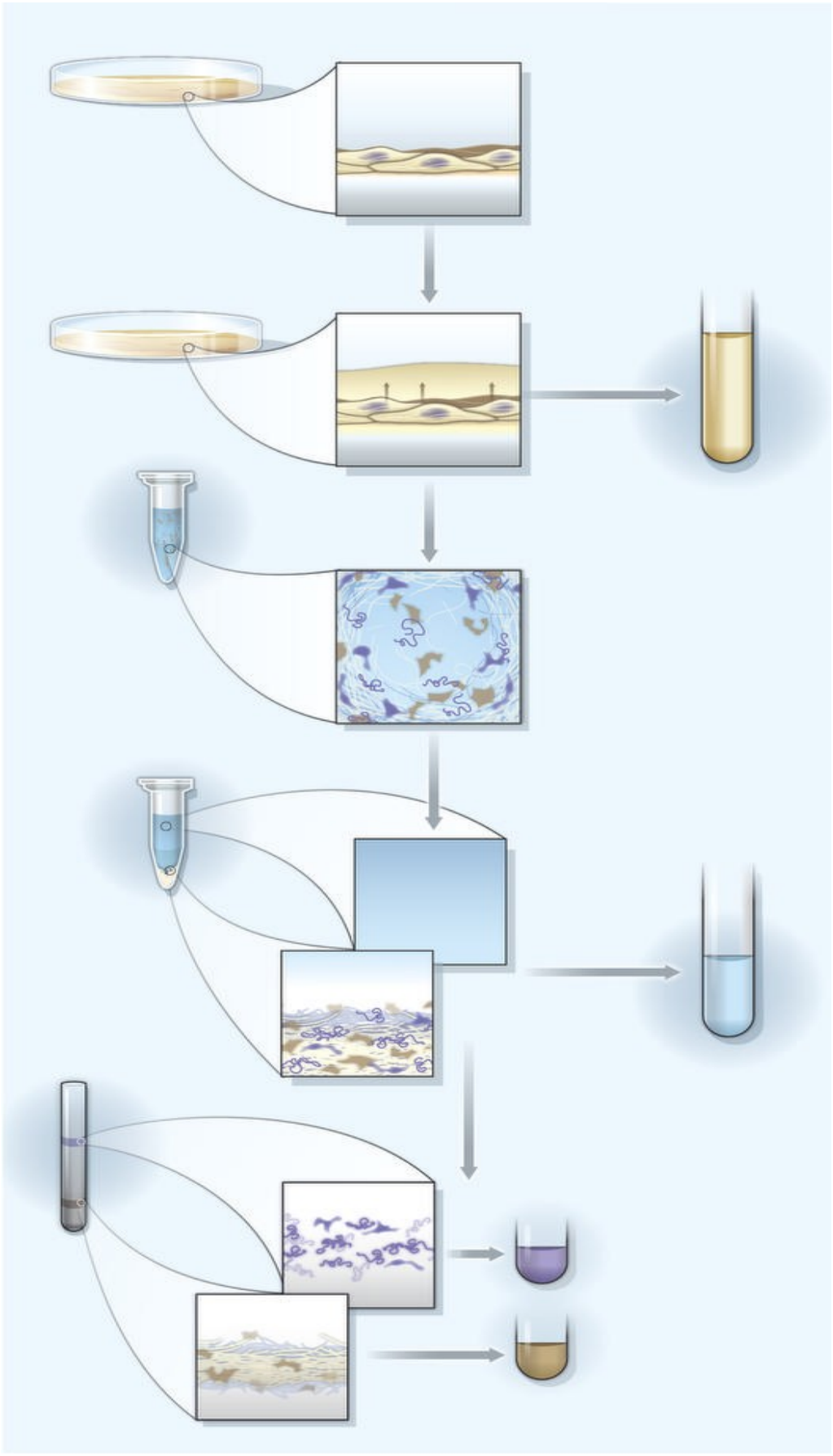

Figure. 2. Separation of cytosolic, nucleosolic, insoluble nuclear, and membrane components.

A. Western blot analysis of the various fractions from L cells. D, digitonin fraction; T, total homogenate after removal of digitonin fraction; s1 and p1, supernatant and pellet of the first 10-min 1000g centrifugation; s2 and p2, supernatant and pellet of the second 30-min 80,000g centrifugation; 2 to 11, fractions from the Percoll gradient. The lightest fraction 1 is not shown because it did not contain any detectable markers. Labels on top indicate the final cellular fractions: Cs, cytosol; Ns, nucleosol; Insol Nuc, insoluble nuclear material; Mbr/Ctk, membranes and actin cytoskeleton; X, centrosomes, cytoskeleton, and "debris." The following relative volumes of each fraction were loaded: D, T, p1, s1, p2, s2: 2%; fractions 2 to 11: 5%.

B. Total cell surface labeling, performed by biotinylation (0.5 mg/ml sulfo-NHS-biotin at 4 ℃ for 45 min). Biotinylated proteins in the various cellular fractions were detected on Western blot with neutravidin conjugated to peroxidase.

C. Fractionation of HEK293 cells. Cadherin adhesion molecules were detected with a pan-cadherin antibody raised against the highly conserved cytoplasmic tail (Pan-cad).

White lines indicate where parts of the same blot were cut and then reassembled for presentation.

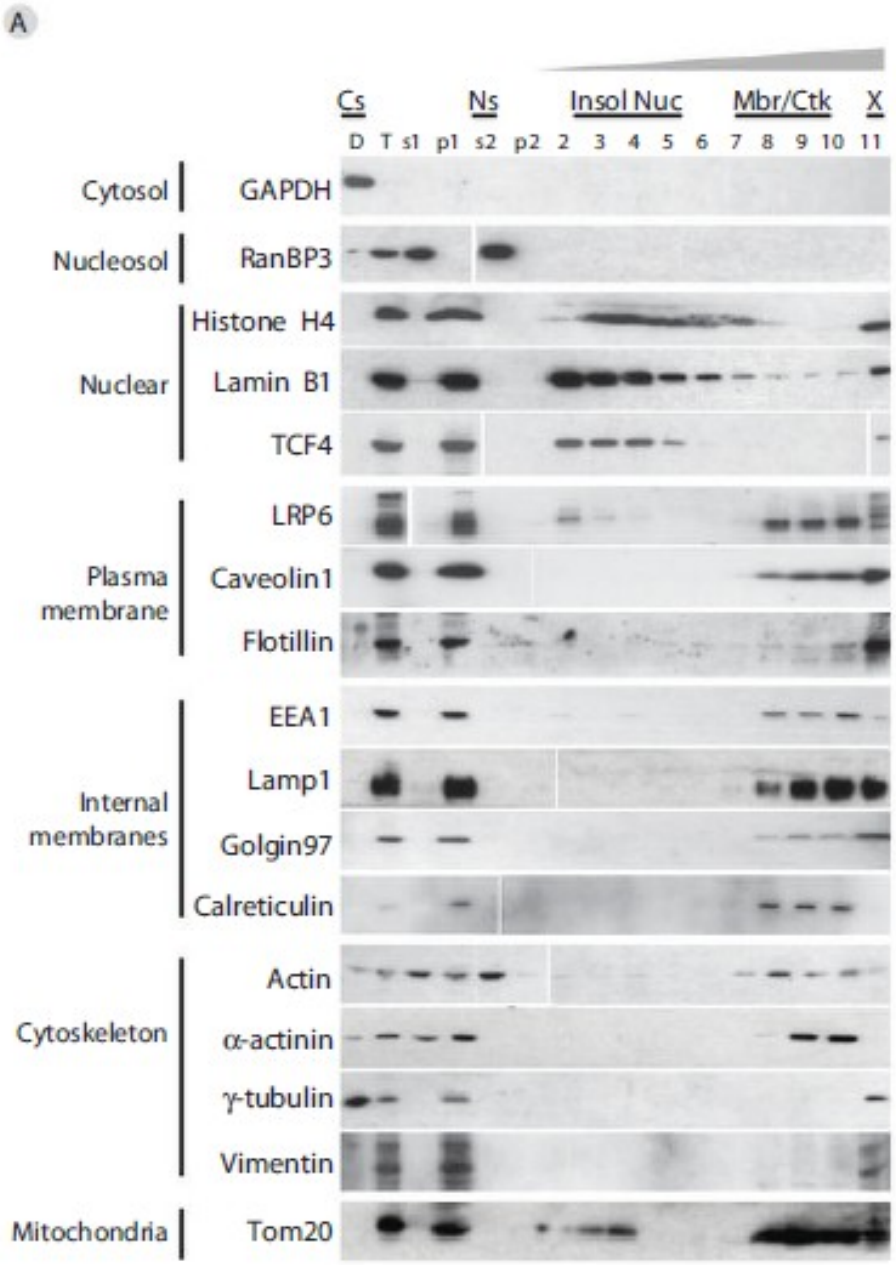
A
Cs
Ns
Insol Nuc
Mbr/Ctk
X
D T s1 p1 s2 p2 2 3 4 5 6 7 8 9 10 11
Cytosol
GAPDH
Nucleosol
RanBP3
Nuclear
Histone H4
Lamin B1
TCF4
Plasma membrane
LRP6
Caveolin1
Flotillin
Internal membranes
EEA1
Lamp1
Golgin97
Calreticulin
Cytoskeleton
Actin
α-actinin
γ-tubulin
Vimentin
Mitochondria
Tom20

B

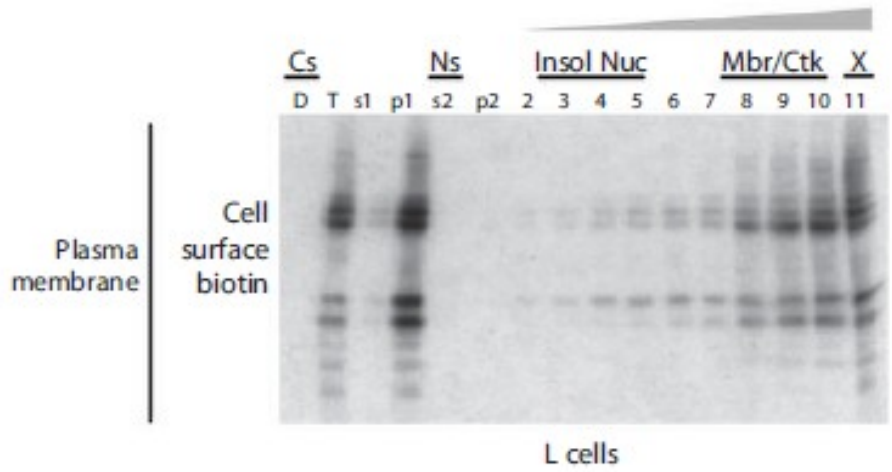

L cells

C

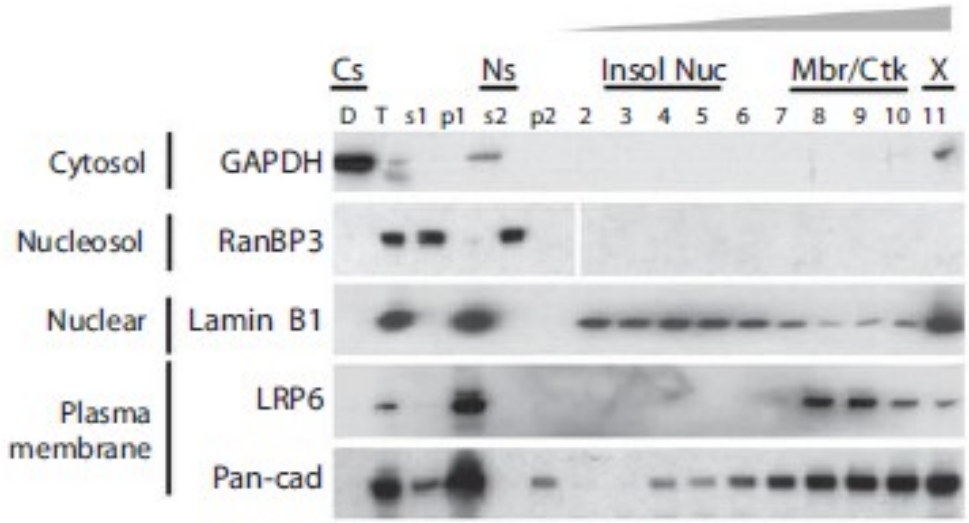

HEK293

Figure. 3. Example of application of the fractionation protocol: analysis of the subcellular distribution of activated ERK.

A–**D.** Nuclear P-ERK is preserved after digitonin semi-permeabilization. L cells were treated for 20 min with 50 ng/ml PMA. They were then either fixed directly in 4% paraformaldehyde (A) or first incubated with digitonin (B), as in the semipermeabilization step of the cell fractionation protocol, before fixation. Samples were immunolabeled with mouse anti-phospho-ERK1/2 antibody and goat Alexa488-conjugated anti-mouse secondary antibody. Arrows: nuclear P-ERK; arrowheads: cytoplasmic P-ERK. Pseudocolor display of the cells in (A) and (B) is shown (C and D). These images are representative of three independent experiments. Fluorescent intensity quantification indicated that 72 ± 10% of nuclear P-ERK was retained after digitonin permeabilization.

E. Western blot showing the subcellular distribution of P-ERK in untreated and PMA treated cells. P-ERK was detected with mouse anti-phospho-ERK1/2 antibody. Total ERK1/2 was detected with a mouse ERK2 antibody.

Cs, cytosol (fraction D in Fig. 2); T, total homogenate; S1, s1 fraction in Fig. 2; P1, p1 fraction in Fig. 2; Ns, nucleosol (fraction s2 in Fig. 2); P2, p2 fraction in Fig. 2; N, insoluble nuclear (fractions 2 through 5 in Fig. 2); M, membranes and cytoskeleton (fractions 7 through 10 in Fig. 2); X, centrosomes, cytoskeleton, and debris (fraction 11 in Fig. 2). The data shown are representative of three independent experiments.

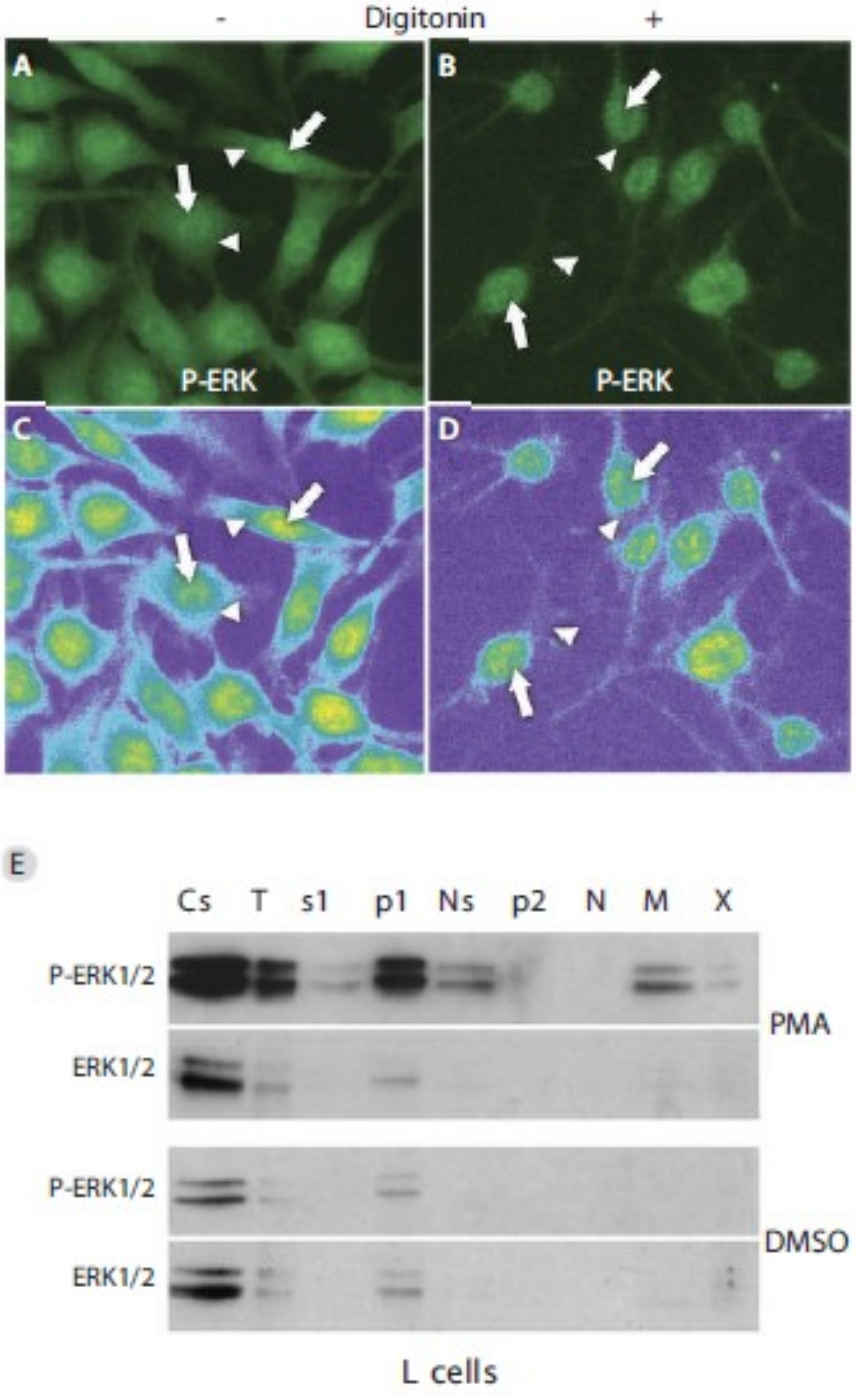
-
Digitonin
+
A
P-ERK
B
P-ERK
C
D
E
Cs
T
s1
p1
Ns
p2
N
M
X
P-ERK1/2
ERK1/2
PMA
P-ERK1/2
ERK1/2
DMSO
L cells

Figure 4. Commonly used cell fractionation methods fail to separate cytosol from nucleosol and plasma membranes from nuclei.

A and B. Differential centrifugation for preparation of "postnuclear" supernatant from mouse L cells (A) and MCF-7 cells (B). Cell homogenates were prepared by osmolysis and Dounce homogenization and then were centrifuged for 10 min at 100, 500, or 1000g, and the resulting supernatants (SN) and pellets (P) were analyzed by Western blot.

C and D. Fractionation samples obtained with the Pierce PER Nuclear and Cytoplasmic Extraction kit (PER kit) in L cells (C) and MCF-7 and HEK293 cells (D).
E. Fractionation samples obtained from HEK293 cells with a published method for separation of nuclei and cytoplasm (43).

F. Plasma membranes are dense and sediment with nuclei in a crude L cell homogenate, prepared by osmolysis and Dounce homogenization and separated on a 0.25 to 2.2 M sucrose discontinuous gradient centrifuged at 80,000g for 4 hours. See Table 1 for a list of the markers of the cellular compartments. Pan-cad, cadherins detected with a pan-cadherin antibody.

The data shown are representative of two to five independent experiments.

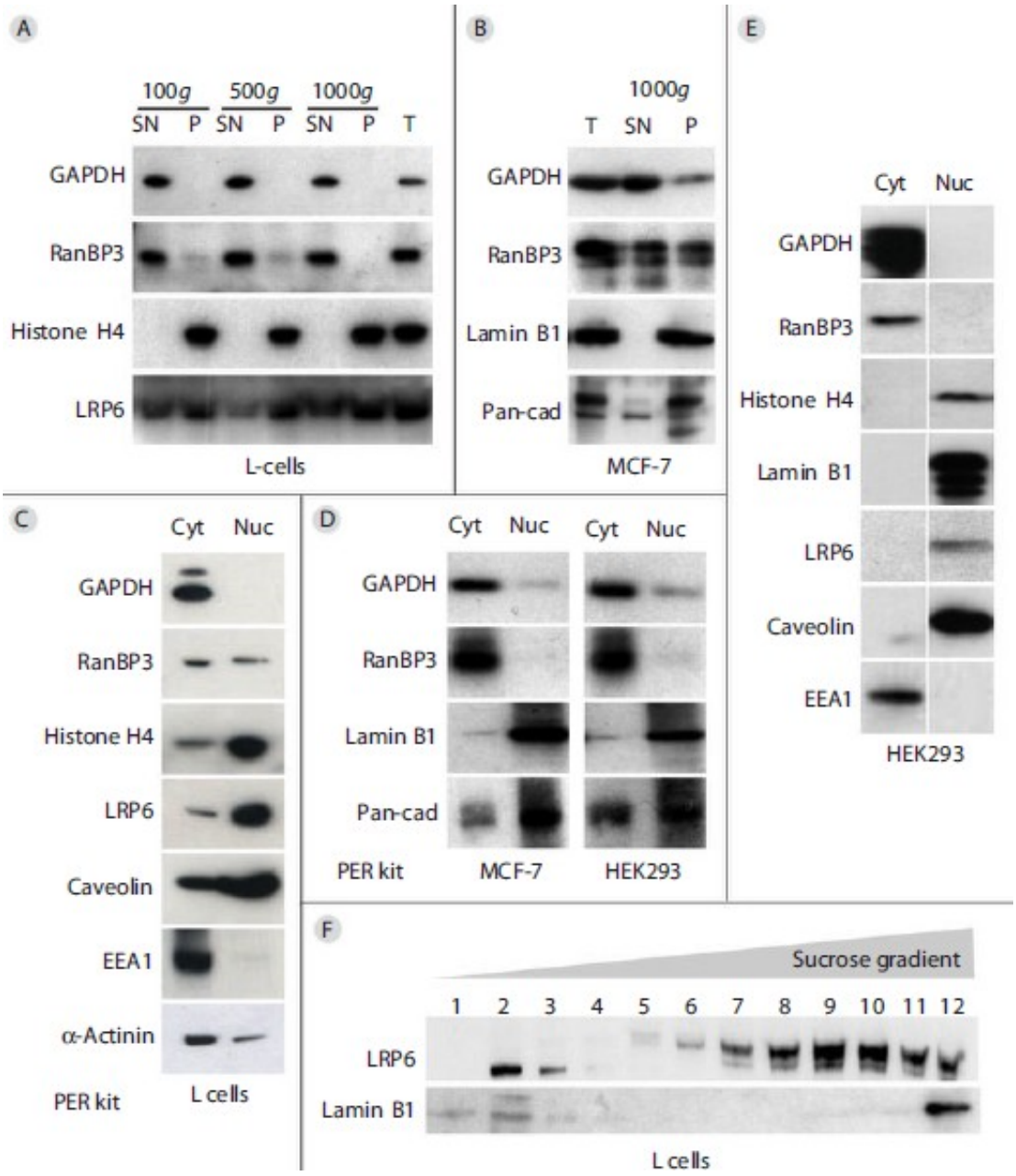
A
100g
500g
1000g
SN P SN P SN P T
GAPDH
RanBP3
Histone H4
LRP6
L-cells
B
1000g
T SN P
GAPDH
RanBP3
Lamin B1
Pan-cad
MCF-7
E
Cyt Nuc
GAPDH
RanBP3
Histone H4
Lamin B1
LRP6
Caveolin
EEA1
HEK293
C
Cyt Nuc
GAPDH
RanBP3
Histone H4
LRP6
Caveolin
EEA1
α-Actinin
PER kit
L cells
D
Cyt Nuc Cyt Nuc
GAPDH
RanBP3
Lamin B1
Pan-cad
PER kit
MCF-7
HEK293
F
Sucrose gradient
1 2 3 4 5 6 7 8 9 10 11 12
LRP6
Lamin B1
L cells

Table 1. Markers for subcellular compartments.

Compartment	Marker protein (antibody source)
Nucleus (insoluble)	Histone H4, 1:2500 (ab10158, Abcam); Lamin B1, 1:2000 (ab16048, Abcam); TCF4, 1:1000 (H125, sc-13027, Santa Cruz Biotechnology).
Nucleosol (nucleus soluble)	RanBP3, 1:1000 (612050, BD Biosciences).
Cytoskeleton (cytosol insoluble)	γ-Tubulin, 1:1000 (C-20, sc-7396, Santa Cruz Biotechnology); Actin, (AC-15, Sigma); Vimentin, 1:1000, (sc-373717, Santa Cruz Biotechnology); α-actinin, 1:1000 (AG6070, Biomol).
Cytosol	GAPDH, 1:5000 to 1:200,000 (6C5, AM4300, Applied Biosystems).
Plasma membrane	Caveolin, 1:2000 (N-20, sc-894, Santa Cruz Biotechnology); Cadherins, 1:5000 (CH-19, C1821, Sigma); LRP6, 1:300 (C-10, sc-25317, Santa Cruz Biotechnology); Serine-phosphorylated LRP6, 1:500 (ab76417, Cell Signaling Technology); Flotilin, 1:800 (3253S, Cell Signaling Technology).
Lysosome, late endosome	Lamp1, 1:100 (1D4B, Developmental Studies Hybridoma Bank, Iowa City, IA).
Early endosome	EEA1, 1:2000 (ab2900, Abcam).
Nucleocytosolic (shuttling protein)	Tyrosine-phosphorylated ERK 1 and 2, 1:1000 (ab50011, Abcam); ERK2, 1:2000 (610103, BD Biosciences).
Golgi	Golgin97, 1:500 (A-21270, Invitrogen).
Mitochondria	Tom20, 1:100 (a gift from G. C. Shore, McGill University).
Endoplasmic reticulum	Calreticulin, 1:500 (ab14234, Abcam); Calnexin, 1:1000 (sc-6465, Santa Cruz).

References

1. J. D. Castle, Purification of organelles from mammalian cells. Curr. Protoc. Immunol. Chapter 8 (1B), 8, 1B (2003).

2. F. Aniento, J. Gruenberg, Subcellular fractionation of tissue culture cells. Curr. Protoc. Immunol. Chapter 8 (1C), 8, 1C (2003).

3. D. M. Wong, K. Adeli, Microsomal proteomics. Methods Mol. Biol. 519, 273-89 (2009).

4. C. E. Au, A. W. Bell, A. Gilchrist, J. Hiding, T. Nilsson, J. J. Bergeron, Organellar proteomics to create the cell map. Curr. Opin. Cell Biol. 19, 376-85 (2007).

5. U. Michelsen, J. von Hagen, Isolation of subcellular organelles and structures. Methods Enzymol. 463, 305-28 (2009).

6. T. Stasyk, L. A. Huber, Zooming in: Fractionation strategies in proteomics. Proteomics 4, 3704-716 (2004).

7. L. A. Huber, K. Pfaller, I. Vietor, Organelle proteomics: Implications for subcellular fractionation in proteomics. Circ. Res. 92, 962-68 (2003).

8. P. G. Sadowski, A. J. Groen, P. Dupree, K. S. Lilley, Sub-cellular localization of membrane proteins. Proteomics 8, 3991-011 (2008).

9. C. Mosimann, G. Hausmann, K. Basler, Beta-catenin hits chromatin: Regulation of Wnt target gene activation. Nat. Rev. Mol. Cell Biol. 10, 276-86 (2009).

10. B. R. Henderson, F. Fagotto, The ins and outs of APC and beta-catenin nuclear transport. EMBO Rep. 3, 834-39 (2002).

11. D. S. Aaronson, C. M. Horvath, A road map for those who don 抉 know JAK-STAT. Science 296, 1653-655 (2002).

12. P. ten Dijke, C. S. Hill, New insights into TGF-beta-Smad signalling. Trends Biochem. Sci. 29, 265-73 (2004).

13. Y. Mebratu, Y. Tesfaigzi, How ERK1/2 activation controls cell proliferation and cell death: Is subcellular localization the answer? Cell Cycle 8, 1168-175 (2009).

14. B. Cox, A. Emili, Tissue subcellular fractionation and protein extraction for use in mass-spectrometry-based proteomics. Nat. Protoc. 1, 1872-878 (2006).

15. A. Essafi, A. R. Gomes, K. M. Pomeranz, A. K. Zwolinska, R. Varshochi, U. B. McGovern, E. W. Lam, Studying the subcellular localization and DNA-binding activity of FoxO transcription factors, downstream effectors of PI3K/Akt. Methods Mol. Biol. 462, 201-11 (2009).

16. P. Holden, W. A. Horton, Crude subcellular fractionation of cultured mammalian cell lines. BMC Res. Notes 2, 243 (2009).

17. L. G. Tilney, K. R. Porter, Studies on the microtubules in heliozoa. II. The effect of low temperature on these structures in the formation and maintenance of the axopodia. J. Cell Biol. 34, 327-43 (1967).

18. P. de Lanerolle, A. B. Cole, Cytoskeletal proteins and gene regulation: Form, function, and signal transduction in the nucleus. Sci. STKE 2002, pe30 (2002).

19. M. Bustin, N. K. Neihart, Antibodies against chromosomal HMG proteins stain the cytoplasm of mammalian cells. Cell 16, 181-89 (1979).

20. R. E. Manrow, A. R. Sburlati, J. A. Hanover, S. L. Berger, Nuclear targeting of prothymosin alpha. J. Biol. Chem. 266, 3916-924 (1991).

21. P. L. Paine, C. F. Austerberry, L. J. Desjarlais, S. B. Horowitz, Protein loss during nuclear isolation. J. Cell Biol. 97, 1240-242 (1983).

22. S. A. Adam, R. S. Marr, L. Gerace, Nuclear protein import in permeabilized mammalian cells requires soluble cytoplasmic factors. J. Cell Biol. 111, 807-16 (1990).

23. I. Schulz, Permeabilizing cells: Some methods and applications for the study of intracellular processes. Methods Enzymol. 192, 280-00 (1990).

24. A. L. Foucher, B. Papadopoulou, M. Ouellette, Prefractionation by digitonin extraction increases representation of the cytosolic and intracellular proteome of Leishmania infantum. J. Proteome Res. 5, 1741-750 (2006).

25. A. L. Dounce, in The Nucleic Acids, E. Chargaff, J. N. Davidson, Eds. (Academic Press, New York, 1955), vol. 2, p. 93.

26. P. Janmey, in Handbook of Biological Physics, R. Lipowsky, E. Sackmann, Eds. (Elsevier Science BV, Amsterdam, 1995), chap. 17.

27. M. Edidin, The state of lipid rafts: From model membranes to cells. Annu. Rev. Biophys. Biomol. Struct. 32, 257-83 (2003).

28. I. C. Morrow, R. G. Parton, Flotillins and the PHB domain protein family: Rafts, worms and anaesthetics. Traffic c 6, 725-40 (2005).

29. E. B. Babiychuk, A. Draeger, Biochemical characterization of detergent-resistant membranes: A systematic approach. Biochem. J. 397, 407-16 (2006).

30. K. van Holde, J. Zlatanova, What determines the folding of the chromatin fiber? Proc. Natl. Acad. Sci. U.S.A. 93, 10548-0555 (1996).

31. E. Nishida, Y. Gotoh, The MAP kinase cascade is essential for diverse signal transduction pathways. Trends Biochem. Sci. 18, 128-31 (1993).

32. M. J. Robinson, M. H. Cobb, Mitogen-activated protein kinase pathways. Curr. Opin. Cell Biol. 9, 180-86 (1997).

33. P. J. Roberts, C. J. Der, Targeting the Raf-MEK-ERK mitogen-activated protein kinase cascade for the treatment of cancer. Oncogene 26, 3291-310 (2007).

34. G. Griffiths, B. Burke, J. Lucocq, in Fine Structure Immunocytochemistry (Springer-Verlag, Berlin, New York, 1993), pp. 27-1.

35. K. L. Dunn, P. S. Espino, B. Drobic, S. He, J. R. Davie, The Ras-MAPK signal transduction pathway, cancer and chromatin remodeling. Biochem. Cell Biol. 83, 1-4 (2003).

36. I. W. Mattaj, L. Englmeier, Nucleocytoplasmic transport: The soluble phase. Annu. Rev. Biochem. 67, 265-06 (1998).

37. L. Warren, Isolation of plasma membrane from tissue culture 榛 cells. Methods Enzymol. 31 (Pt A), 156-62 (1974).

38. J. H. Hartwig, Actin flament architecture and movements in macrophage cytoplasm. Ciba Found. Symp. 118, 42-3 (1986).

39. P. H. Mangeat, Interaction of biological membranes with the cytoskeletal framework of living cells. Biol. Cell 64, 261-81 (1988).

40. A. Bretscher, Microfilament structure and function in the cortical cytoskeleton. Annu. Rev. Cell Biol. 7, 337-74 (1991).

41. M. P. Sheetz, Cell migration by graded attachment to substrates and contraction. Semin. Cell Biol. 5, 149-55 (1994).

42. C. I. Murray, M. Barrett, J.E.Van Eyk, Assessment of ProteoExtract subcellular fractionation kitreveals limitedand incompleteenrichmentofnuclearsubproteomefrom frozen liver and heart tissue. Proteomics 9, 3934-938 (2009).

43. M.T.Maher, A.S.Flozak, A.M. Stocker,A.Chenn, C.J. Gottardi, Activity of the beta-catenin phosphodestruction complex atcell-cellcontacts is enhancedby cadherinbased adhesion. J. Cell Biol. 186, 219-28 (2009).

44. N.G. Kim, C. Xu, B.M. Gumbiner. Identification of targets of the Wnt pathway destruction complex in addition to β-catenin. Proc. Natl. Acad. Sci. USA, 106 (2009), pp. 5165–5170.

Bridge to Chapter III

Since I had now a good fractionation protocol, I decided to reevaluate the subcellular distributions of Wnt signaling pathway components and to characterize the endogenous Axin-based complexes in various subcellular localizations and their roles in regulating Wnt signaling.

In Chapter III, I collaborated with my colleague, Ms. Ekaterina Gusev who established and optimized an *in vitro* kinase assay that allowed us to dissect various aspects of β-catenin phosphorylation. We have first identified several endogenous Axin-based complexes that differ in terms of compositions, activities, and subcellular localizations. We have also analyzed the changes induced by Wnt activation. Our data support a model where Wnt stimulation modulates the dynamic balance and combinations between pre-existing complexes.

Based on the data in Chapter III, we are preparing two manuscripts for publication.

Characterization of the endogenous Axin complexes: properties, activity and Wnt regulation. *In preparation.*

CHAPTER III

Characterization of the Endogenous Axin Complexes: Properties, Activity and Regulation by Wnt

Xiaoyong Liu, Ekaterina Gusev, Brian Siu, and François Fagotto*

Department of Biology, McGill University, Montreal, Quebec, Canada

* Correspondence:
François Fagotto, Department of Biology, McGill University
1205 Dr. Penfield Ave., room W5/15
Montreal, QC H3A 1B1, Canada
Email, francois.fagotto@mcgill.ca

Abstract

β-catenin phosphorylation is the core reaction in regulation of the Wnt pathway. This reaction occurs within a protein complex built around the scaffold protein Axin, and Wnt activation appears to inhibit the function of the complex. However, despite intensive investigation, neither the exact nature of the complex nor the regulatory mechanism have been definitively established.

We present the identification of multiple endogenous Axin complexes, which we characterize in terms of composition, subcellular localization, stability, and specific phosphorylation activity toward β-catenin. We also determine the effect of Wnt stimulation of these complexes. Our results show that multiple complexes co-exist, which contribute to different degrees to β-catenin phosphorylation and are differentially regulated by Wnt. We discuss how these results validate several aspects of current models, but contradict some of the recently proposed hypotheses and suggest an integrative mechanism of β-catenin regulation.

Introduction

The Wnt-β-catenin signaling pathway is essential in mediating cell-cell communication in embryos and in adult tissues, and its de-regulation is involved in the development of many cancers (Cadigan and Peifer 2009). β-catenin is the central protein that transduces the signal from the cell surface to the nucleus, where it functions as a transcriptional co-activator (Cadigan and Peifer 2009). Regulation of signaling seems to revolve around β-catenin stability (MacDonald and He 2012): In the absence of Wnt, cytosolic β-catenin is captured by the Axin-based complex, where it is phosphorylated. Phosphorylation by casein kinase 1 on serine residue 45 serves as priming for the subsequent phosphorylation by GSK3 on three consecutive residues, threonine 41, serine 37 and serine 33. These four phosphorylated residues serve as recognition sequence (called a "phosphoedron") for ubiquitination and proteasomal degradation (Verheyen and Gottardi 2009). Thus levels of free cytosolic β-catenin are maintained extremely low in non-stimulated cells. Upon Wnt stimulation, β-catenin appears to be stabilized, building a progressively larger cytosolic pool. It then enters the nucleus, where it binds HMG-box transcription factors of the TCF/LEF1 family and activates a series of target genes (Mosimann *et al* 2009).

β-catenin is phosphorylated within a protein complex assembled by the scaffold protein Axin (Cadigan and Peifer 2009, Zeng, Fagotto *et al.,* 1997, Fagotto *et al.,* 1999, Yamamoto *et al.,* 1999, Ikeda *et al* 1998, Behrens *et al* 1998, Hart *et al* 1998). Axin can directly bind many partners, including most of the components involved in the Wnt pathway (Zeng, Fagotto *et al.,* 1997, Kishida 1998, Yamamoto *et al.,* 1999, Ikeda 1998, Fagotto 1999, Kishida 1999, Luo and Lin 2004). The major accepted function of Axin is to bring together the substrate β-catenin and its kinases, casein kinase 1 (CK1) and glycogen synthase kinase 3 (GSK3), thus enormously increasing the efficiency of the phosphorylation reactions. Another important component is adenomatous polyposis coli (APC), which can bind simultaneously Axin and

β-catenin, and is often depicted as the forth core component of the complex. APC is essential for β-catenin regulation (Hinoi *et al* 2000, Xing *et al* 2004, Kimelman *et al* 2006), more specifically, for β-catenin phosphorylation (Ha *et al* 2004, Kimelman, *et al.,* 2006, Wang *et al.,* 2014), although the details of its function are still unclear. Axin also recruits protein phosphatase 2A, which efficiently dephosphorylates phosphorylated β-catenin (Hsu *et al* 1999, Su, Fu *et al.,* 2008). Axin and APC are also phosphorylated by CK1 and GSK3, and dephosphorylated by PP2A. Axin is destabilized by dephosphorylation, which is one of the possible mechanisms regulating the pathway, while APC phosphorylation increases its affinity for β-catenin. Note that two CK1 and two GSK3 isoforms have been implicated. Both GSK3α and β seem to provide a similar function. The isoform of casein kinases, CK1α or CK1ε, that is responsible for phosphorylation of β-catenin and/or of the other components has not been yet solved conclusively, with a contribution from both being a likely possibility.

How Wnt inhibits the function of the complex is still not definitively understood. What is well established is that Wnt binds to two co-receptors, Frizzled (Fz) and LRP5/6, and that the cytoplasmic tail of LRP5/6 then gets phosphorylated by GSK3 and CK1γ, another CK1 isoform (Davidson *et al* 2005, Zeng *et al* 2005), on multiple contiguous consensus motifs. It has been shown that phosphorylation of LRP5/6 increases its affinity for Axin (Mao *et al* 2001). It has also been proposed that the same phosphorylation inhibits GSK3 activity (Piao *et al* 2008, Wu *et al* 2009). The mechanism through which Frizzled contributes to activation of the pathway is less clear, although it probably relates to the recruitment of Dishevelled (Dvl in vertebrates; Gonzalez-Sancho *et al.,* 2004). A Frizzled-Dvl dependent mechanism also seem to recruit Amer1, another scaffold protein, to the plasma membrane via phosphoinositol phosphates, which may, in turn, contribute to recruitment of Axin to LRP5/6 receptors (Tanneberger *et al* 2011). Based on these and other observations, different models have been proposed. Most models assume that regulation occurs at the level of β-catenin phosphorylation: for instance, Dvl interacts with GBP (GSK3 binding protein, also called Frat), which inhibits GSK3 catalytic activity. Since Dvl can

heterodimerize with Axin, it may directly bring GBP in contact with Axin-bound GSK3 (Yost, Farr *et al.,* 1998, Farr, Ferkey *et al.,* 2000). Axin recruitment to phosphorylated LRP5/6 receptors is another reaction that may directly inhibit GSK3 (Zeng, Huang *et al.,* 2008), decrease the efficiency of the complex by causing dissociation of APC (Valvezan, Zhang *et al.,* 2012), dissociate the Axin complex altogether (Bilic 2007, Wu, Huang *et al.,* 2009), and/or inhibit phosphorylation of Axin (or stimulate its de-phosphorylation; Zeng, Huang *et al.,* 2008, MacDonald, Tamai *et al.,* 2009, MacDonald and He 2012, Kim, Huang *et al.,* 2013, Jho *et al* 1999, Willert *et al* 1999). Dephosphorylated Axin may adopt an inactive conformation (Kim, Huang *et al.,* 2013) and/or be ubiquitinated and degraded (Willert *et al* 1999, Yamamoto *et al* 1999). It is easy to conceive that these mechanisms cooperate: for instance, a feed forward loop is likely to form, where Axin binding to LRP5/6 brings GSK3 in close proximity to LRP5/6 and thus favours additional phosphorylation of LRP5/6, either on the same tail, or on adjacent LRP5/6 molecules. This in turn would lead to recruitment of more Axin molecules (Bilic 2007, Wu, Huang *et al.,* 2009). Also, dissociation of the complex may favour Axin dephosphorylation and vice versa. In any case, LRP5/6 would serve as a catalyzer of Axin complex inactivation, in the sense that a dissociated complex is expected to be rapidly replaced by a new complex.

Another quite radically different model suggests internalization of LRP5/6-bound Axin-GSK3 complex inside multivesicular bodies, thus physically sequestering GSK3 away from β-catenin (Taelman *et al.,* 2010). While all these models present β-catenin phosphorylation as the major processes being regulated, a recent model considered the association of β-TrCP with the Axin complex as the real target of the regulation. It proposed that phosphorylation is directly coupled to ubiquitination. Activation with Wnt would cause dissociation of β-TrCP, thus blocking the degradation of phosphorylated β-catenin, which would saturate and block the complex (Li, Ng *et al.,* 2012).

Note that all current models are explicitly or implicitly based on a series of assumptions: in particular, the process of β-catenin degradation results from the activity of a single type Axin complex. Yet, several pools of Axin have been detected

by centrifugation and cell fractionation, indicating the existence of more than one complex (Nathke 1996, Reinacher-Schick and Gumbiner 2001, Gottardi and Gumbiner 2004, Wang *et al.,* 2014). If distinct Axin complexes indeed coexist, the interpretation of data obtained by generic approaches, e.g. by immunoprecipitation from total cell extracts may not be as straightforward as presented (Taelman *et al.,* 2010, Li, Ng *et al.,* 2012, Kim, Huang *et al.,* 2013). Most models also assume that Axin is the limiting factor for the complex, a notion that is based on measurements from a single system, i.e. Xenopus eggs (Salic, Lee *et al.,* 2000, Lee, Salic *et al.,* 2003). This now appears to be an exception withAxin being much more abundant in mammalian cell lines (Tan, Gardiner *et al.,* 2012). Consistently, increasing Axin levels does not necessarily lead to increased β-catenin phosphorylation (Wang *et al.,* 2014). Another debatable assumption that has been previously made is that the phosphorylation activity can be determined by measuring the levels of β-catenin and its phosphorylation state (phosphorylated/non-phosphorylated) in cell extracts, cell fractions, or in association with Axin complexes (Taelman *et al.,* 2010, Li, Ng *et al.,* 2012, Valvezan, Zhang *et al.,* 2012, Kim, Huang *et al.,* 2013). Yet, the levels of the product or substrate that remain bound to an immunoprecipitated enzymatic complex are not a good readout of the enzymatic activity. Similarly, steady-state cellular levels do not necessarily reflect the rate of enzymatic reactions, since they can also be controlled by other parameters, such as association with other components that could casue sequestration in subcellular compartments (membranes, nucleus), or differential stability. e.g. In the case of β-catenin, it can bind to cadherins, indapendently of Wnt signalling, and it binds to TCF/LEF1 upon Wnt induced stimulation), Note also that much of the current knowledge on molecular details of this pathway is largely based on analysis of interactions between single pairs of the molecular components, which are generally overexpressed. Virtually nothing is known about potential cooperativity or on the contrary competitivity, nor about the actual proportion of each component that is actually associated with the complexes.

These considerations illustrate the need to re-evaluate the status of the Wnt signaling pathway using approaches that would be more systematic, would take into

account the abovementioned caveats to minimize potential sources of misinterpretation. As a first step toward this goal, we have performed a biochemical analysis of endogenous Axin-based complexes that included their separation, characterization of their subcellular distribution, composition, sensitivity to proteasomal degradation, and most importantly their relative activity toward β-catenin phosphorylation. We have compared these properties in unstimulated and Wnt-treated cells, in order to determine the effect of activation of the Wnt pathway and infer characteristics of the mechanism of regulation. Mouse L-cell fibroblasts were chosen as model system, because of their lack of cadherins and of their extremely low basal Wnt activity, two important features that significantly simplify the interpretation of the results.

Results

Characterization of endogenous β-catenin phosphorylation activity in L cell extracts

Steady-state levels of β-catenin are classically used as read-out of the Wnt pathway activity (MacDonald *et al.,* 2009, Logan and Nusse 2004, Cadigan and Peifer 2009). However, neither total β-catenin levels, nor levels of de-phospho or phosphorylated β-catenin forms can reflect the actual phosphorylation activity, since they also depend on additional parameters, including ubiquitination/ degradation as well as stabilization/sequestration (e.g. by association to other components; MacDonald *et al.,* 2009, Cadigan and Peifer 2009). In particular, soluble phosphorylated β-catenin is immediately ubiquitinated and degraded, and is typically barely detectable in cell extracts.

The only adequate approach is to measure the actual rate of phosphorylation in a classical enzymatic assay. Note that standard methods to monitor GSK3 activity use small peptides (Cole and Sutherland, 2008) or Tau (Taelman, 2010) as the substrate, which cannot be used here, since the Axin complex is considered to confer high substrate specificity to the process. We thus set to establish an *in vitro* assay to

monitor the endogenous activity responsible for β-catenin N-terminal phosphorylation (Fig. 1A, Gusev, 2012, Wang *et al.,* 2014): Recombinant his-tagged β-catenin, which was used as the substrate, was mixed with cell extract, and the degree of phosphorylation was determined by immunoblotting with anti-phospho antibodies recognizing the CK1 priming site (pSer45, abbreviated here p45) or the residues of the GSK3-consensus site (pSer33/pSer37/pThr41, abbreviated here p33/37/41; Fig. 1B, see Material and Methods). Phosphorylated β-catenin is known to be the target of protein phosphatases PP1 and PP2A (Janssens and Goris 2001, Kimelman and Xu 2006, Kim *et al.,* 2013), which are therefore expected to antagonize kinase activities in our assay.

Indeed, we found that the addition of okadaic acid (OA), a potent inhibitor of PP1 and PP2A strongly boosted the reaction (Fig. 1B). Sensitivity to OA was thus systematically tested in this study. Note that Axin and APC are also targets of CK1, GSK3 and PP2A, and that these reactions are also expected to affect β-catenin phosphorylation, a complication that should be taken into account when interpreting the results of this kinase assay.

We verified the sensitivity of p45 priming and p33/37/41 phosphorylation to CK1 and GSK3 inhibitors (Fig.1B, C). We chose concentrations approximately five-fold above the IC50 (Fig.1D), which should be sufficient to inhibit the activities almost completely. Because CK1α is more sensitive than CK1ε to IC261, we tested two concentrations, the lowest being expected to only marginally affect CK1α but block CK1ε activity. In the presence of OA, the CK1 inhibitor IC261 strongly inhibited both p45 and p33/37/41 reactions, consistent with the obligatory priming for the subsequent phosphorylation steps. Note that a low IC261 concentration was only partially effective, suggesting an important contribution of CK1ε. The GSK3α+β inhibitor IX had a mild effect on p45 signal but strongly decreased p33/37/41, fully consistent with the expected CK1-GSK3 sequence. TWS119, an inhibitor of GSK3β, but not GSK3α, had little effect. This observation contradicted the common assumption that GSK3β was specifically involved in the Wnt pathway (Ikeda *et al.,* 1998, Jho *et al.,* 1999, Yamamoto *et al.,* 1999), and supported a contribution of both

isoforms (Siegfried *et al.,* 1990, Wu and Pan 2010).

Results with IC261 were similar in the absence of OA, but more complex effects were observed for the GSK3 inhibitors (Fig.1B, C): in the presence of OA, inhibitor IX had little effect on p33/37/41 but blocked p45 phosphorylation, while TWS119 led to an increase in both signals. These effects presumably reflect the importance of other phosphorylation/ dephosphorylation reactions (on APC and Axin). The dissection of this complicated issue is beyond the scope of this study.

Next, we asked what happens to β-catenin once the phosporylation reaction completed. It remains unknown whether phosphorylated β-catenin gets released, or remains associated in the Axin complex. To test this, we ran kinase reactions, which were then loaded on blue native gels to separate free β-catenin from larger macromolecular complexes. Note that we favoured blue native gel electrophoresis (BNGE) over gel filtration, because the former method minimizes dilution, thus better preserving non-covalent interactions. As shown in Fig.2A, two crude fractions were tested as the source of kinase activity, the cytosol and the rest of the cell content (i.e. insoluble fraction plus nucleosol). Both yielded essentially the same general patterns, for both p45 and p33/37/41: When the assay was run under standard conditions, we only detected signal on the top of the gel, indicating phospho-β-catenin association with a very large complex. As presented later, these are high molecular Axin complexes. When the assay was performed in the presence of okadaic acid, the signal was strongly increased, and a second strong band appeared in the low region of the gel, where it perfectly coincided with the position of the free recombinant β-catenin (Fig.2A). The relative signal intensity of the high band compared to the low band was strikingly higher for p45.

These observations suggest that β-catenin is partially retained in the Axin complex after priming but largely released once fully phosphorylated. Partial retention of the intermediate product would explain the partial inhibition of p45 activity by the GSK3 inhibitor, which may “jam” the complex.

General characterization of Wnt activation

In a preliminary analysis of the effects of Wnt activation, we examined the total levels of β-catenin forms and of components of the Axin complex at different time points of stimulation (supplementary Fig.S1A). We detected the expected rises of phosphorylated LRP6, reflecting receptor activation, and of total β-catenin, with a rapid decrease of p45 β-catenin and a slower and more partial decrease of Axin levels. Note that phosphorylated LRP6 was already present in non-stimulated cells, and that it appeared to increase relatively linearly over the time of Wnt stimulation, while β-catenin stabilization started to be detectable relatively late (> 20min activation, at a time when p45 had almost disappeared), and then increased exponentially (supplementary Fig.S1B). Based on these data, we selected 30min as our standard length of Wnt treatment, i.e. at a stage were activation was already robustly detectable in terms of LRP6 phosphorylation and β-catenin accumulation, yet phosphorylated β-catenin was still abundant, indicating that we may be able to capture the action of Wnt activation, rather than long term effects, which could be complex and indirect. As shown below, we also tested additional time points in some experiments, i.e. 15 and 60 min.

Activation of the Wnt pathway is generally thought to antagonize β-catenin phosphorylation by inhibiting GSK3, but the issue has remained controversial in the absence of direct measurements. We found that both p45 and p33/37/41 phosphorylation were significantly decreased (20-50 % inhibition) in extracts from Wnt-stimulated L cells (Fig. 2B). It had been proposed that Wnt activation blocks the transfer of phosphorylated β-catenin from the Axin complex to the ubiquitination machinery (Kimelman and Xu 2006, MacDonald *et al.,* 2009). However, BNGE analysis of kinase assays showed that phosphorylated recombinant β-catenin was released from the Axin complex to a roughly similar extent in both control and Wnt-treated cell extracts (data not shown).

Identification and characterization of multiple Axin pools

The existence of different Axin pools/complexes has been previously reported (Nathke 1996, Reinacher-Schick and Gumbiner 2001, Gottardi and Gumbiner 2004),

but not yet systematically analyzed. In particular, previous studies had omitted dense plasma membrane and cytoskeletal element fractions (see Chapter II and Introduction). To obtain a global overview of Axin pools, we fractionated crude cell extracts by zonal-rate centrifugation on a broad sucrose gradient (SG; Fig.3 and supplementary Fig.S2). Despite the crudeness of the samples, the obtained sedimentation patterns appeared very reproducible in terms of peak position and relative levels for the various molecules tested. Axin showed a wide distribution: while the largest pool remained near the top of the gradient (fraction F2-F4), a significant amount sedimented to denser fractions (F5-F10, F5-8 defined as "intermediate" pools, F9-F10 as dense pool), as well as in the pellet (F13). These differences in sedimentation were much too large to be explained by small variations in composition/stoichiometry of Axin complexes, but rather indicated the existence of complexes of widely different sizes and/or associated with different subcellular structures. Various criteria confirmed that each pool had distinct properties in terms of kinase activity, composition, stability and membrane association:

We first analyzed the SG fractions for kinase activity toward β-catenin (Fig.3A) and compared it to Axin distribution (Fig.3B). We first present the results for unstimulated cells. The changes observed upon Wnt activation will be described below:

p45 activity showed three distinct peaks, coinciding with part of the large light pool (F3-4), the dense pool (F9-10) and the pellet (F13). p33/37/41 activity had a more spread distribution but the same three peaks. The two activities were not proportional to Axin levels: the "specific activities", expressed as relative activity/Axin level, were generally higher for the dense and insoluble pools, and lowest for the light pool (supplementary Fig.S2D). These pools further differed in p45 and p33/37/41 activity (see supplementary Fig.S2D, E). The effect of PP2A inhibition by OA also differed: it boosted the kinase activity of the light fractions, but decreased it in the dense factions (see also below). These observations argue for the co-existence of complexes with quantitatively and qualitatively different intrinsic activities. Note that several Axin pools may overlap in these SG, in particular in the top of the

gradient where resolution was the lowest. Thus the moderate relative activity of F3-F4 could be equally explained by an abundant but weakly active complex or, on the contrary, by the existence of a small pool of a highly active complex overlapping with inactive Axin.

We also systematically tested the distribution of the other components of the Wnt pathway (Fig.3B, supplementary Fig.S2A). APC sedimented in a pattern relatively similar to Axin, but several other core components of the complex showed distinct distributions, which may at least partially account for the differences in kinase activity. In particular, CK1α and CK1ε were remarkably concentrated in F9-10, perfectly coinciding with the peak of high kinase activity. Note however that the relative kinase activities correlated only partially with kinase levels. For instance, F5-8 had comparatively less CK1 but as much GSK3 (Fig.3B), consistent with their relatively higher p33/37/41 activity, but F3-4 had lower CK1 levels than F9-10, yet twice higher p45 activity. Protein phosphatase 2A (PP2A) was abundant in light fractions and in the pellet, which correlated with the boost of activity in the presence of OA. Consistently, the activity pattern in the presence of OA matched closely Axin distribution, in particular producing a more prominent peak for p33/37/41 in F2-3 (Fig.3C, D). We conclude that dephosphorylation by PP2A was a significant parameter that lowered the apparent specific activity of these pools. The smaller PP2A pool present in dense fractions F9-10 clearly has a different function, since, as mentioned above, OA inhibited both p45 and p33/37/41 activities (Fig.3A, C, D and supplementary Fig.S2D). As we will see later, this effect was confirmed when the complexes were further fractionated. We presume that these contrasting effects reflect the dual function of PP2A: dephosphorylation of β-catenin is antagonistic to the pathway, but, on the other hand, PP2A is probably required to ensure the cycle of phosphorylation/dephosphorylation of APC, which was proposed to control capture and release of β-catenin by the complex (Seeling, Miller *et al.,* 1999). Due to this complexity, we concluded that it was not possible to determine “absolute” CK1 and GSK3 activities in these pools, but only “apparent activities” in the absence or presence of phosphatase activity.

Effect of Wnt stimulation

Comparison of SG from crude extracts of unstimulated and Wnt stimulated cells showed that the activities of the pools were affected differently (Fig.3 C, D and supplementary Fig.S2F): the activity of the light pool remained largely unaffected, with the notable exception of p33/37/41 activity measured in the presence of OA, which was slightly lowered by Wnt. On the contrary, the activities of the dense pool and of the pellet were more strongly inhibited, particularly in the pellet fraction.

In terms of Axin levels, Wnt caused a decrease throughout the SG, with the exception of the dense pool F9-10. Note that the pellet, F13, was the only pool where changes in Axin and kinase activities correlated, suggesting that decreased activity could be simply due to displacement, dissociation or degradation of the complex. The effect on the other pools, respectively strong decrease in Axin but little effect on activity for F3-4, no change in Axin but a decrease in activity for F9-10, were apparently contradictory. The simplest interpretation of the results in the light fractions was that they contained different types of Axin complexes with different intrinsic activities, stabilities, and sensitivity to Wnt. The comparatively huge pool of Axin relative to CK1 suggested that only a small fraction may be actually forming a functional complex with the kinases. We thus hypothesized the existence of a minor pool of active Axin complexes that would be relatively stable, while the rest of the light fractions would be degraded upon Wnt stimulation. This hypothesis was tested below by examining the composition of these fractions in more detail. As for F9-10, GSK3 and CK1α/ε were all decreased in Wnt-treated samples, suggesting that the decreased activity was possibly due to the dissociation of the kinases from this complex.

Membrane association

The three main Axin/β-catenin phosphorylation pools all overlapped with plasma membrane markers, in particular with LRP6 (compare Fig.3B and supplementary Fig.S2A). To examine a potential membrane association, we tested the effect of

adding a mild detergent CHAPS to the SG. We observed important changes in the Axin sedimentation pattern, with the almost complete disappearance of the intermediate-dense pools (F7-10) and a concomitant increase in both light fractions and pellet (Fig.4B and supplementary Fig.S3A). The same trend was also observed for GSK3, LRP6 and Fz (supplementary Fig.S3A). These data suggested that the Axin complexes recovered in these dense fractions were all membrane associated. Note that a shift was also observed for the light pool (Fig.4B and supplementary Fig.S3A), suggesting that at least part of this pool was associated to membranes. We directly evaluated the extent of this association for F3-4 and F9-10 by equilibrium density centrifugation in the presence and absence of CHAPS (flotation assay). Membrane-associated proteins are expected to float to a lower density than the density of the corresponding solubilized protein complexes. Note that the absolute density is difficult to predict, as it depends on the intrinsic density of each particular protein complex as well as the amounts of associated detergent/lipid molecules. For F3-4, half of Axin was shifted to a higher density in the presence of CHAPS (Fig.4A). The fact that the rest remained at the same position in the presence or absence of CHAPS suggested the presence of a second pool, either soluble or associated with a detergent-insoluble lipid membrane domains (Schuck *et al* 2003). In the case of F9-10, the majority of Axin floated in the absence of detergent, and was completely shifted in the presence of CHAPS, confirming that the whole pool was membrane-associated (Fig.4A). Note that its sedimentation to a particularly high density in the presence of CHAPS suggested either a particularly dense protein structure and/or association with the actin cytoskeleton. Other Axin-interacting components, GSK3, APC, Dvl2, and CK1ε behaved similar to Axin, in both pools (Fig.4A).

Instability of the membrane-associated pool

Another interesting property was observed in extracts of cells that were treated with proteasome inhibitors. Incubation with MG132 (Fig.4B) or lactacystine (not shown) caused a specific increase of Axin (and GSK3) levels in F7-10. Note that this peak included both the very active CK1-rich F9-F10 and the less active F7-F8 fractions.

We conclude that this region of the gradient contains one or multiple Axin complexes that are normally destabilized by a proteasome-dependent mechanism.

The pool of Axin and associated components that accumulated in SG fractions F7-10 after MG132 treatment were completely eliminated by the addition of CHAPS (supplementary Fig.S3B), indicating that it was membrane-associated. We confirmed these results by comparing the subcellular distribution of Axin from control and MG132-treated cells. We used a protocol that separates crude cell extracts into five fractions, corresponding to five major subcellular compartments, cytosol (Cs), nucleosol (Ns), nuclear insoluble material (Ni), membranes (M), and dense insoluble material (called fraction X, containing mostly cytoskeletal components; Liu, Fagotto 2011). This experiment unambiguously identified the membrane fraction and, to a lesser extent, the insoluble fraction X as the major sites where Axin was stabilized by the MG132 inhibitor (Fig.4C).

Subcellular distribution

We used the same cell fractionation protocol to measure the relative kinase activities and determine the distribution of the various constituents of the Axin complex. The nuclear insoluble fraction (Ni) had high background signal (data not shown) and was not further considered. The other fractions showed robust activity both for both p45 and p33/37/41 (Fig.5B, C, and supplementary Fig.S4A). The cytosol was particularly active for p33/37/41 phosphorylation, both for the wild type β-catenin substrate and for the "primed" phosphomimetic S45D. p45 activity was more broadly distributed. We do not have information about the relative volumes of the different compartments. Yet, if one assumes that the membrane activity corresponded to plasma membrane (and potentially early endosomes), the "volume" of the fraction would clearly be very small, particularly compared to the cytoplasm, and thus the p45 activity was comparatively elevated in this fraction.

Among the constituents of the Axin complex, most of them were most abundant in the cytosol, including Axin, GSK3, CK1α, APC and Dvl2 (Fig.5D and supplementary Fig. S4). All the components were also present in the other fractions,

consistent with their β-catenin phosphorylation activity. Note that the cytosol was much less active than the other fractions relative to the Axin levels or levels of the kinases.

Effects of Wnt activation

We identified the compartments where Wnt stimulation caused inhibition of β-catenin phosphorylation (Fig.5A-C and supplementary Fig.S4A). We found that both p45 and p33/37/41 activities were decreased in the Cs (~40% inhibition) and fraction X (25-35% inhibition). The nucleosol was not greatly affected, while the membrane-associated activities tended to be slightly increased. These changes were generally consistent with changes in Axin levels, which decreased in Cs and X, but not Ns nor M fractions (supplementary Fig.S4B). CK1 and GSK3 levels did not appear significantly changed, except for a slight increase of CK1ε and GSK3α in the membrane-associated pool (Supplementary Fig.S4B). Other components underwent more important changes. For instance, Dvl2 phosphorylation strongly increased in the cytoplasm, while Dvl2 accumulated in the membrane and insoluble fractions (supplementary Fig.S4B). Additional details about these changes are given in supplementary legends. Note that non-phosphorylated β-catenin accumulated in all fractions, although somewhat faster in the cytosol and slowest in the nuclear fractions (supplementary Fig.S4B).

It should be mentioned that we could not exclude that complexes and some activity may be lost during cell fractionation. Nevertheless, it appeared that the major properties were largely preserved. Most importantly, the total p45 and p33/37/41 activities, calculated as the sum of the fractions, were decreased by Wnt to a similar degree as when measured in total extracts. We were thus confident that the results accurately reflect the endogenous conditions.

In summary, all fractions were capable of phosphorylating β-catenin to different degrees. They differed in their sensitivity to Wnt activation. The comparison of Cs and X suggested differences in inhibition by Wnt: in fraction X, it could be explained by the decrease in Axin, but in the cytosol kinase inhibition was clearly stronger than

what could be accounted for by the decrease in Axin levels (40% versus 15%). Note also the surprisingly strong kinase activity of the membrane fraction, which should be the site of Axin inactivation according to classical models. We thus set to dissect the complexes and activities present in these three fractions, cytosol, insoluble dense material and membranes.

Characterization of cytosolic complexes

We used BNGE to analyze the composition of the Axin complexes, as this "non-invasive" method provided excellent resolution. Note that immunoprecipitation, which we used to verify the global association of the components of Axin-based complexes (supplementary Fig.S8), cannot discriminate between multiple complexes present in the same sample. Furthermore, the antibody-antigen binding may compete with interactions between components of a complex, leading to artefacts such as failure to capture some of the complexes when the antigen is masked, or on the contrary dissociation of the competing interaction upon antibody binding.

BNGE detected several cytosolic complexes with apparent sizes ranging from approximately 300kDa to greater than 1MDa (Fig.6A). Complexes of similar sizes were also found in the nucleosolic fraction (Mostly fragments of Axin; Fig.6A). To draw a correlation between these various complexes and their kinase activity, we partially separated them by fractionation of the cytosol: We first used size exclusion chromatography, which gave a broad Axin elution profile (Fig.6B). BNGE confirmed that complexes of different sizes were separated (Fig.6C). When analyzed for β-catenin phosphorylation, the fractions containing the largest complexes showed the highest activity both for p45 and p33/37/41 (Fig.6D). They also showed the highest specific activities compared to Axin levels (Fig.6D" and E). The intermediate complexes were the most abundant but had a moderate activity. They were however most sensitive to OA. In fact, their p45 activity became the strongest when measured in the presence of OA. The small complexes had the lowest activity, which was partly increased by OA for p45 but not p33/37/41.

Gel filtration causes a large dilution of the sample, and it does not allow

simultaneous analysis of multiple samples. To perform a more systematic dissection of the cytosolic complexes, we resorted to SG. BNGE of SG fractions yielded Axin complexes that were overall similar to those separated by gel filtration, although here large complexes were more spread along the gradient (supplementary Fig.S5). We systematically analyzed the BNGE profiles of these SG for all components of the Axin complex, and in parallel we measured the kinase activity. Detailed analysis, including quantification, is provided in supplementary materials (Figs.S5-S7). Examples of BNGE are shown in Fig.7, and here we present a summary of the most salient observations.

The Axin pattern showed that the top fractions (pool 1-3) contained mostly ~200-500kDa complexes, but also larger complexes in the 700-1200kDa range (supplementary Fig.S5). The denser fractions were progressively enriched in the larger complexes. The densest fractions F11-13 had even higher complexes (>1300kDa). The sum of all the fractions recapitulated the Axin pattern observed in whole Cs (Fig.7C). This indicates that the complexes remained stable through the 4hr-long ultracentrifugation, a stability that validates our results based on various fractionation steps.

The kinase activities spread through light and intermediate fractions, with a peak at F4-5 for p45 and two peaks at F4 and F7-8 for p33/37/41 (Fig.6A, B). The effect of OA was similar to that observed for crude SG: Both kinase activities were significantly boosted in light fractions but not in dense fractions. Under these conditions, the general distribution resembled that of Axin (Fig.6C).

The analysis of the complexes by BNGE involved stringent determination of co-migration of the various components and systematic quantification of relative abundance. This was performed by aligning the scan profiles for the blots of each component and measuring relative peak intensities (examples in Fig.8, see also supplementary Fig.S5). The profiles turned out to be very reproducible. Despite the extensive peak overlap, in particular in the top SG fractions, peak quantification turned out to be rather accurate, as validated by the fact that the sum of the patterns of all SG fractions gave values very close to those obtained from BNGE of crude

cytosol.

The results, summarized in supplementary Fig.S6 revealed the existence of a variety of complexes, differing in sedimentation, apparent size, and composition. One feature that appeared common to all large complexes (850kDa and above) was the striking correlation between Axin and APC levels (supplementary Fig.S6), from which we could conclude that these two scaffold proteins are probably present with a similar stoichiometry, consistent with their basic role in organizing these structures. Note that the smaller complexes abundantly present in the light fractions F3-4 did not contain APC.

The other components were present in different ratios. For instance, CK1α and GSK3, also detected in all complexes, showed parallel levels in the large complexes of F11-13, but opposed trends in 850 and 1100-1200 kDa complexes, with CK1α most abundant in dense fractions and GSK3 in light fractions (supplementary Fig.S5,S6). This was consistent with the observation that p45 was also proportionally more efficiently phosphorylated than p33/37/41 by dense fractions (Fig.6A, B). β-TrCP distribution closely resembled GSK3's, while PP2A resembled CK1α's. These correlations suggest that the occurrence of multiple complexes of well-defined composition. Some of the largest complexes, in particular those recovered in F11-13, appeared to contain all tested components (Fig.6B). A minimal complex containing one copy of each component, including the substrate β-catenin would have a theoretical size of ~ 1000kDa, but one expects complexes to be more compact than the individual components, and thus likely to migrate faster than the standard molecular weight markers. The markers should therefore only be considered as internal references rather than accurate indicators of the actual size of the complexes. The largest complexes may accommodate more than one copy of each molecule, in particular for small size proteins such as CK1α and GSK3, consistent with multiple possible interactions (e.g. association with either Axin, or APC, or both). This would explain the different relative ratios observed for these molecules.

Note also that the size of the complexes could not account for the differences in sedimentation alone, since similarly large complexes were found throughout the

gradient. Additional interactions, likely weaker and not preserved during BNGE, may need to be invoked. These could involve multimerization via Axin and/or APC, or with uncharacterized partners.

To be able to compare the data from BNGE and the kinase activities of the SG fractions, we computed the relative levels of each component relative to Axin for each complex, as well as the relative kinase activities (also to Axin levels; supplementary Fig. S6, 7). In this comparison we also included the levels of the various forms of β-catenin (total, non-phosphorylated, p45 and p33/37/41) detected in association with these complexes.

Several conclusions could be made: 1) Activities appeared to be related to the presence of large complexes (700-1300kDa): They were close to nil in F1-2, despite the presence of small~250-500 kDa complexes. 2) The activities in the rest of the fractions could not be assigned to one single type of complex, nor to complexes of one particular size, but seemed best accounted as the result of the contribution of the multiple large complexes. The 850 and 1200KDa complexes appeared to be the best candidates for high activity: a) They were systematically enriched in APC, CK1α and GSK3 relative to Axin. b) They also systematically contained high levels of phosphorylated β-catenin. c) Their combined Axin levels roughly correlated with relative activities, with the exception of F5-6. 3) The most active complexes were found in fractions F3-4 and F7, 8. F5-6 fractions, on the contrary, were significantly less active. This latter fraction correlated with low CK1α, PP2A and β-TrCP to Axin ratios. 4) The activity was also low in dense fractions F11-13, despite Axin levels equivalent to F9-10, suggesting that the largest complexes (>1300kDa) were less active. This weak activity also correlated with high levels of non-phosphorylated β-catenin and low levels of phosphorylated β-catenin associated with these complexes, suggesting that β-catenin, while efficiently recruited to these complexes, was only slowly phosphorylated.

In summary, the cytosol appeared to contain different types of complexes functioning in different modes: complexes of light fractions were particularly active but β-catenin was also quickly dephosphorylated, resulting in a moderate net activity.

The dense complexes (F7-8) were comparatively more efficient, apparently due to lower product dephosphorylation. Finally, the largest and densest complex found at the bottom of the SG showed weak activities.

Effects of Wnt activation on cytosolic complexes

After Wnt treatment, p45 phosphorylation was partially decreased throughout most of the fractions of the SG (Fig.7A). There was also a significant decrease in p33/37/41 activity, but this was restricted to the light fractions (Fig.7B). Axin levels were decreased in the same light fractions (Fig.7C). Thus Axin levels accounted for changes in p33/37/41, but not entirely for p45.

In terms of complex levels and composition, BNGE showed that in the light fractions (F3-F4) the intermediate complexes (500-850kDa) were affected (compare levels of Axin, APC, CK1α and GKS3 in supplementary Fig.S5, see quantification for Axin in supplementary Fig.S7), but not the large complexes (1100-1200kDa). As for the second major pool of kinase activity, F7-F8, Axin levels remained largely unchanged in all the complexes. The only significant change was a clear dissociation of β-TrCP within the 1200kDa complex. In summary, it appears that the decrease in β-catenin phosphorylation by cytosolic complexes is mostly due to the disappearance of medium sized complexes, which constitute the most abundant pool, but display only a relatively moderate activity. The larger pools, which show the strongest specific activity, remain stable, at least during this early phase of Wnt activation.

Insoluble complexes

The characterization of the activity detected in the fraction X was challenging due to its insolubility, even in the presence of mild detergents such as TritonX100 (present in the cell fractionation) or CHAPS (not shown). While neither immunoprecipitation nor BNGE were applicable in this case, we obtained some interesting information by simply analyzing fraction X by rate-zonal centrifugation. We knew that this fraction contained a variety of components, including a minor fraction of the nuclear markers lamin and histones, as well as an abundant contribution from the cytoskeleton (Fig.9C

and Liu and Fagotto 2011). Quite conspicuously, centrosomal markers γ-tubulin and pericentrin concentrated in this fraction (Fig.9C, Liu and Fagotto 2011, Wang *et al.,* 2014).

Figure 9A shows that both p45 and p33/37/41 kinase activities concentrated in the lower part of the gradient with a peak at F9 (trailing respectively upwards for p45 and downwards for p33/37/41). A weaker secondary peak was found in F3. Altogether, the distribution of the kinase activities correlated well with the very characteristic sedimentation patterns of specific components of the Axin complex, first of all of Axin itself (Fig.9B), but also APC (and APC fragments, see discussion below), CK1ε, and β-TrCP (Fig.9B and supplementary Fig.S9). A weak peak of PP2A and a "shoulder" of GSK3 were also detected in F9-12. The low levels of GSK3 may correspond to a weak interaction, which could be lost during centrifugation, and/or to low intrinsic levels of GSK3 in this complex, consistent with a relatively low p33/37/41 activity compared to p45 (Fig.5B). Note that while most of the activity of fraction X corresponded to a very dense component, the distribution did not coincide with centrosome markers. Consistently, little Axin and APC were found co-localized with γ-tubulin/pericentrin by immunofluorescence (data not shown).

The decreased activity upon Wnt activation can be explained by a partial but general shift from dense to light fractions of most constituents of the complex. Presumably the insoluble complexes are either dissociated by activation of the pathway, or at least substantially weakened such that they dissociated during isolation.

Membrane-associated complexes

The membrane fraction is particularly interesting because it is considered to be the site of regulation of the Axin complex by activated LRP receptors. The membrane pool of Axin also appeared conspicuous as it was stabilized upon proteasome inhibition (Fig.4C). We thus explored the composition of these membrane-associated complexes using BNGE. We compared four conditions: untreated cells, cells incubated with MG132 proteasome inhibitor, with Wnt, and with both. The rational of MG132 treatment was to try to stabilize and thus capture labile complexes.

We first observed a clear accumulation of phosphorylated LRP6 (p-LRP6) upon Wnt stimulation, consistent with previous observations (Fig.10). We also observed a similar accumulation upon MG132 treatment. In both cases, p-LRP6 showed a sharp peak with an apparent molecular weight of 1100-1200kDa. Secondary peaks below and above this band also increased under these two conditions. In particular, a broad band migrating around 800-900kDa coincided with the bulk of total LRP6. We probed these gels for all the major components of the pathway. Examples and quantification are shown in Fig.10. Here we summarize the most striking observations:

1) The large complexes were highly enriched in p-LRP6 signal relative to total LRP6 compared to the 850kDa complex. We hypothesize that the larger complexes may have contained LRP6 phosphorylated on multiple sites (Ranganathan 2004, Balic 2007).

2) We found clear co-migration of LRP6 and Axin. Axin was prominently enriched together with p-LRP6 in the 1200 and 1300kDa peaks compared to the 850kDa peak (Fig.10C). We interpret this observation as reflecting the recruitment of multiple Axin molecules, consistent with poly-phosphorylation of the LRP6 cytoplasmic tail (Balic 2007, Zeng 2008, MacDonald, Tamai *et al.,* 2009, MacDonald and He 2012).

3) All LRP6-Axin complexes also appeared to contain GSK3, and the three major complexes (850, 1200 and 1300kDa) also contained CK1α and CK1ε. Thus LRP6 appears to recruit with intact core Axin-based complexes. The 1200kDa appeared to be the most enriched (compare LRP6 levels with Axin, CK1 and GSK3). Several additional components were found to co-migrate with the major 850 and 1200kDa complexes: Frizzled and Dvl, as well as Amer1 and CK1γ, two proteins known to be involved in regulation of LRP6 complexes. In addition, APC was present only in a particular subset of complexes, most conspicuously absent from the most abundant 850kDa complex. PP2A and β-TrCP were not detected.

4) The apparent sizes of the complexes fit very well with the theoretical size calculated from the individual molecular weights. The 850kDa complex, for instance could correspond to: LRP6 + Fz + Dvl + Axin + GSK3 + CK1α or CK1ε + CK1γ + Amer + β-catenin = 200 + 70 + 80 + 100 + 50 + 40 + 40 + 150 + 100 = 830kDa. The

1000kDa had the same composition, but with APC and without Amer1 = +300 – 150 = 980kDa. Although, as mentioned above, the actual sizes may differ from the apparent migration, these data fit well with the assumption of a relatively simple stoichiometry.

5) Wnt significantly stimulated LRP6 phosphorylation and recruitment of the other components. However, there was already a surprisingly high basal level of p-LRP6 in unstimulated cells. Similarly, the increase in Axin levels was modest. Thus significant amounts of Axin already appeared recruited under unstimulated conditions. The same was true for most components, which where enriched less than 2 fold (Fig.10D). The only strong increases were observed for CK1γ in the 1200kDa complex (4 fold), consistent with its role in LRP6 phosphorylation (Davidson, Wu *et al.,* 2005), and for Amer1 (two folds).

6) Furthermore, proteasome inhibition caused essentially the same changes as Wnt, not only an increase in association of Axin and other components, but also increased LRP6 phosphorylation. The similarity held for the fold increases (Fig.10D) as well as the relative distribution in the different peaks (Fig.10B). On the contrary, proteasome inhibition did not significantly co-operate with Wnt stimulation (Fig.10A, B).

7) The endogenous β-catenin forms (phosphorylated and non-phosphorylated) also comigrated with the LRP6/Axin bands, with distinct patterns (Fig.10A and supplementary Fig.S10). Although these steady-state levels cannot provide direct information on rates of kinase activity, they confirm that all complexes must be capable of at least some β-catenin phosphorylation. Both Wnt and MG132 treatments caused comparatively important changes in distribution of the different forms.

Discussion

This study represents the first systematic analysis of endogenous Axin-based complexes, and the first direct investigation of the activity of these complexes in β-catenin phosphorylation. Our results give a picture of the pathway where multiple

complexes contribute to β-catenin phosphorylation, and suggest that Wnt stimulation preferentially targets some of these complexes. The data are consistent with a mechanism of inactivation based on Axin degradation and consequent decrease in levels of active complexes.

Multiplicity of Axin complexes

Any biochemical separation carries the intrinsic caveat of causing dissociation of multimolecular complexes, simply due to dilution compared to the natural intracellular conditions. It is most likely that some of the Axin complexes have dissociated during homogenization and subsequent fractionation, yet our results indicate that Axin complexes tend to be relatively stable, and that multiple complexes coexist in the cellular environment. For instance, the typical patterns of Axin cytosolic complexes observed by blue native gel electrophoresis seem to resist to both sucrose density centrifugation and gel filtration, two conditions where one would expect extensive dissociation. The most striking evidence for stability comes from the dense fractions of the sucrose gradients, which appear to contain exclusively very large complexes: if these complexes would easily dissociate, they should also do so while the fractions are collected and loaded on the native gels. In principle, one would expect then to observe similar small complexes and free monomeric proteins in all fractions. On the contrary, both gel filtration and sucrose gradients separated a range of complexes that corresponded to the expected sizes, arguing that these complexes were already present before fractionation, and by extension probably before homogenization.

In fact, previous quantitative models on Axin complex composition predicted a low fraction of large complexes, and a large amount of free Axin (Lee *et al.,* 2003, Tan *et al.,* 2012). On the contrary, we could detect only a very small pool of free Axin. Provided that published affinities between the various components of the complex are accurate, one must assume that multiple components interact cooperatively, thus stabilizing the complexes. Consistent with this possibility, most Axin complexes show an apparent size and composition corresponding to complexes made of at least three

or more components. Cooperativity may explain the particularly high stability of the largest complexes separated in the dense fractions of the sucrose gradient from cytosolic fractions, and those detected in the membrane fraction. The complexes associated with the insoluble fraction, although of unknown size, are probably also relatively large and stable. It is conceivable that additional factors could contribute to the composition and stability of the Axin complexes. Yet, their size can generally be explained very easily simply by the known components, thus no additional unknown component need to be hypothesized.

One interesting question is whether some of the complexes are built for a specific function, or whether the observed spectrum of complexes merely reflects the inevitable equilibrium based on mass action. Our extensive analysis of the patterns obtained by blue native electrophoresis show the presence of many combinations: for example, some complexes contain only CK1, GSK3 or PP2A, some both kinases but not PP2A, others CK1 and PP2A but not GSK3, and so forth. Similarly, there are complexes that contain APC and others not, again in both cases with combinations of the other components. These observations suggest that the system is an equilibrium that depends on relative affinities, but with strong cooperative effects.

One fascinating consequence of this system is that β-catenin must be regulated by the combined effect of multiple complexes with distinct activities. Some will only prime Ser45, others build on primed substrate, while others still perform the whole phosphorylation sequence. Our analysis of the cytosolic activities clearly shows that there isn't a single "mature" complex, but multiple forms, all of them active to different degrees.

It should be noted, however, that some components appear more intimately associated with the complex than others: CK1ε, in particular, seems to be almost exclusively in an associated form, with virtually no free pool, neither in the cytosol, nor in the insoluble fraction. On the contrary, a large pool of GSK3 migrating with an apparent low size are systematically detected in about all fractions. Unfortunately, GSK3α and β are enzymes that are involved in so many processes that one cannot determine how much of the pool corresponds to free GSK3 dissociated from Axin

complexes, as opposed to GSK3 originating from other unrelated complexes. This uncertainty prevents determining whether the insoluble complexes are more specialized for Ser45 priming, as indicating based on our phosphorylation data, or if they have simply lost GSK3 during fractionation.

What happens to phosphorylated β-catenin?

Classical enzymes capture the substrate, modify it, and release the product in the cytosol. In the case of sequential reactions, nature has often optimized the process by coupling the reactions. Similar mechanisms have been proposed for β-catenin phosphorylation. In particular, it has been hypothesized that the role of APC could be to help dissociating β-catenin from Axin once phosphorylated (Hinoi *et al.,* 2000, Xing *et al.,* 2003, Kimelman, *et al.,* 2006), and the model was recently pushed further: APC would not only take β-catenin from Axin, but would transfer it directly to β-TrCP (Su, Fu *et al.,* 2008). The Axin-APC complex would look then like a factory where the entire processing of β-catenin up to its degradation would be performed. Note, however, that the model has only been inferred based on global immunoprecipiation data, without attempts to follow the fate of β-catenin during and after phosphorylation.

Our analysis of the products of β-catenin phosphorylation has provided some answers to this issue. We did detect a significant amount of phosphorylated β-catenin associated with a very large complex. This complex seems to correspond to the largest complex identified in dense cytosolic fractions, which was also prominently enriched with β-TrCP. However, we also detected a pool migrating as would be expected for free β-catenin. These observations are not consistent with the hypothesis that β-catenin would remain associated with a large complex and/or directly transferred via APC to β-TrCP, and that this step would be rate-limiting (Su, Fu *et al.,* 2008). This conclusion is further supported by the strong phosphorylation activity of the light cytosolic fractions, where none of the complexes seem to contain β-TrCP.

What are the changes induced by Wnt?

We have reported here the first direct evidence that β-catenin phosphorylation is inhibited by Wnt. Although such inhibition had been indirectly supported by numerous observations, including changes in relative steady state levels of various β-catenin forms, these were also consistent with other explanations, including differences in subsequent steps, or differential sequestration/stabilization.

Our data also bring some insight into the potential mechanism of regulation. We did not detect any obvious qualitative change, e.g. in the composition of the Axin complexes, or their localization, which could account for the decreased activity. In fact, the specific activities remain largely unaffected by Wnt (Fig.5 and 7). The major effect seemed to be a decrease in the levels of Axin complexes, observed both in light cytosolic fractions and in insoluble fractions. The data fit best with a model where Wnt activation causes recruitment of intact complexes to LRP6, resulting in Axin dephosphorylation and degradation (or at least dissociation of the complex). Recruitment to LRP6 did not seem to inhibit the activity of the complex, thus inconsistent with other models of complex inactivation.

The destabilizing effect of Wnt was clearly affecting only a subset of complexes. The largest cytosolic complexes in general appeared resistant to the action of Wnt. On the contrary, Wnt acted strongly on the intermediate complexes of the light fractions, as well as on the insoluble complexes. We do not know the exact cause of these differences, but part of the answer for the insensitivity of the large complexes may reside in their intrinsic stability. Assuming that Axin dephosphorylation is the trigger for complex inactivation, one may hypothesize that the structure of the large complexes makes Axin inaccessible to PP2A action, or that even when dephosphorylated, Axin does not get degraded nor dissociated, due to the abovementioned strong cooperative binding that must hold these complexes together. Note however that PP2A is present abundantly in the dense and large cytosolic complexes (supplementary Fig.S6A, B), but that it does not antagonize but rather stimulates β-catenin priming (Fig.7A, A'). The simplest explanation for this action is its known action on CK1, releasing its inhibitory autophosphorylation (Gietzen and Virshup 1999).

Note that the loss of Axin in light cytosolic fractions is larger than the loss in activity, also supporting the idea that partial complexes are the most sensitive, which are also those with lower specific activity.

The regulation of the insoluble complex of fraction X remains unclear. Considering the fair assumption that Axin complexes must be recruited to the cell membrane receptors to be inactivated, and the fact that we could not detect any trace of LRP6 in association with this complex, one has to assume that the complex must be translocated during Wnt stimulation. Determining the mechanism responsible for this process will be an interesting but challenging future question.

The membrane-associated complexes

The use of native electrophoresis showed that the Axin pool detected in the membrane fraction perfectly comigrated with LRP6, with strong enrichment in the 1200-1300kDa bands, closely matching the relative distribution of p-LRP6, providing a clear confirmation of the published models of Axin recruitment by the phosphorylated receptor (Bilic *et al.,* 2007, Schwarz-Romond 2007, Pan 2008).

While p-LRP6 levels showed a large increase during Wnt stimulation, the amount of membrane-associated Axin only slightly increased (Fig.5, Fig.10, and supplementary Fig.S1). This can be readily explained based on the model where recruitment to LRP6 leads to Axin degradation. One thus expects that hyper-phosphorylation of the receptor will not only increase Axin binding, but also its subsequent degradation, thus not necessarily changing the steady-state levels at the membrane. This model is fully consistent with the fact that Axin levels in the dense membranes (Fig.4B) and its recruitment to LRP6 (Fig.10) were significantly boosted when proteasomal degradation was inhibited.

These considerations, while confirming previous published data, also lead to a new an interesting observation: that Axin recruitment to the membrane does not require Wnt stimulation. The LRP6-bound pool clearly exists in unstimulated cells, and can be increased by proteasome inhibition in the absence of Wnt. In fact, MG132 treatment mimics most of the effects of Wnt on the membrane fraction, including the

Axin distribution between the various complexes, but also the distribution of most of the associated components, and even increased LRP6 phosphorylation, as well as recruitment of the scaffold protein Amer1 and of CK1γ (Fig.10).

This relates to another surprising observation, the detection of intact complexes in association with LRP6, apparently composed of Axin, CK1α and ε, GSK3 and even APC.

Furthermore, these complexes were clearly still active for β-catenin phosphorylation (Fig.5), further confirmed by the significant levels of various β-catenin forms associated with these complexes (Fig.10 and supplementary Fig.S10). This was not only the case under unstimulated conditions, but also upon Wnt activation (Fig.5, 10, supplementary Fig.S4). Thus membrane recruitment does seem associated with Wnt activation and with Axin destabilization, but it does not inhibit its activity. Taken together, our data suggest that the major mechanism responsible for regulation of the pathway acts via degradation of Axin, triggered by its recruitment to LRP6 receptors.

Conclusion

The regulation of the pathway does not seem to follow the traditional scheme of specific switches in complex composition or activity that is characteristic of classical signaling pathways. Rather it appears to be based on a shift in the balance of a pre-existing process, through which Axin complexes are constitutively recruited by LRP5/6 receptors, leading to Axin destabilization and consequently complex dissociation. We have discovered that different Axin complexes that are differently sensitive/ resistant to Wnt-induced dissociation, either because of differences in binding to LRP6, or to more general differences in complex stability or accessibility to Axin. It is plausible that the largest and most stable complexes, which have also the highest specific activity, may be specifically required to provide a strong baseline β-catenin phosphorylation activity even during Wnt stimulation. Alternatively, the

system could be seen as a “quasi” continuum of multiple complexes with different compositions, activities, stabilities, and kinetics for recruitment to LRP6 and for subsequent dissociation, all of them contributing to an integrated regulation of β-catenin. In this model, there would be different equivalent ways for β-catenin to be sent for degradation, from being released at each individual step and re-captured by another complex, to full processing within one complex. The fate of the various Axin complexes would similarly be diverse, from addition/loss/exchange of components, to movement between cytosolic and insoluble pools, or complete dissociation due to Axin degradation after binding to LRP6. Wnt activation would then modulate this system, perhaps simply by changing the dynamics of receptor interactions/cycling, such that a higher proportion is routed toward the LRP6-degradation pathway.

Material and methods

Antibodies

anti-actin (AC-15) and anti-β-catenin 6F9 (C7082) were from Sigma; anti-α-actinin (BT-GB-276S, Babraham tech); anti-APC C-20 (sc-896), anti-APC N-15 (sc-895), anti-β-catenin H102 (sc-7199), anti-CK1α H-57 (sc-28886), anti-CK1α C-19 (sc-6477), anti-CK1ε C-20 (sc-6471), anti-Dvl2 10B5 (sc-8026), anti-LRP6 C-10 (sc-25317), anti-β-TrCP (sc-8863) and anti-γ-Tubulin C-20 (sc-7396) were from Santa Cruz; anti-Axin2 (ab32197), anti-Lamin B1(ab16048) and anti-γ-Tubulin (ab11316) were from Abcam; anti-GPS-non-phospho-β-catenin (06-734), anti-GSK3 (05-412) and anti-PP2A (05-421) were from Millipore; anti-phospho-β-catenin Ser33/37/Thr41 (9561), anti-phospho-β-catenin Ser45 (9564), anti-Dvl2 30D2 (3224), anti-phospho-LRP6 Ser1490 (2568) and anti-β-TrCP (4394) were from Cell Signaling; anti-APC (mAPC, kindly provided by Inke Nathke); affinity purified anti-Axin (Wiechens *et al.,* 2004); anti-proteasome antibody (I571, kindly provided by K. B. Hendil).

HRP-conjugated secondary antibodies: Donkey anti-Mouse (715-035-150), Donkey

anti-Rabbit (711-035-152), Donkey anti-Goat (705-035-147), Mouse anti-Rabbit, Light Chain (211-032-171), Goat anti-Mouse, Light Chain (115-035-174) (Jackson ImmunoResearch).

Inhibitors

IC261 (400090), GSK3 Inhibitor IX (CAS 667463-62-9), TWS119 (361554) were from Calbiochem); Okadaic Acid (AC328390000, Acros Organics BVBA, final 2μM).

Recombinant His/S-tagged β-catenin

E. coli BL21 cells were transformed with 2 ng of the plasmid. Proteins were then purified on Ni-NTA agarose column and exchanged into kinase buffer (200mM Sucrose, 150mM NaCl, 20mM Hepes-NaOH). Final concentration was adjusted to 1 μg/μl. Purified proteins were aliquoted and stored at -80 °C.

Cell Culture

HEK293 cells and Mouse fibroblast L cells were obtained from American Type Culture Collection (ATCC), and were maintained in Dulbecco's modified Eagle's medium (DMEM, 11965, Gibco) supplemented with 10% fetal bovine serum (FBS, 12483, Gibco).

L-Wnt3a-cells were obtained from ATCC and were grown in DMEM plus 10% FBS and 0.4mg/ml G418 (10131, Gibco). This cell line can express a non-tagged form of Wnt3A protein.

Conditional medium production

L cells and L-Wnt3a-cells were used to produce control and Wnt-conditional medium, respectively. Cells were grown for 2~3 days until 85% confluency in maintaining medium. Old medium of both cell lines was then switched to fresh DMEM plus 10% FBS and cells were left to overgrow for 3~4 days. Produced medium was then collected and filtered. The medium was aliquoted and stored at -80°C.

Cell homogenization

Cells grown in 10cm tissue culture dishes were washed with ice-cold PBS and Osmolysis Buffer (20 mM Hepes-NaOH, 0.2 mM EDTA), and harvested by scraping in 300μl Osmolysis Buffer supplemented with protease inhibitors. Cells were incubated on ice for 5 min to allow swelling, then passed in a Dounce homogenizer

(40 stokes). An equal volume (500 µl) of High Na Buffer (400mM Sucrose, 300mM NaCl, 20mM Hepes-NaOH, and 0.2mM EDTA) was added in the homogenizer, followed by 20 additional strokes. Crude cell homogenate was then collected and kept on ice. When detergents were used, a 2x concentration of detergent was added into the High Na Buffer.

Cell fractionation

The cell fractionation was described in Chapter II. The concentrated membrane fraction was prepared as below: Percoll was removed by spinning at 80000rpm for 1h. The soluble fraction was concentrated with spin tubes from 1ml to ~100 ul. The insoluble materials were resuspended from the filter.

Rate-Zonal Centrifugation

Discontinuous gradients (17%-78%) were prepared by laying 11 successive 340µl layers (final 3.74ml) of sucrose gradient buffer containing 150mM NaCl, 20mM Hepes-NaOH pH 7.4, 0.2mM EDTA, 10mM dithiothreitol and sucrose ranging from 400mM to 2M. 500µl of crude cell homogenate from two 10cm dishes were loaded onto the gradients. Gradients were spun in a Beckman Coulter SW 55Ti rotor at 45,000rpm for 4h at 4°C. Thirteen 340µl fractions were collected, diluted 1:1 with 2xLaemmli sample buffer for analysis by immunoblotting.

Flotation

Crude cell homogenate was separated on SG as described above. Fractions 3+4 and 9+10 were pooled and mixed with an equal volume of 2.2 M sucrose in sucrose gradient buffer. Each pool was then split into 2 aliquots to test density in the presence of absence of 0.1% CHAPS. The samples were laid in a 4ml tube over a 340µl of 2.0M sucrose and covered by two successive 680µl lighter layers. Sucrose in these lighter layers was 1.0M and 0.3M for the light pool, and 1.3M and 0.3M for the intermediate pool. To test for the effect of detergent solubilization, 0.5%CHAPS was added to all solutions. The 4-layer-gradients were spun at 40 300rpm (200 000g) overnight at 4°C.

In vitro Kinase Assay

L-cells were cultured and homogenized or fractionated as mentioned above. The KA

reaction system contained 100mM recombinant β-catenin substrates, 1mM ATP, 1-10μl cell samples (depended on the type of the experiment). The final volume was adjusted to 50μl with kinase buffer. The reaction was carried out by adding the samples and incubating at 37°C for 15 min. The inhibitor was also added in the system for incubation, if necessary. The reaction was stopped by adding 4xLaemmli sample buffer with 20mM EDTA and boiled immediately 2-3 min at 100°C. Relative levels of phosphorylated S45 and S33/S37/T41 were measured by quantitative immunoblotting using commercial phospho-β-catenin antibodies.

Immunoprecipitation

Cytosol was extracted from control and Wnt-stimulated L-cells as mentioned above. Cytosol was then centrifuged at 14,000g for 10min and the supernatant was saved. A small aliquot of the supernatant was mixed with 2x sample buffer as the input, while the rest was incubated with 5–8μg of an appropriate antibody in lysis buffer plus 0.5%NP-40 for 4h at 4°C with constant rotation. 50μl of protein G-plus agarose (sc-2002, Santa Cruz) was added and the incubation continued for an additional 1.5h. Immunoprecipitates were pelleted, washed three times with lysis buffer and were analyzed by SDS-PAGE and western blot.

Immunoblotting and quantification

Samples were separated on SDS-PAGE and transferred to nitrocellulose membranes. Membranes were blocked with Sigma blocking buffer in PBS with 0. 1%Tween-20, incubated overnight with primary antibodies diluted in blocking buffer, and 1-2 hrs with HRP-conjugated secondary antibodies. HRP activity was visualized by a chemiluminescence detection reagent (WBKLS0500, Millipore) with a 12-bit digital camera (Alpha Innotech MultiImage or DNR MicroChemi 2.0). Band intensities were quantified using the Gene Tools software (Syngene) or Image J. And relatively activities were calculated after background subtraction.

Note: Anti-phospho-β-catenin Ser33/37/Thr41 antibody displayed a strong background of non-phosphorylated β-catenin. This reactivity was eliminated by pre-incubating the antibody with 50μg/ml recombinant β-catenin at room temperature for 1h before adding on the membrane. Note that I found that adding too much

recombinant β-catenin may also deplete all the phospho-antibodies.

Blue native gel electrophoresis (BN)

Samples were collected from the above experiments and mixed with 4x Native sample buffer with NO HEATING. The samples were separated on BN (BN1003, Invitrogen), according to manufacturer's instructions. The gel was transferred and immunoblotted as above.

Immunofluorescence staining

Cells were grown on poly-L-lysine-coated coverslips in 24-well plate. Cell were washed rapidly with PBS and immediate fixation with 4% PFA in PBS (10min at room temperature) followed by 5 min permeabilization with 4% PFA, 0.1% Triton-X100. Primary antibody was rabbit anti-Axin. Secondary antibody was Alexa488 (Invitrogen). Nuclei were stained with DRAQ5. Samples were observed under a DMIRE2 microscope (Leica) equipped with a 40 X/1.40 IMM Corr CS oil immersion objective and a Hamamatsu ORCA-ER camera. Images were acquired using MetaMorph (Molecular Devices) software.

Reference

Behrens J., Jerchow B.A., Wurtele M., Grimm J., Asbrand C., Wirtz R., Kuhl M., Wedlich D., Birchmeier W.(1998) Functional interaction of an axin homolog, conductin, with β-catenin, APC, and GSK3β. Science 280:596–599.

Bilic, J. (2007). "Wnt induces LRP6 signalosomes and promotes dishevelled-dependent LRP6 phosphorylation." Science **316**: 1619-1622.

Cadigan, K. M. and M. Peifer (2009). "Wnt Signaling from Development to Disease: Insights from Model Systems." CSH Perspectives in Biology **1**(2).

Cliffe, A., *et al.,* (2003). "A role of Dishevelled in relocating Axin to the plasma membrane during Wingless signaling." Curr Biol **13**: 960-966.

Cole A.R., Sutherland C.. Measuring GSK3 expression and activity in cells. Methods Mol. Biol., 468 (2008), pp. 45–65.

G. Davidson, W. Wu, J. Shen, J. Bilic, U. Fenger, P. Stannek, A. Glinka, C. Niehrs. Casein kinase 1 gamma couples Wnt receptor activation to cytoplasmic signal transduction. Nature, 438 (2005), pp. 867–872.

Fagotto, F. (1999). "Domains of axin involved in protein-protein interactions, wnt pathway inhibition, and intracellular localization." J. Cell Biol. **145**: 741-756.

Farr, I. G., *et al.,* (2000). "Interaction among GSK-3, GBP, Axin, and APC in *Xenopus* axis specification." J Cell Biol **148**: 691-702.

Fumoto, K., *et al.,* (2006). "GSK-3beta-regulated interaction of BICD with dynein is involved in microtubule anchorage at centrosome." EMBO J **25**: 5670-5682.

González-Sancho, J. M., *et al.,* (2013). "Functional Consequences of Wnt-induced Dishevelled 2 Phosphorylation in Canonical and Noncanonical Wnt Signaling." Journal of Biological Chemistry **288**(13): 9428-9437.

González-Sancho JM, Brennan KR, Castelo-Soccio LA, Brown AM. Wnt proteins induce dishevelled phosphorylation via an LRP5/6- independent mechanism, irrespective of their ability to stabilize beta-catenin. Mol Cell Biol. 2004 Jun;24(11):4757-68.

Gottardi, C.J., B.M. Gumbiner. 2004a. Distinct molecular forms of β-catenin are targeted to adhesive or transcriptional complexes. J. Cell Biol. 167:339–349.

Gusev, E. (2012). "Regulation of the Wnt pathway: analysis of ß-catenin phosphorylation by the endogenous Axin-based complexes." Thesis, MSc. McGill University.

Ha, N. C., *et al.,* (2004). "Mechanism of phosphorylation-dependent binding of APC to [beta]-catenin and its role in [beta]-catenin degradation." Mol Cell 15: 511-521.

Hart M.J., de los Santos R., Albert I.N., Rubinfeld B., Polakis P.(1998) Downregulation of beta-catenin by human Axin and its association with the APC tumor suppressor, beta-catenin and GSK3 beta. Curr. Biol. 8:573–581.

Hendriksen, J., *et al.,* (2008). "Plasma membrane recruitment of dephosphorylated beta-catenin upon activation of the Wnt pathway." J Cell Sci **121**: 1793-1802.

Hernández, A. R., *et al.,* (2012). "Kinetic Responses of β-catenin Specify the Sites of Wnt Control." Science **338**(6112): 1337-1340.

Hinoi, T., *et al.,* (2000). "Complex formation of adenomatous polyposis coli gene product and axin facilitates glycogen synthase kinase-3 beta-dependent phosphorylation of beta-catenin and down-regulates beta-catenin." J Biol Chem 275(44): 34399-34406.

Hsu, W., Zeng, L. and Costantini, F. (1999) Identification of a domain of Axin that binds to the serine/threonine protein phosphatase 2A and a self-binding domain. JBC 274, **3439-3445.**

Ikeda S, Kishida S, Yamamoto H, Murai H, Koyama S, Kikuchi A. Axin, a negative regulator of the Wnt signaling pathway, forms a complex with GSK-3beta and beta-catenin and promotes GSK-3beta-dependent phosphorylation of beta-catenin. EMBO J. 1998;17:1371–1384.

Janssens, J. Goris. Protein phosphatase 2A: a highly regulated family of serine/threonine phosphatases implicated in cell growth and signaling. Biochem. J., 353 (2001), pp. 417–439.

Jho E, Lomvardas S, Costantini F. A GSK3beta phosphorylation site in axin modulates interaction with beta-catenin and Tcf-mediated gene expression. Biochem Biophys Res Commun. 1999;266:28–35.

Kim, S.-E., *et al.,* (2013). "Wnt Stabilization of beta-Catenin Reveals Principles for Morphogen Receptor-Scaffold Assemblies." Science **340**(6134): 867-870.

Kimelman D, Xu W. beta-catenin destruction complex: insights and questions from a structural perspective. Oncogene. 2006;25:7482–7491.

Lee, E., *et al.,* (2003). "The roles of APC and Axin derived from experimental and theoretical analysis of the Wnt pathway." PLoS Biol **1**: E10.

Li, V., *et al.,* (2012). "Wnt signaling inhibits proteasomal [beta]-catenin degradation within a compositionally intact Axin1 complex." Cell.

Liu, G., *et al.,* (2003). "A novel mechanism for Wnt activation of canonical signaling through the LRP6 receptor." Mol Cell Biol **23**: 5825-5835.

Liu, X., *et al.,* (2005). "Rapid, Wnt-induced changes in GSK3[beta] associations that regulate [beta]-catenin stabilization are mediated by G[alpha] proteins." Curr Biol **15**: 1989-1997.

Liu X., Fagotto F. (2011). A method to separate nuclear, cytosolic, and membrane-associated signaling molecules in cultured cells. Sci Signal 4: pl2

Logan, C. Y. and R. Nusse (2004). "The Wnt signaling pathway in development and disease." Annu. Rev. Cell Dev. Biol. **20**: 781-810.

Luo, W. and S. C. Lin (2004). "Axin: a master scaffold for multiple signaling pathways." Neurosignals **13**(3): 99-113.

Luo, W., *et al.,* (2007). "Protein phosphatase 1 regulates assembly and function of the beta-catenin degradation complex." EMBO J **26**(6): 1511-1521.

MacDonald, B. T. and X. He (2012). "Frizzled and LRP5/6 Receptors for Wnt/β-catenin Signaling." CSH Perspectives in Biology **4**(12).

MacDonald, B. T., *et al.,* (2009). "Wnt/beta-catenin signaling: components, mechanisms, and diseases." Dev Cell **17**: 9-26.

Mao, J. (2001). "Low-density lipoprotein receptor-related protein-5 binds to Axin and regulates the canonical Wnt signaling pathway." Mol. Cell **7**: 801-809.

Mosimann, G. Hausmann, K. Basler. Beta-catenin hits chromatin: regulation of Wnt target gene activation. Nat. Rev. Mol. Cell Biol., 10 (2009), pp. 276–286

Nathke IS, Adams CL, Polakis P, Sellin JH, Nelson WJ. The adenomatous polyposis coli tumor suppressor protein localizes to plasma membrane sites involved in active

cell migration. J Cell Biol. 1996;134:165–179.

Piao S, Lee S-H, Kim H, Yum S, Stamos JL, Xu Y, Lee S-J, Lee J, Oh S, Han J-K, Park B-J, Weis WI, Ha N-C (2008) Direct inhibition of GSK3beta by the phosphorylated cytoplasmic domain of LRP6 in Wnt/beta-catenin signaling. PLoS ONE 3:e4046

Pan, W. (2008). "Wnt3a-mediated formation of phosphatidylinositol 4,5-bisphosphate regulates LRP6 phosphorylation." Science **321**: 1350-1353.

Ranganathan S, Liu CX, Migliorini MM, Von Arnim CA, Peltan ID, Mikhailenko I, Hyman BT, Strickland DK. Serine and threonine phosphorylation of the low density lipoprotein receptor-related protein by protein kinase Calpha regulates endocytosis and association with adaptor molecules. J Biol Chem. 2004;**279**:40536–40544.

Reinacher-Schick A, Gumbiner BM. Apical membrane localization of the adenomatous polyposis coli tumor suppressor protein and subcellular distribution of the beta-catenin destruction complex in polarized epithelial cells. J Cell Biol. 2001;152:491–502.

Roberts, D. M., *et al.,* (2012). "Defining components of the ss-catenin destruction complex and exploring its regulation and mechanisms of action during development." PLoS ONE **7**(2): e31284.

Roberts, D. M., *et al.,* (2011). "Deconstructing the szcatenin destruction complex: mechanistic roles for the tumor suppressor APC in regulating Wnt signaling." Mol Biol Cell **22**: 1845-1863.

Saito-Diaz, K., *et al.,* (2013). "The way Wnt works: components and mechanism." Growth Factors **31**(1): 1-31.

Salic, A., *et al.,* (2000). "Control of [beta]-catenin stability: reconstitution of the cytoplasmic steps of the wnt pathway in *Xenopus* egg extracts." Mol. Cell **5**: 523-532.

Schuck S, Honsho M, Ekroos K, Shevchenko A, Simons K. 2003. Resistance of cell membranes to different detergents. Proc. Natl. Acad. Sci. USA 100:5795–800

Seeling, J. M., Miller, J. R., Gil, R., Moon, R. T., White, R. and Virshup, D. M. (1999) Regulation of β-catenin signaling by the B56 subunit of protein phosphatase 2A. Science 283, 2089–2091

Siegfried E, Perkins LA, Capaci TM, Perrimon N. Putative protein kinase product of the *Drosophila* segment-polarity gene zeste-white3. Nature. 1990 345(6278):825-9.

Su, Y., *et al.,* (2008). "APC is essential for targeting phosphorylated beta-catenin to the SCFbeta-Trcp ubiquitin ligase." Mol Cell **32**: 652-661.

Taelman, V. F. (2010). "Wnt signaling requires sequestration of glycogen synthase kinase 3 inside multivesicular endosomes." Cell **143**: 1136-1148.

Tan, C. W., *et al.,* (2012). "Wnt signalling pathway parameters for mammalian cells." PLoS ONE **7**(2): e31882.

Tanneberger K., Pfister A. S., Brauburger K., Schneikert J., Hadjihannas M. V., Kriz V., Schulte G., Bryja V., Behrens J. (2011) Amer1/WTX couples Wnt-induced formation of PtdIns(4,5)P2 to LRP6 phosphorylation. EMBO J. 30, 1433–1443.

Tran, H. and P. Polakis (2012). "Reversible modification of adenomatous polyposis coli (APC) with K63-linked polyubiquitin regulates the assembly and activity of the beta-catenin destruction complex." J Biol Chem **287**(34): 28552-28563.

Valvezan, A. J., *et al.,* (2012). "Adenomatous polyposis coli (APC) regulates multiple signaling pathways by enhancing glycogen synthase kinase-3 (GSK-3) activity." J Biol Chem **287**(6): 3823-3832.

Wang L., Liu X., Gusev E., Wang C., Fagotto F. (2014). Regulation of β-catenin phosphorylation and nuclear/cytoplasmic transport by APC and its cancer-related truncated form. In process.

Willert K, Shibamoto S, Nusse R. Wnt-induced dephosphorylation of axin releases beta-catenin fromthe axin complex. Genes Dev 1999; 13:1768-73.

Wu D., Pan W. (2010). GSK3: a multifaceted kinase in Wnt signaling. Trends Biochem. Sci. 35 161–168.

Wu, G., *et al.,* (2009). "Inhibition of GSK3 phosphorylation of β-catenin via phosphorylated PPPSPXS motifs of Wnt coreceptor LRP6." PLoS ONE **4**: e4926.

Xing, Y., *et al.,* (2004). "Crystal structure of a [beta]-catenin/APC complex reveals a critical role for APC phosphorylation in APC function." Mol Cell **15**: 523-533.

Yamamoto, H., *et al.,* (2001). "Inhibition of the Wnt signaling pathway by the PR61 subunit of protein phosphatase 2A." J Biol Chem 276(29): 26875-26882.

Yamamoto, H., *et al.,* (1999). "Phosphorylation of axin, a Wnt signal negative regulator, by glycogen synthase kinase-3beta regulates its stability." J Biol Chem 274: 10681-10684.

Yamamoto H., Komekado H., Kikuchi A. 2006. Caveolin is necessary for Wnt-3a-dependent internalization of LRP6 and accumulation of beta-catenin. Dev. Cell. 11:213–223.10.1016.

Hideki Yamamoto, Hiroshi Sakane, Hideki Yamamoto, Tatsuo Michiue, Akira Kikuchi. Wnt3a and Dkk1 Regulate Distinct Internalization Pathways of LRP6 to Tune the Activation of β-catenin Signaling. Developmental Cell, 2008, 15:1, 37-48.

Yost, C., *et al.,* (1998). "GBP, an inhibitor of GSK-3, is implicated in *Xenopus* development and oncogenesis." Cell **93**: 1031-1041.

Zeng, L., *et al.,* (1997). "The mouse Fused locus encodes Axin, an inhibitor of the Wnt signaling pathway that regulates embryonic axis formation." Cell **90**: 181-192.

.
Zeng, X., Tamai, K., Doble, B., Li, S., Huang, H., Habas, R., Okamura, H., Woodgett, J. and He, X. (2005). A dual-kinase mechanism for Wnt co-receptor phosphorylation and activation. Nature **438**, 873-877.

Zeng, X., *et al.,* (2008). "Initiation of Wnt signaling: control of Wnt coreceptor Lrp6 phosphorylation/activation via frizzled, dishevelled and axin functions." Development **135**: 367-375.

Figure

Figure 1. Establishment of an *in vitro* β-catenin phosphorylation assay.

A) Diagram of β-catenin and detail of the N-terminal phosphorylation sites. Phosphorylation occurs in sequential steps, starting by priming at serine 45 by CK1, followed by stepwise phosphorylation at threonine 41, serine 37 and serine 33 by GSK3. Commercial antibodies are available to recognize phosphorylated β-catenin forms. **A'**) β-catenin phosphorylation is antagonized by dephosphorylation performed by phosphatase PP2A.

B) Basic characterization of the phosphorylation reactions: Effect of kinase and phosphatase inhibitors on the activity from crude L cell homogenate. Reactions were incubated for 15 min in the absence (ctrl) or presence of the various inhibitors. The reactions were analyzed by quantitative immunoblotting using anti-pSer45 and anti-pSer33/37/Thr41 antibodies.

C) Quantification. Average of 2-3 experiments. Error bars, SD.

D) Characteristics of the inhibitors. IC261 was used at two different concentrations, the lowest inhibiting specifically CK1δ/ε.

Figure 1

A

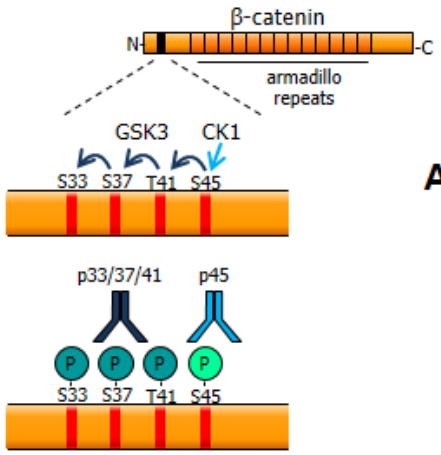

A'

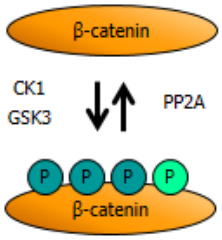

B

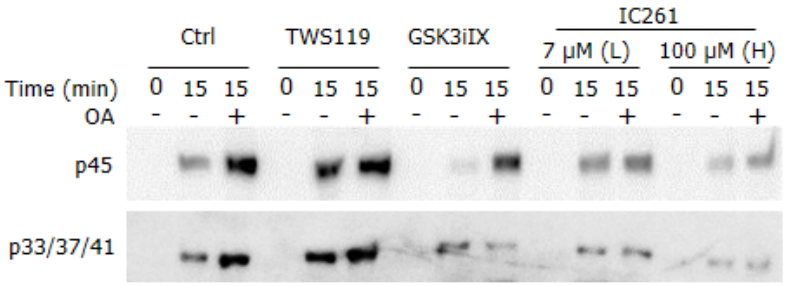

C

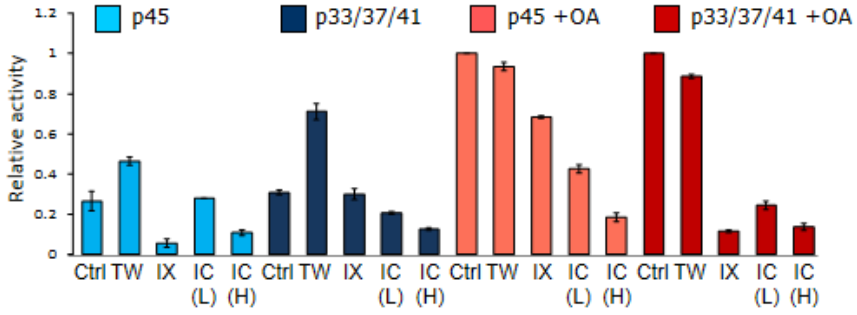

D

Inhibitor	Specificity	IC50	Final conc. in assay
GSK3iIX	GSK3α/β	5 nM	25 nM
TWS119	GSK3β	30 nM	150 nM
IC261	CK1 δ/ε	0.6-1.4 μM	7 μM (Low) 100 μM (High)
	CK1 α	11-21 μM	

Figure 2. Characterization of endogenous β-catenin phosphorylation activity.

A) Analysis of phosphorylated β-catenin product from the reaction by blue native gel electrophoresis. *In vitro* kinase assay was performed using wild type recombinant β-catenin and cytosol (Cs) and insoluble material (insol) from L cells. Reactions were incubated for 15 min and 60 min in the absence or presence of OA. Pure recombinant β-catenin blotted for total β-catenin antibodies was used as control. A small amount of phosphorylated β-catenin appears associated with a large complex (double arrow), but most migrates with an apparent low molecular weight, indicating that it is released from the complex. The fraction associated with the large complex is larger for p45 than p33/37/41. The free pool is more sensitive to de-phosphorylation by PP2A (compared +/- OA). The patterns are very similar for reactions using cytosolic and insoluble material.

B) Effects of Wnt stimulation on β-catenin phosphorylation by crude L cell homogenate. L cells were treated for 30 min with control and Wnt conditioned medium, respectively. Both p45 and p33/37/41 activities were inhibited by Wnt stimulation, both in the absence or presence of OA.

B') Quantification, expressed as relative activity compared to control 15 min. Average of 2-3 experiments. Error bars, SD.

Figure 2

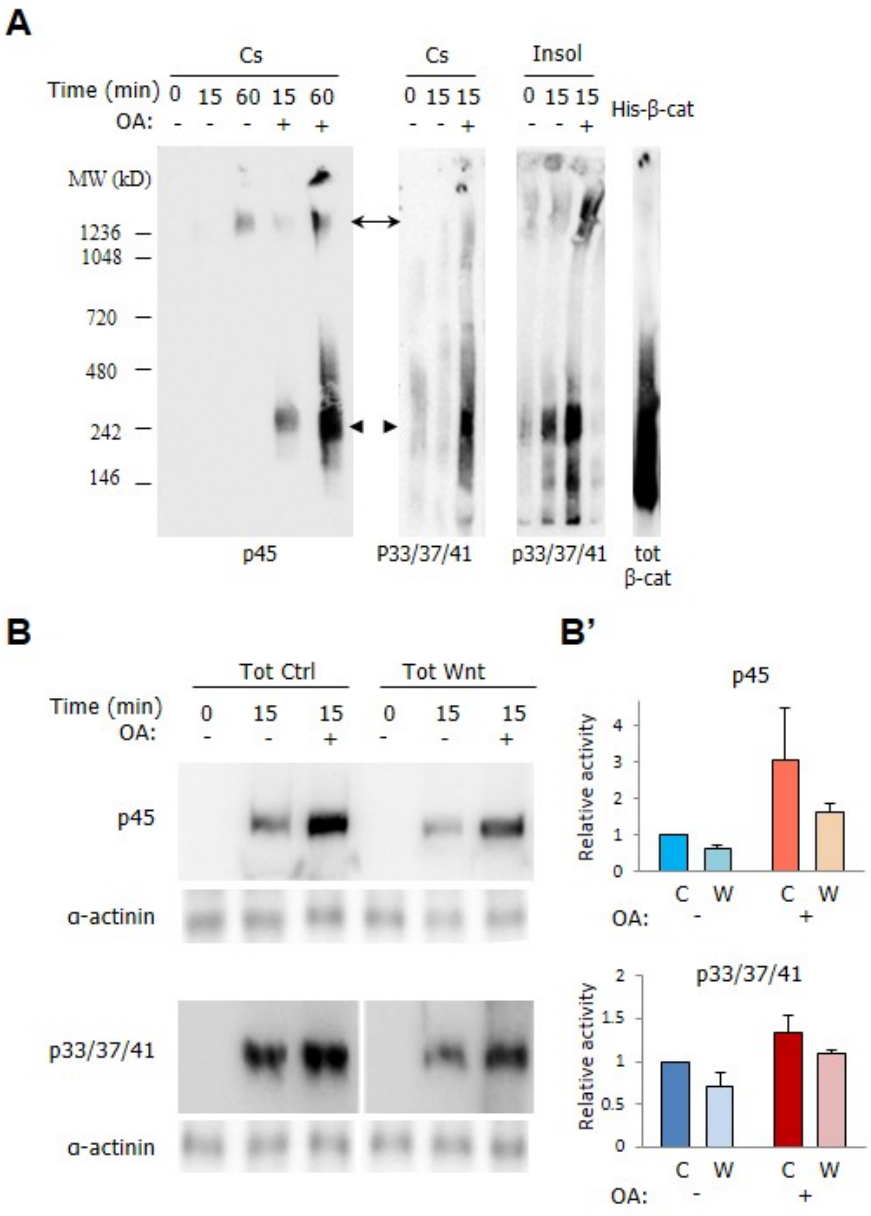
A
Cs
Cs
Insol
Time (min) 0 15 60 15 60
0 15 15
0 15 15
OA: - - - + +
- - +
- - +
His-β-cat
MW (kD)
1236
1048
720
480
242
146
p45
P33/37/41
p33/37/41
tot β-cat
B
B'
Tot Ctrl
Tot Wnt
Time (min) 0 15 15 0 15 15
OA: - - + - - +
p45
α-actinin
p33/37/41
α-actinin
p45
Relative activity
C W C W
OA: - +
p33/37/41
Relative activity
C W C W
OA: - +

Figure 3. Identification of multiple Axin-based complexes.

L cells were treated with control or Wnt conditioned medium for 30 min. Crude homogenates were separated by zonal-rate centrifugation on a sucrose gradient (SG).

A) *In vitro* phosphorylation assay.

B) Distribution of Axin and various associated components.

C-E) Quantification. Activities and Axin levels are expressed as fraction of total (sum of all fractions). Average of 2-3 experiments.

C', D', E') Same graphs with enlarged scale to show details of the weakest signals.

Figure 3

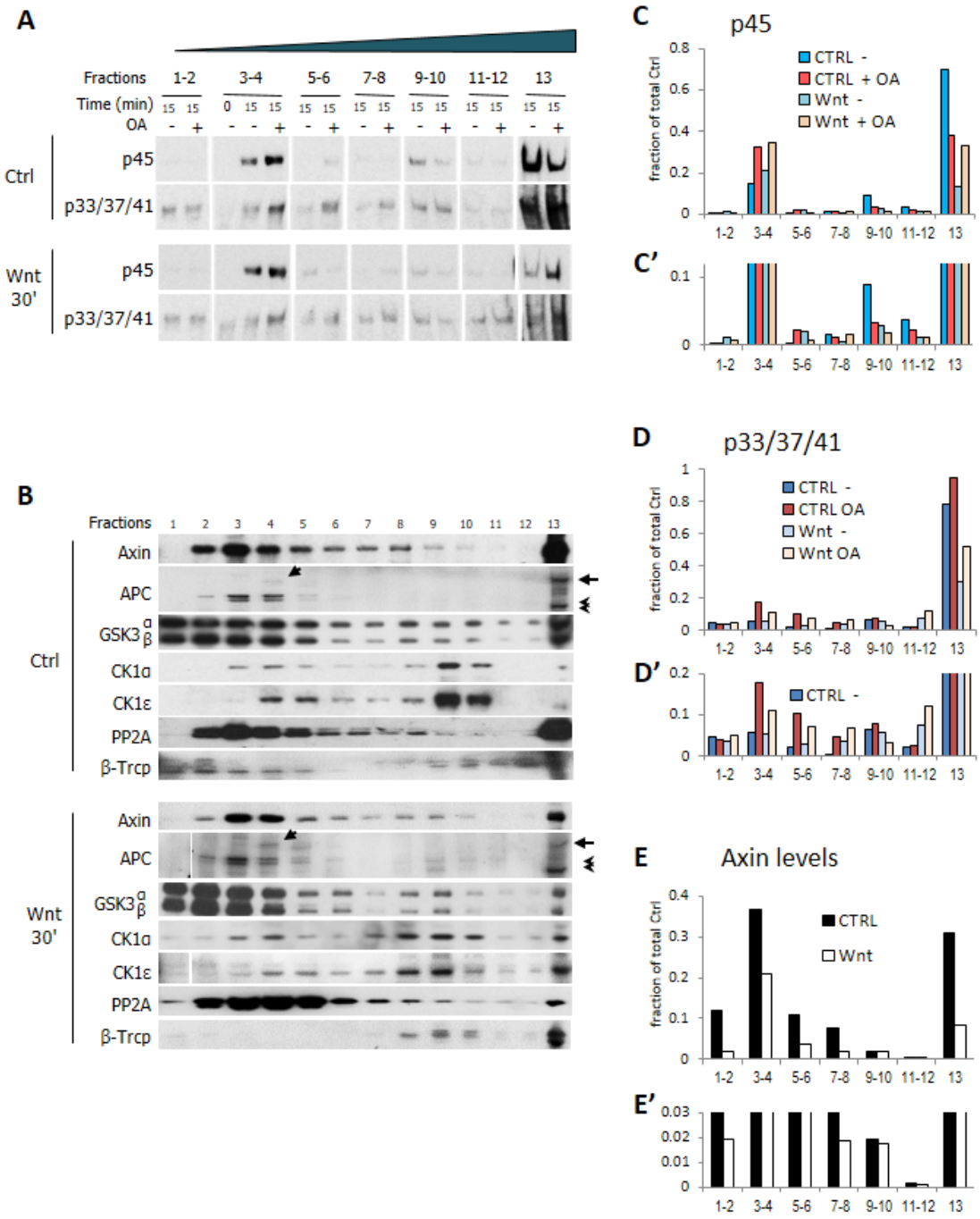
A
Fractions 1-2 3-4 5-6 7-8 9-10 11-12 13
Time (min) 15 15 0 15 15 15 15 15 15 15 15 15 15 15
OA - + - - + - + - + - + - + - +
Ctrl
p45
p33/37/41
Wnt 30'
p45
p33/37/41
B
Fractions 1 2 3 4 5 6 7 8 9 10 11 12 13
Ctrl
Axin
APC
GSK3 α β
CK1α
CK1ε
PP2A
β-Trcp
Wnt 30'
Axin
APC
GSK3 α β
CK1α
CK1ε
PP2A
β-Trcp
C
p45
fraction of total Ctrl
CTRL -
CTRL + OA
Wnt -
Wnt + OA
1-2 3-4 5-6 7-8 9-10 11-12 13
C'
D
p33/37/41
fraction of total Ctrl
CTRL -
CTRL OA
Wnt -
Wnt OA
1-2 3-4 5-6 7-8 9-10 11-12 13
D'
CTRL -
E
Axin levels
fraction of total Ctrl
CTRL
Wnt
1-2 3-4 5-6 7-8 9-10 11-12 13
E'

Figure 4. Membrane association and sensitivity to proteasomal degradation.

A) Detection of Axin membrane association by flotation. Two pools, separated on SG from crude extract, were analyzed by equilibrium density centrifugation (four layer discontinuous gradients) in the absence or presence of 0.5% mild detergent CHAPS. Arrows indicate the initial position of the samples. Part of the light pool and most of the dense pool showed a higher apparent density in the presence of CHAPS, indicating membrane association.

B-C) Instability of the dense membrane-associated pool.

B, B') L cells were treated with either DMSO (CTRL) or MG132 for 4h. Crude homogenates were separated on a SG in the absence (**B**) or presence of CHAPS (**B'**). MG132 caused a strong increase in Axin and GSK3 levels in dense fractions F7-10. The pool was absent when CHAPS was included in the SG, indicating that it was membrane associated.

C) Control and MG132-treated cells were fractionated in cytosol (Cs), nucleosol (Ns), nuclear insoluble (Ni), membrane (M) and dense insoluble (X) fractions, which were analyzed for Axin.

C') Quantification. The membrane fraction was the only one showing significant increased Axin levels upon MG132 treatment.

Figure 4

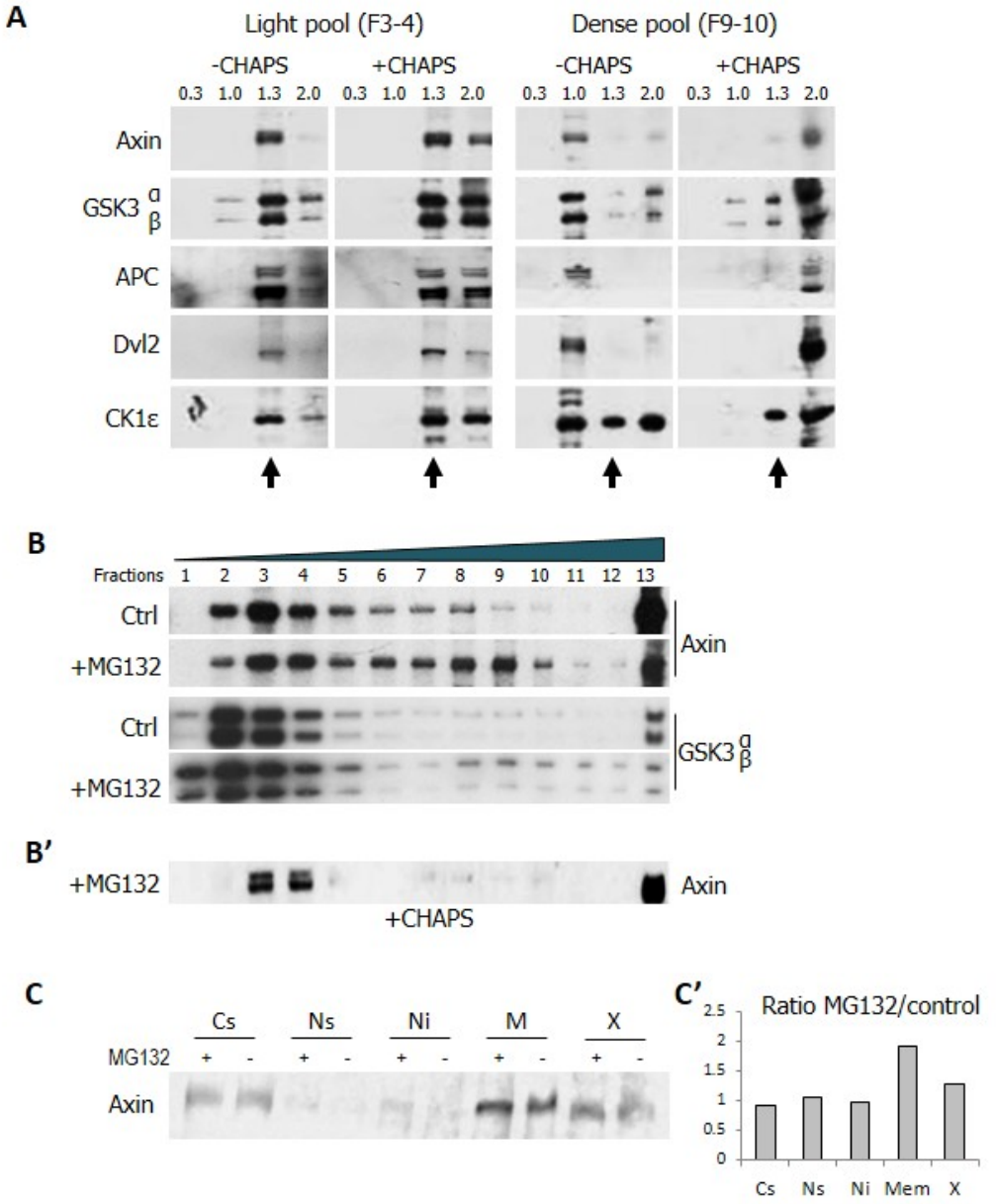
A
Light pool (F3-4)
Dense pool (F9-10)
-CHAPS
+CHAPS
-CHAPS
+CHAPS
0.3 1.0 1.3 2.0 0.3 1.0 1.3 2.0 0.3 1.0 1.3 2.0 0.3 1.0 1.3 2.0
Axin
GSK3 α β
APC
Dvl2
CK1ε
B
Fractions 1 2 3 4 5 6 7 8 9 10 11 12 13
Ctrl
+MG132
Ctrl
+MG132
Axin
GSK3 α β
B'
+MG132
Axin
+CHAPS
C
Cs Ns Ni M X
MG132 + - + - + - + - + -
Axin
C'
Ratio MG132/control
2.5
2
1.5
1
0.5
0
Cs Ns Ni Mem X

Figure 5. Subcellular localization of β-catenin phosphorylation activities.

A) Example of *in vitro* kinase assay on cell fractions from control and Wnt-treated cells.

B, C) Quantification. Average of 2-3 experiments. Error bars, SD.

B) Activities are expressed as relative activities, control cytosol values were set at 1. The values were corrected for fraction volumes, and corresponded to the total activities in each cell compartment. p45 phosphorylation was determined using wild type recombinant β-catenin, 33/37/41 using both wild type and S45D β-catenin substrates. S45D mimicked CK1 primed β-catenin, and was used to monitor p33/37/41 activity independently of the priming step. p45 phosphorylation was distributed in all fractions, p33/37/41 was proportionally enriched in the cytosol.

C) Ratio between the activity in Wnt-treated and control conditions. Wnt stimulation appeared to mostly affect the cytosol, where all activities were decreased to about 60% of control levels. A smaller decrease was observed for fraction X. The activities were increased in the membrane fraction. Average of 3-5 experiments. Error bars, SD. P values, Student's t-test.

D) Subcellular distribution of Axin and GSK3.

D') Quantification of Axin. Average of 2 experiments. Error bars, SD. ** indicate $p<0.01$ between Wnt-treated and controls, Student's t-test.

E) Comparison of relative activities (ratio β-catenin phosphorylation to Axin). Control activities in the cytosol were set to 1. p45 relative activity was relatively lower in the cytosol.

E') Comparison of relative activities between Wnt-treated and control conditions. Relative cytosolic activities were in all cases significantly inhibited. p45 relative activity was increased in the other fractions. Error bars, SD. P values, Student's t-test.

Figure 5

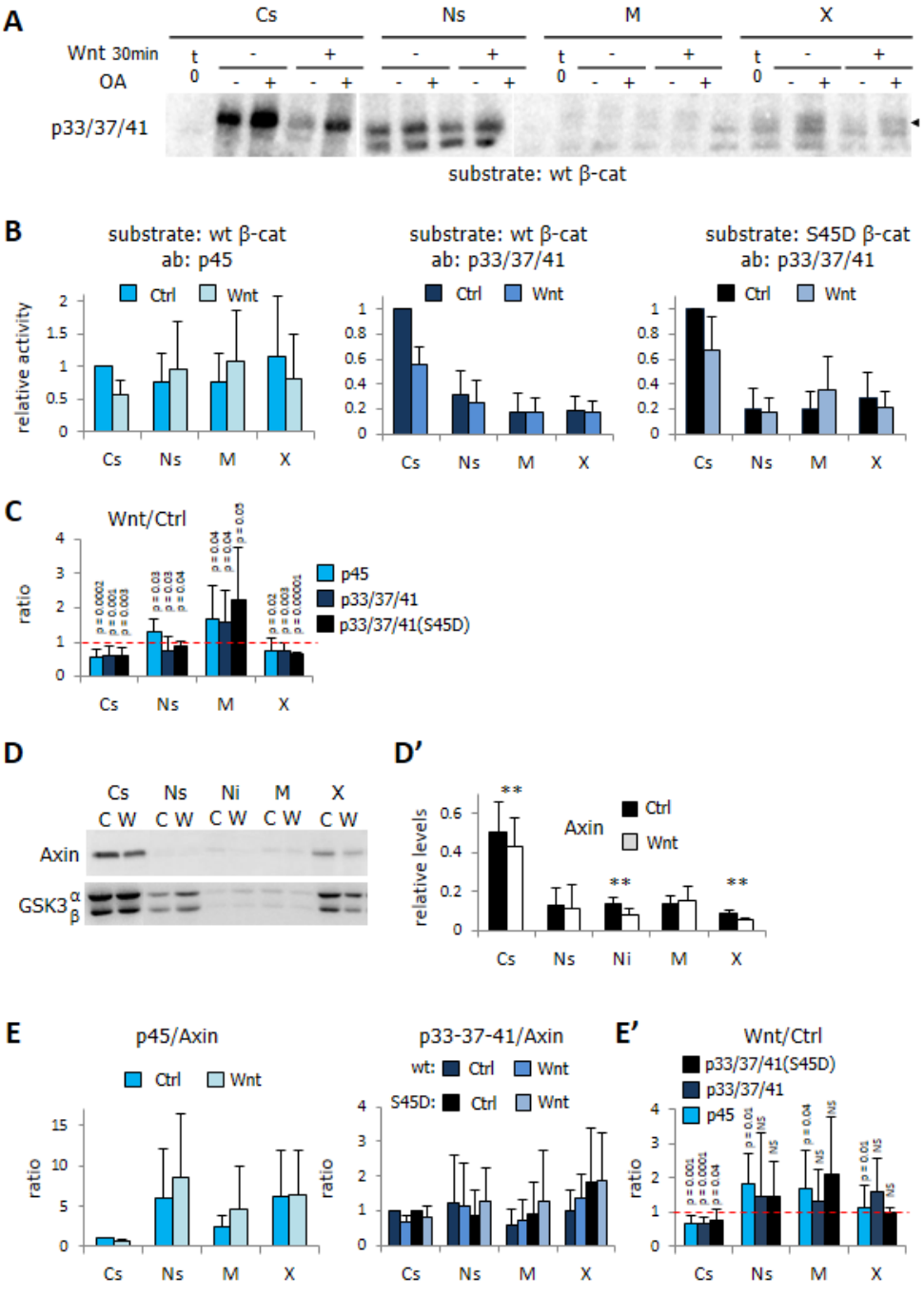
A
Cs
Ns
M
X
Wnt 30min
OA
t 0
p33/37/41
substrate: wt β-cat
B
substrate: wt β-cat
ab: p45
substrate: wt β-cat
ab: p33/37/41
substrate: S45D β-cat
ab: p33/37/41
Ctrl
Wnt
relative activity
C
Wnt/Ctrl
ratio
p45
p33/37/41
p33/37/41(S45D)
D
Cs Ns Ni M X
C W C W C W C W C W
Axin
GSK3 α β
D'
relative levels
Axin
Ctrl
Wnt
E
p45/Axin
p33-37-41/Axin
wt: Ctrl Wnt
S45D: Ctrl Wnt
ratio
E'
Wnt/Ctrl
p33/37/41(S45D)
p33/37/41
p45

Figure 6. Identification of Axin complexes with distinct sizes.

A) Blue native gel electrophoresis (BNGE) of cytosolic (Cs), nucleosolic (Ns) and membrane (M) fractions from control (C) and 30min Wnt-treated (W) cells. Axin migrated as multiple discrete bands, indicating the existence of several complexes. Soluble fractions reproducibly showed major bands on the 300-500kDa range and at least three additional bands with much higher apparent size (colored arrows). Note the very low levels of free Axin (black arrow). Arrowhead: Axin fragment. Membrane fractions also show several bands. Wnt activation leads to a general decrease of most soluble complexes, and an increase in membrane complexes.

B) Axin elution from a S200 gel filtration column loaded with a cytosolic extract.

C) BNGE of pools from gel filtration fractions.

D) Example of β-catenin phosphorylation assay using total cytosol (Cs) and pooled fractions from a S200 gel filtration. **D'** and **D"**) Quantification. Average of 2-3 experiments. Error bars, SD. **D'**) Total activities. **D"**) Specific activities (ratio to Axin levels). Note the strikingly different patterns and sensitivity to okadaic acid.

E, E') Corresponding immunoblot for Axin levels and quantification. Average of 2-3 experiments. Error bars, SD.

Figure 6

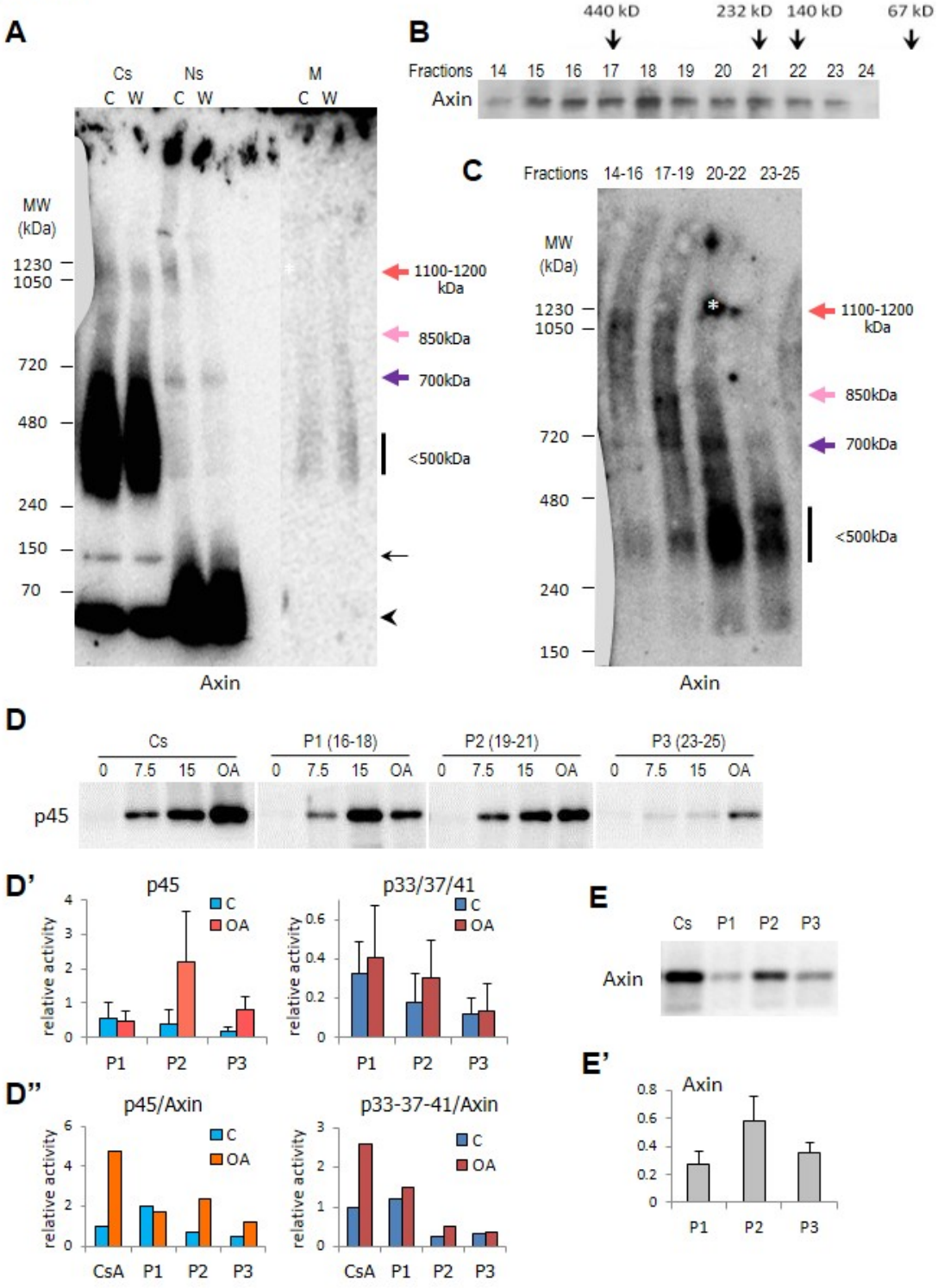
A
Cs
Ns
M
C W C W C W
MW (kDa)
1230
1050
720
480
240
150
70
1100-1200 kDa
850kDa
700kDa
<500kDa
Axin
B
440 kD
232 kD
140 kD
67 kD
Fractions 14 15 16 17 18 19 20 21 22 23 24
Axin
C
Fractions 14-16 17-19 20-22 23-25
MW (kDa)
1230
1050
720
480
240
150
1100-1200 kDa
850kDa
700kDa
<500kDa
Axin
D
Cs
P1 (16-18)
P2 (19-21)
P3 (23-25)
0 7.5 15 OA
p45
D'
p45
p33/37/41
C
OA
relative activity
P1 P2 P3
D''
p45/Axin
p33-37-41/Axin
CsA P1 P2 P3
E
Cs P1 P2 P3
Axin
E'
Axin
P1 P2 P3

Figure 7. Analysis of cytosol from control and Wnt-stimulated cells by rate-zonal centrifugation.

Cytosol from control and 30min Wnt-treated cells were separated on a sucrose gradient. Fractions were analyzed for β-catenin phosphorylation (**A** and **B**) and for Axin levels (**C**).

A, **B**, **C**) Examples of immunoblots.

A', **B'**, **C'**) Quantifications. Different pools showed distinct total and specific activities, sensitivity to okadaic acid (OA) and Wnt stimulation (see main text). Average of 3-4 experiments. Error bars, SD. * indicate $p<0.05$ between OA conditions +/- Wnt, Student's t-test (**A'** and **B'**). **C'**) Average of 3-4 experiments. Error bars, SD. * indicate $p<0.05$ and ** indicate $p<0.01$ between Wnt-treated and controls, Student's t-test (3-4 experiments).

Figure 7

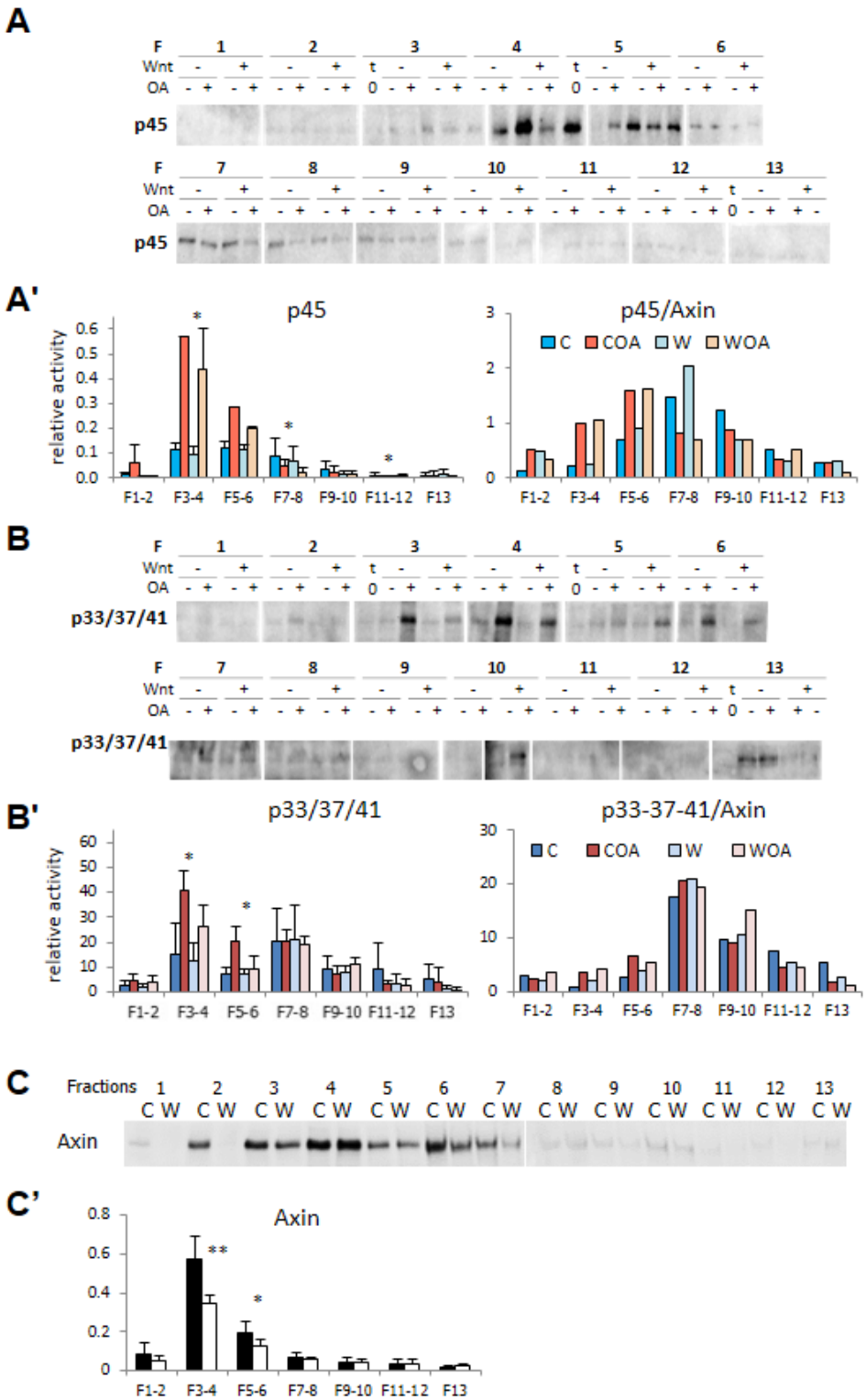
A
F 1 2 3 4 5 6
Wnt - + - + t - + - + t - + - +
OA - + - + - + - + 0 - + - + - + - + 0 - + - + - + - +
p45
F 7 8 9 10 11 12 13
Wnt - + - + - + - + - + - + t - +
OA - + - + - + - + - + - + - + - + - + 0 - + + -
p45
A'
p45
p45/Axin
C COA W WOA
relative activity
F1-2 F3-4 F5-6 F7-8 F9-10 F11-12 F13
B
p33/37/41
B'
p33-37-41/Axin
C
Fractions 1 2 3 4 5 6 7 8 9 10 11 12 13
C W C W C W C W C W C W C W C W C W C W C W C W C W
Axin
C'
Axin

Figure 8. BNGE analysis of cytosolic Axin complexes.

Cytosol from control and 30min Wnt-treated cells were separated on a sucrose gradient. Pools of fractions were separated by BNGE, which were systematically analyzed for components of the Axin complex. Precise co-migration was interpreted as evidence for complex association.

A) Example of a migration patterns for a subset of components from intermediate fractions F7-F8. Major Axin complexes were similar to those detected in whole cytosol, see Fig.6A. Note that some Axin bands are broader (here 1200kDa) than for other markers (e.g. CK1α), but peaks nevertheless reproducibly colocalize. Note strong differences in the relative intensities of the bands, consistent with distinct compositions and activities. For instance, the 850 and 1200kDa complexes were enriched in phosphorylated β-catenin compared to the 700kDa complex, despite similar CK1α levels, and the much lower signal for Axin.

B) Example of BGNE gels for the pellet fraction (F13). Only the top part is shown, since it contained most of the signal (see supplementary figure S5 for image of the whole lanes). All analyzed components co-migrated in a very high position (apparent MW > 1500kDa).

Complete analysis of all pools and components is shown in supplementary figure S5, and quantitative analysis is provided in supplementary figure S6 and S7.

Figure 8

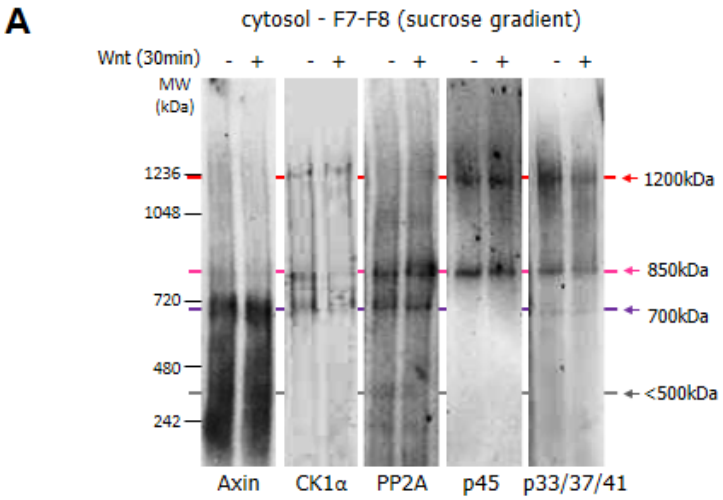
A
cytosol - F7-F8 (sucrose gradient)
Wnt (30min) - + - + - + - + - +
MW (kDa)
1236
1048
720
480
242
1200kDa
850kDa
700kDa
<500kDa
Axin
CK1α
PP2A
p45
p33/37/41

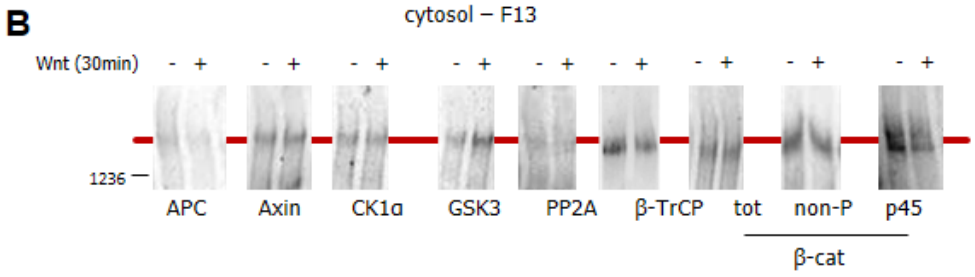
B
cytosol – F13
Wnt (30min) - + - + - + - + - + - + - + - +
1236
APC
Axin
CK1α
GSK3
PP2A
β-TrCP
tot
non-P
p45
β-cat

Figure 9. Characterization of insoluble Axin complex.

The insoluble fraction (X) was re-suspended and further separated by a sucrose gradient.

A) β-catenin phosphorylation activity. Activities are concentrated in dense fractions 8-11.

B) Distribution of Axin, CK1ε and GSK3. See supplementary Fig.S9 for complete analysis.

B') Quantification of A and B.

C) Distribution of the organelle markers. The major peak of Axin and phosphorylation activity does not cosediment with any of the markers.

Figure 9

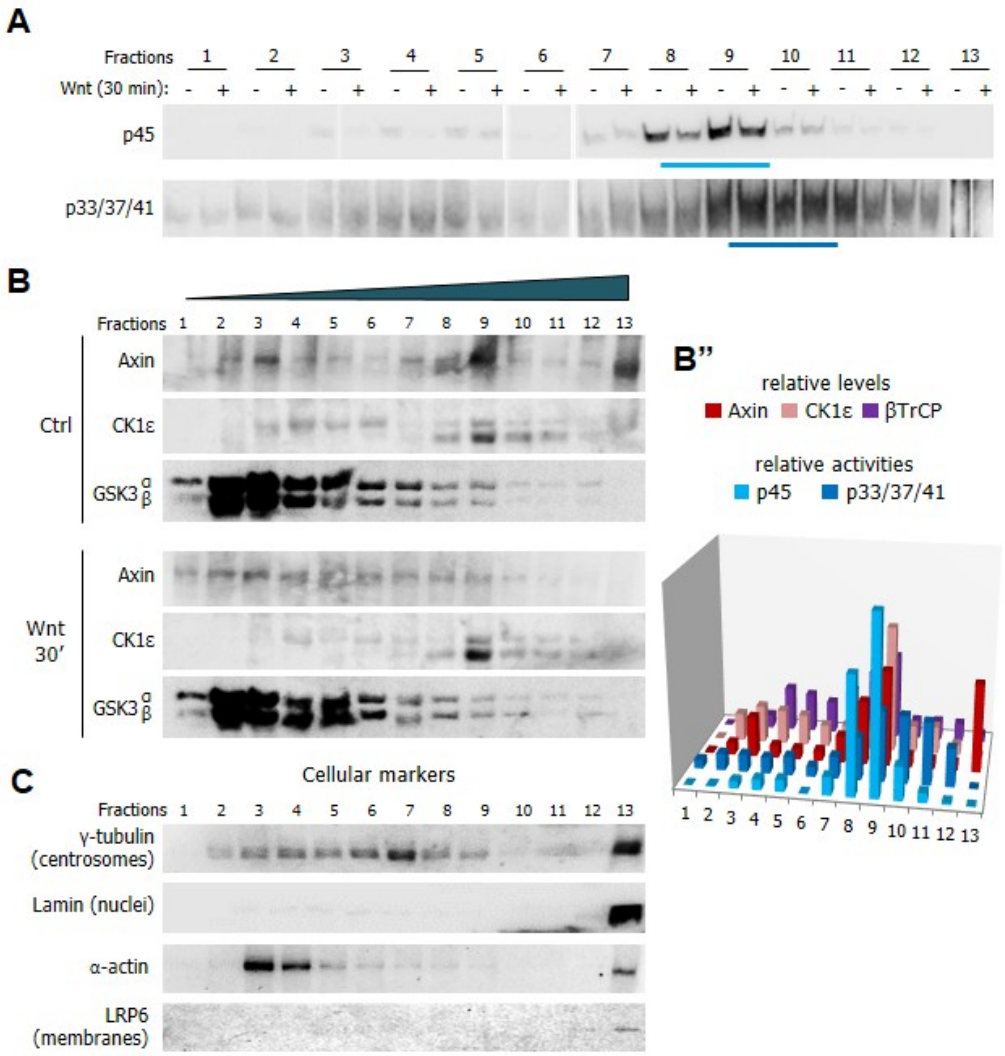
A
Fractions 1 2 3 4 5 6 7 8 9 10 11 12 13
Wnt (30 min): - + - + - + - + - + - + - + - + - + - + - + - + - +
p45
p33/37/41
B
Fractions 1 2 3 4 5 6 7 8 9 10 11 12 13
Ctrl
Axin
CK1ε
GSK3 α β
Wnt 30′
Axin
CK1ε
GSK3 α β
B”
relative levels
Axin CK1ε βTrCP
relative activities
p45 p33/37/41
1 2 3 4 5 6 7 8 9 10 11 12 13
C
Cellular markers
Fractions 1 2 3 4 5 6 7 8 9 10 11 12 13
γ-tubulin (centrosomes)
Lamin (nuclei)
α-actin
LRP6 (membranes)

Figure 10. Characterization of insoluble Axin complex.

A) Native gels of membrane fractions blotted for Wnt pathway components. Membrane fractions we prepared from extracts from cell treated with for 30min with control medium (C) or Wnt conditioned medium (W), MG132 (MG, 4hrs) or both (W+MG). Most antibodies recognized only bands above 500kDa. Axin, CK1α and PP2A were the only components that showed lower bands, in all cases located at the bottom of the gel, thus corresponding to free monomeric forms (not shown).

B) Quantification of relative levels.

C) Quantification of Axin to LRP6 ratio. Note that the Wnt only causes a relatively modest increase in Axin.

D) Relative changes in the 1200 and 850kDa complexes upon Wnt and MG132 treatments. Major changes upon Wnt treatment are increased LRP6 phosphorylation, and increased recruitment of Amer1 and CK1γ for 1200kDa complex.

Figure 10

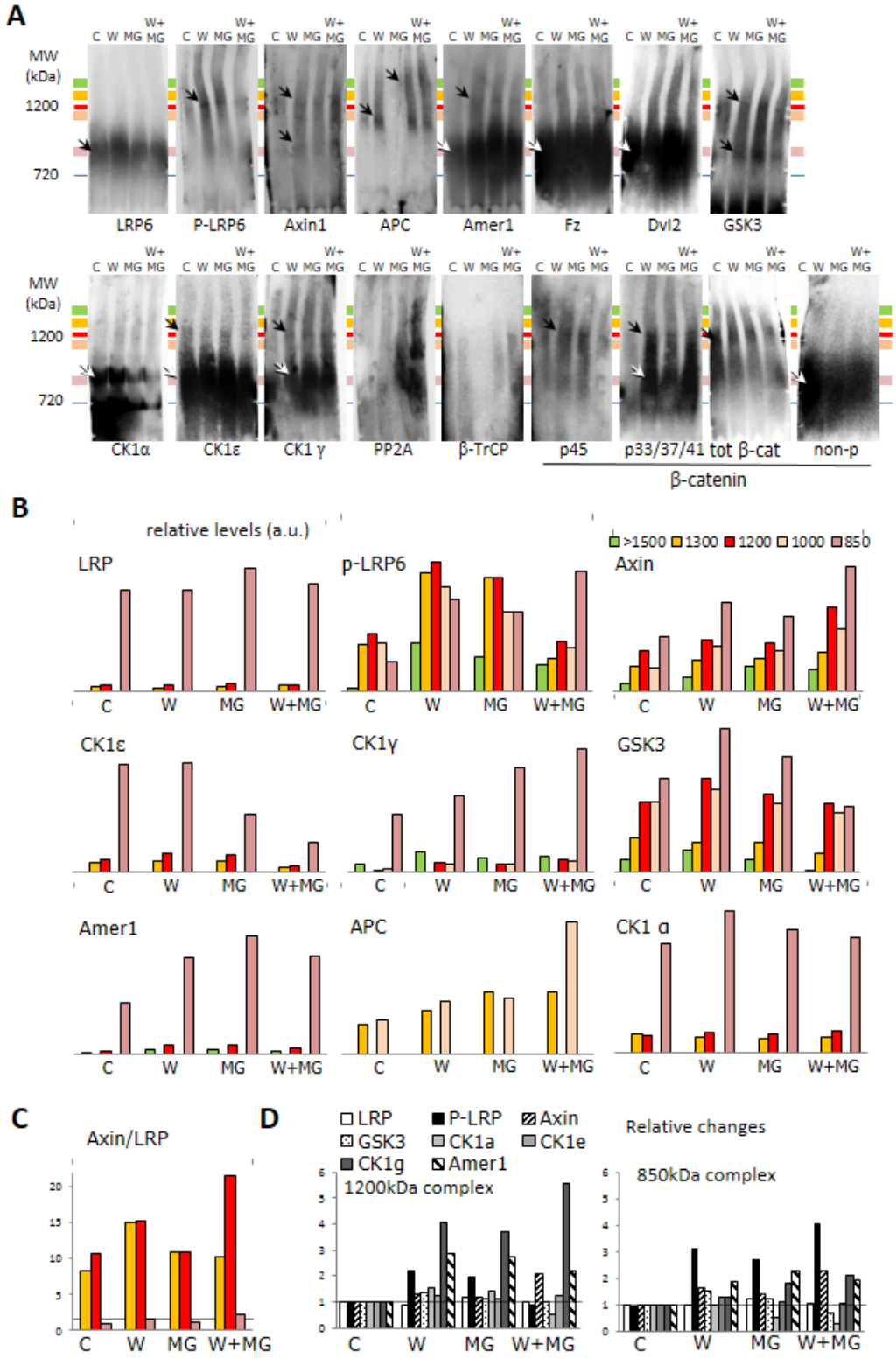
A
C W MG W+MG
MW (kDa)
1200
720
LRP6
P-LRP6
Axin1
APC
Amer1
Fz
Dvl2
GSK3
CK1α
CK1ε
CK1 γ
PP2A
β-TrCP
p45
p33/37/41
tot β-cat
non-p
β-catenin
B
relative levels (a.u.)
>1500 1300 1200 1000 850
LRP
p-LRP6
Axin
CK1ε
CK1γ
GSK3
Amer1
APC
CK1 α
C W MG W+MG
C
Axin/LRP
D
LRP
P-LRP
Axin
GSK3
CK1a
CK1e
CK1g
Amer1
1200kDa complex
Relative changes
850kDa complex

Supplementary figures

Figure S1. Effect of Wnt stimulation of global levels of components of the Wnt pathway.

A) Total β-catenin, Axin and GSK3. **A'**) Phospho-LRP6, LRP6, p45 and 33/37/41 β-catenin.

B) Quantification.

β-catenin levels remain low for the first 30min of stimulation, and then increase exponentially. Axin progressively decreases, while GSK3 remains stable. Phospho-LRP6 increases steadily. The pool of p45 β-catenin disappears very rapidly, but the low levels of p33/37/41 β-catenin remain relatively constant.

C) Immunofluorescence for Axin in control cells and cell stimulated 60min with Wnt. Inserts: higher magnification. Axin distributes throughout the cell, including in the nucleus. Wnt activation leads to a general decrease.

Figure S1

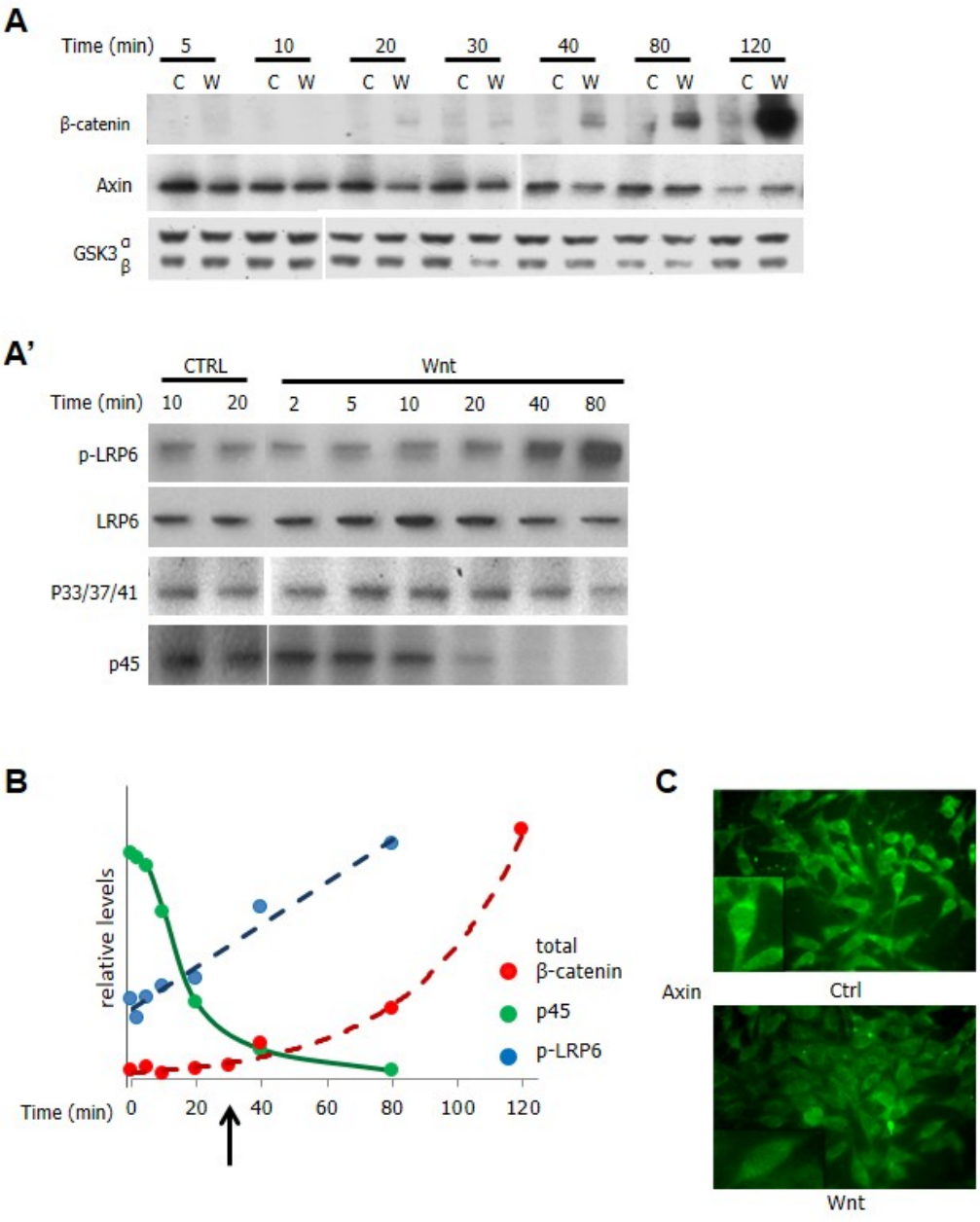
A
Time (min) 5 10 20 30 40 80 120
C W C W C W C W C W C W C W
β-catenin
Axin
GSK3 α β
A'
CTRL Wnt
Time (min) 10 20 2 5 10 20 40 80
p-LRP6
LRP6
P33/37/41
p45
B
relative levels
Time (min) 0 20 40 60 80 100 120
total β-catenin
p45
p-LRP6
C
Axin
Ctrl
Wnt

Figure S2. Distribution of Axin complex components on a sucrose gradient.

A) Distribution of LRP6 and Frizzled receptors and of G protein Gαo on a sucrose gradient from crude cell extracts. Arrow: full length LRP6. Arrowhead: high molecular weight bands corresponding to phosphorylated LRP6.

B) Distribution of subcellular markers: EEA1 (early endosomes), ER68 (endoplasmic reticulum), Lamin (nuclei), proteasomes, and Commassie staining of total proteins.

C) Position of purified his-tagged β-catenin on a similar sucrose gradient, as monitor for soluble monomeric proteins.

D) Quantification of specific activity from *in vitro* β-catenin phosphorylation using pooled fractions from sucrose gradients (see Fig.3A, C-E).

E) Comparison of priming (p45) and p33/37/41 activities. Different fractions showed distinct properties. For example, intermediate fractions F5-8 seemed to phosphorylate better p33/37/41 than p45 compared to other fractions. On the contrary, the light pool F3-4 had proportionally a weak p33/37/41 specific activity. The dense pool F9-F10 showed the strongest specific activity for both p45 and p33/37/41.

F) Effect of Wnt on specific activities, expressed as Wnt/control ratio.

Figure S2

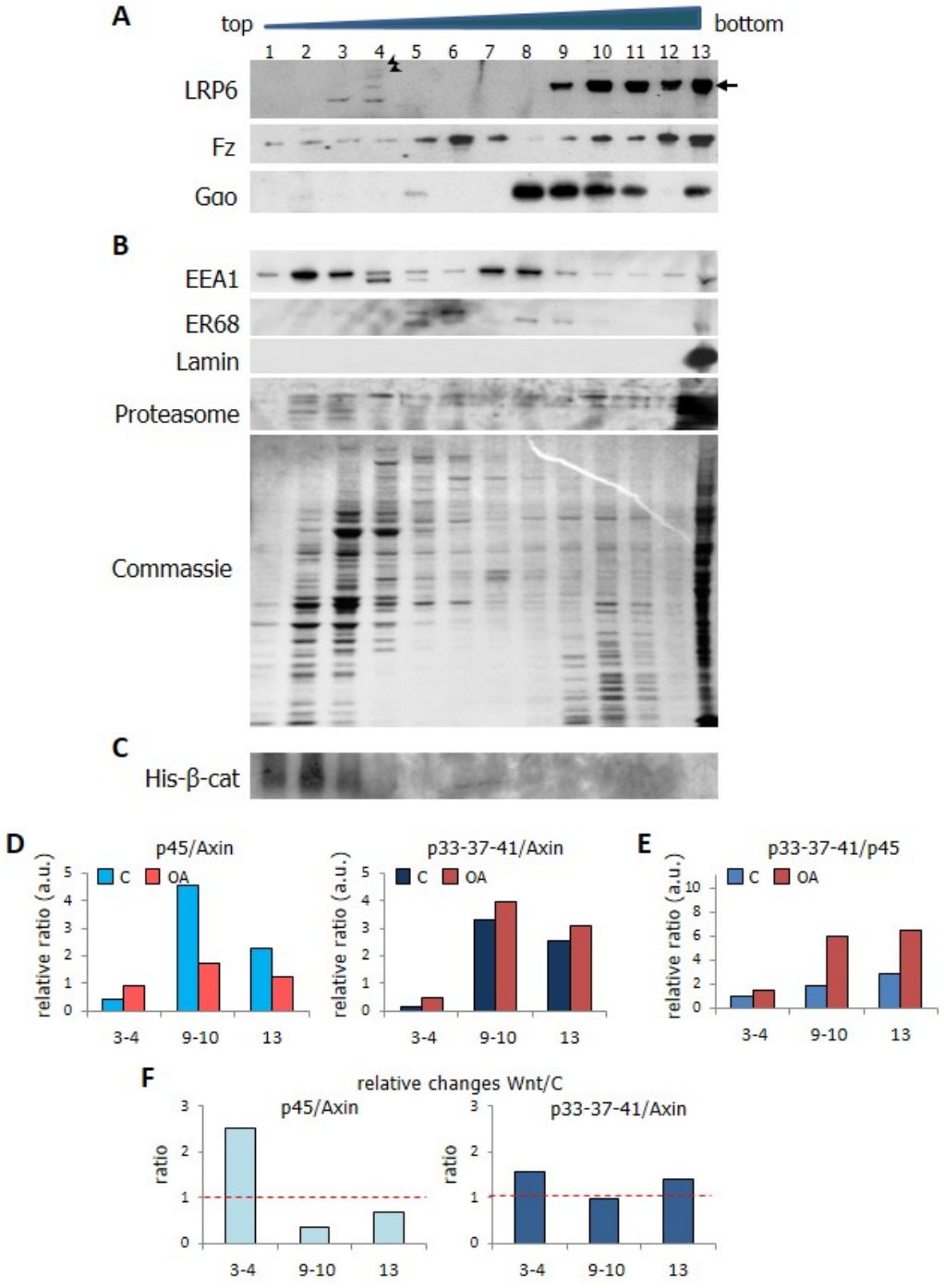
A
top
bottom
1 2 3 4 5 6 7 8 9 10 11 12 13
LRP6
Fz
Gαo
B
EEA1
ER68
Lamin
Proteasome
Commassie
C
His-β-cat
D
p45/Axin
p33-37-41/Axin
C
OA
relative ratio (a.u.)
3-4
9-10
13
E
p33-37-41/p45
F
relative changes Wnt/C
p45/Axin
p33-37-41/Axin
ratio

Figure S3. Effect of mild detergent on sedimentation of components of the Wnt pathway.

Crude extracts were fractionated in the absence of presence of CHAPS. Membrane-associated components are expected to show a shift between the two conditions.

A) Untreated cells.

B) Cells treated for 4 hrs with proteasomal inhibitor MG132 prior to extraction.

Figure S3

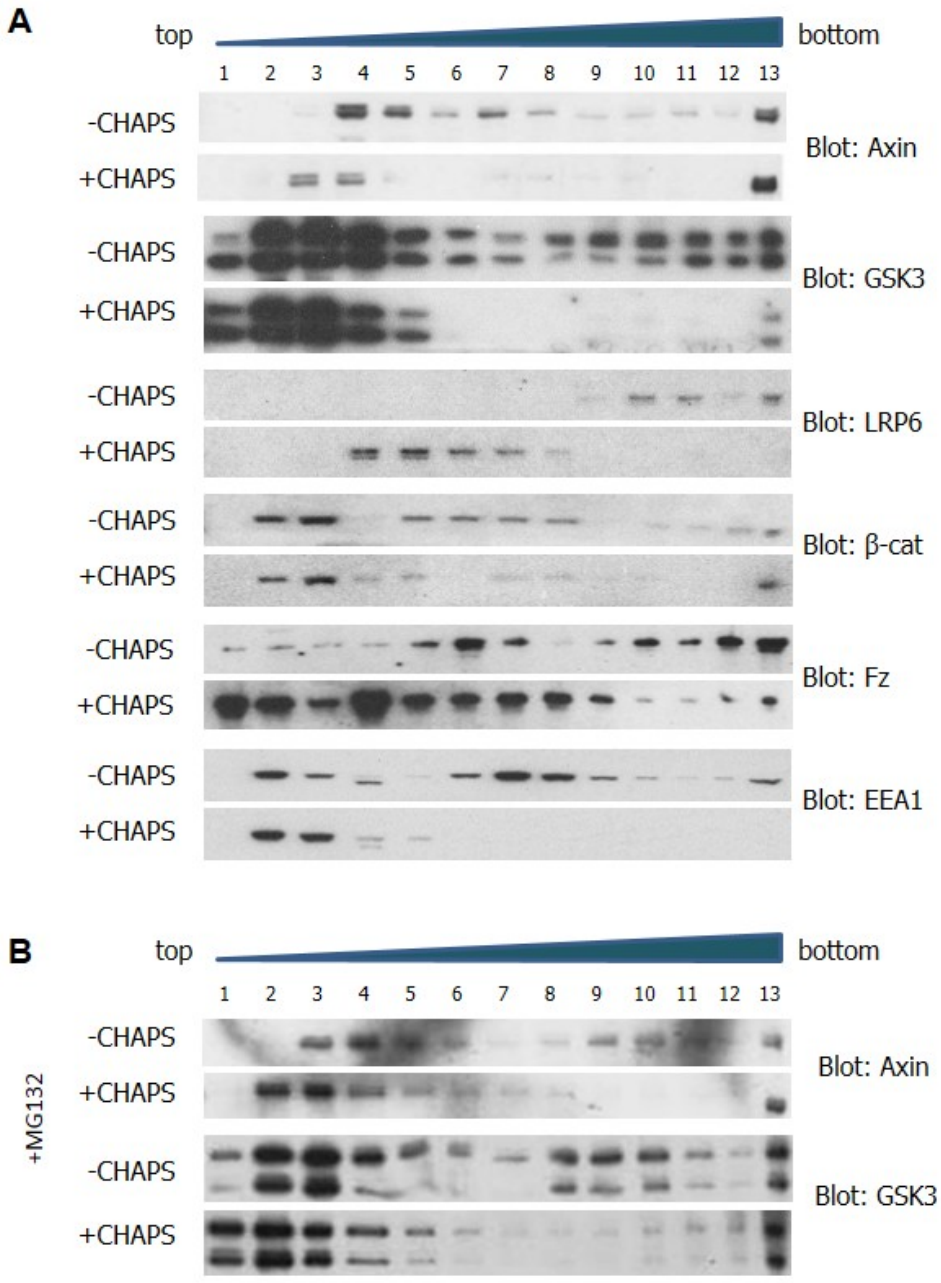
A
top
bottom
1 2 3 4 5 6 7 8 9 10 11 12 13
-CHAPS
+CHAPS
Blot: Axin
-CHAPS
+CHAPS
Blot: GSK3
-CHAPS
+CHAPS
Blot: LRP6
-CHAPS
+CHAPS
Blot: β-cat
-CHAPS
+CHAPS
Blot: Fz
-CHAPS
+CHAPS
Blot: EEA1
B
top
bottom
1 2 3 4 5 6 7 8 9 10 11 12 13
+MG132
-CHAPS
+CHAPS
Blot: Axin
-CHAPS
+CHAPS
Blot: GSK3

Figure S4. Cell fractionation.

A) p45 phosphorylation activity in cytosolic (Cs), nucleosolic (Ns), membrane (M) and insoluble (X) fractions. Cells were either control or Wnt stimulated. The kinase reaction was performed in the absence or presence of the PP2A inhibitor okadaic acid. See Fig.5 for quantification.

B) Subcellular distribution of the major components of Wnt pathway. Arrowheads in p33/37/41 indicate the possible ubiquitinated bands after phosphorylation. Arrow in APC indicates the full length APC and the arrowhead indicates the APC fragment. Arrowheads in Dvl indicates the phosphorylation of Dvl. Arrow in Dvl indicate the non-phosphorylated Dvl.

C-F) Quantification of **B**. Average of 2-3 experiments. Error bars, SD. * indicate $p<0.05$, Student's *t*-test.

Figure S4

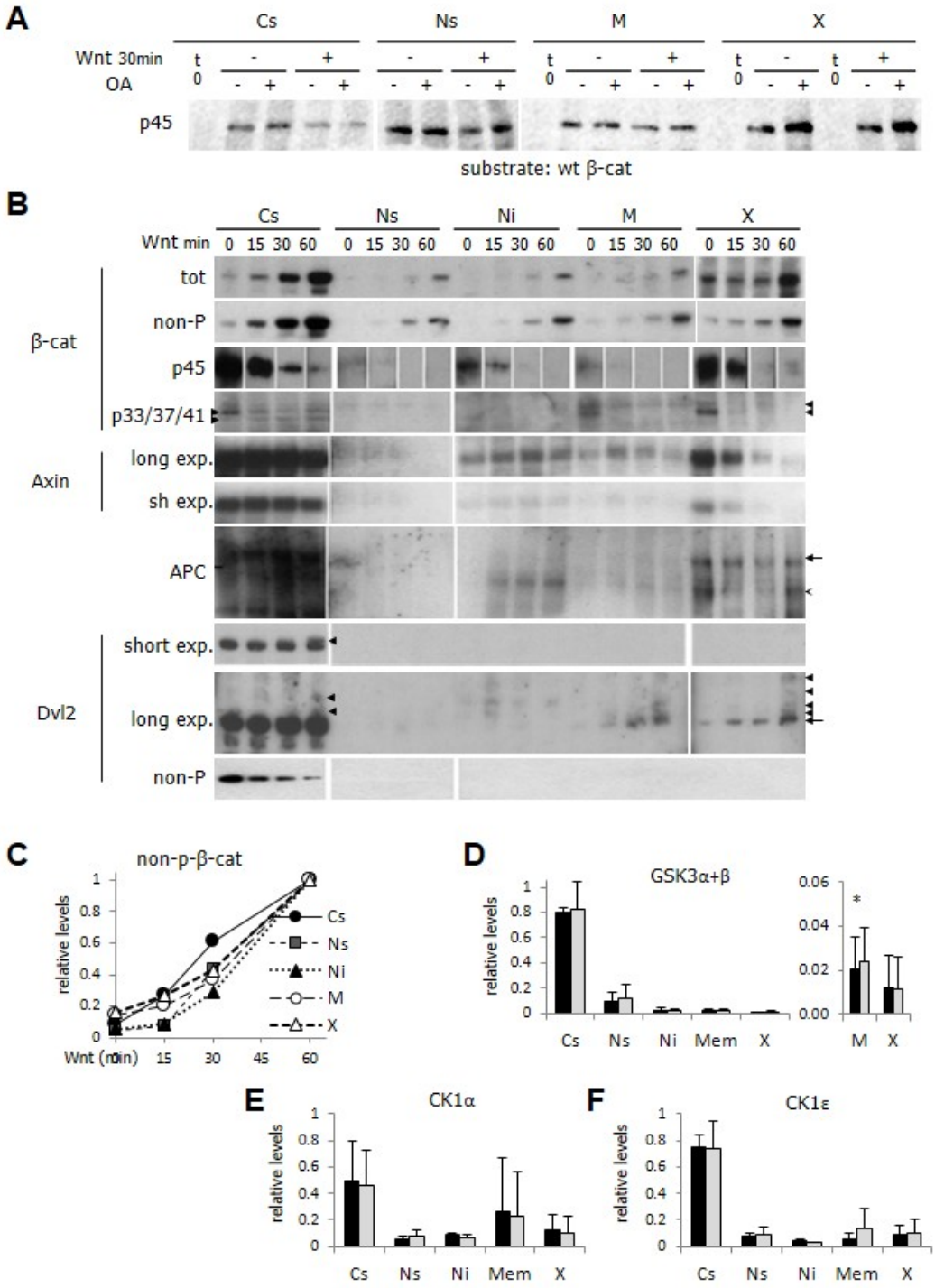
A
Cs
Ns
M
X
Wnt 30min
OA
p45
substrate: wt β-cat
B
Cs
Ns
Ni
M
X
Wnt min
0 15 30 60
β-cat
tot
non-P
p45
p33/37/41
Axin
long exp.
sh exp.
APC
Dvl2
short exp.
long exp.
non-P
C
non-p-β-cat
relative levels
Wnt (min)
Cs
Ns
Ni
M
X
D
GSK3α+β
relative levels
Cs Ns Ni Mem X
M X
E
CK1α
relative levels
Cs Ns Ni Mem X
F
CK1ε
relative levels
Cs Ns Ni Mem X

Figure S5. Analysis of cytosolic Axin complexes by native gel electrophoresis.

Cytosol, prepared from control or 30min Wnt-stimulated cells, was separated on sucrose gradient. The fractions, pooled by two, were directly loaded on native gels, transferred on membranes and blotted for various components of the Axin complex, as well as various forms of β-catenin. All fractions were loaded on single gels, but to help compare migration of different components, for the figure lanes were cropped and aligned for each pool. Note that brightness and contrast were kept identical for all the lanes of a same marker, thus relative levels can be directly compared between pools. In a few cases, two exposures are shown (LE, DE = respectively light and dark exposure), in order to show both the abundant lower bands and the paler high bands. Again, similar exposures can be quantitatively compared between pools.

For quantification (Figure S6), intensity profiles were obtained by line scans, shown alongside with each lane. A series of bands were detected, where several components precisely comigrated. They were designated by apparent size as >1300kDa, 1100-1200kDa (generally double band), 850kDa, 700kDa and several lower bands collectively classified as < 500kDa, which are here indicated with color coded arrowheads. Bands migrating as free monomers are indicated in orange.

Figure S5

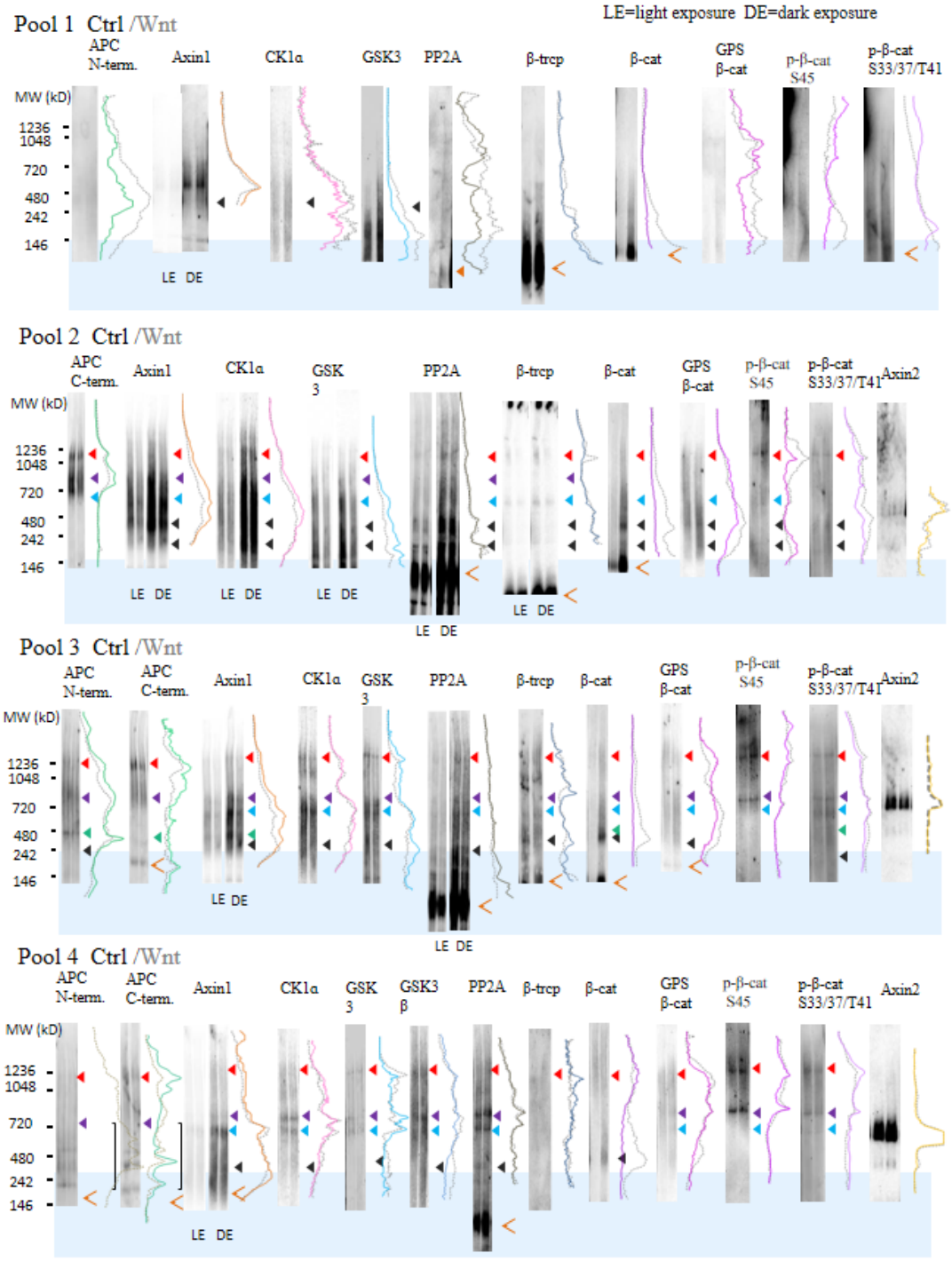
LE=light exposure DE=dark exposure
Pool 1 Ctrl /Wnt
APC N-term.
Axin1
CK1α
GSK3
PP2A
β-trcp
β-cat
GPS β-cat
p-β-cat S45
p-β-cat S33/37/T41
MW (kD)
1236
1048
720
480
242
146
LE DE
Pool 2 Ctrl /Wnt
APC C-term.
Axin1
CK1α
GSK 3
PP2A
β-trcp
β-cat
GPS β-cat
p-β-cat S45
p-β-cat S33/37/T41
Axin2
Pool 3 Ctrl /Wnt
APC N-term.
APC C-term.
Axin1
CK1α
GSK 3
PP2A
β-trcp
β-cat
GPS β-cat
p-β-cat S45
p-β-cat S33/37/T41
Axin2
Pool 4 Ctrl /Wnt
APC N-term.
APC C-term.
Axin1
CK1α
GSK 3
GSK3 β
PP2A
β-trcp
β-cat
GPS β-cat
p-β-cat S45
p-β-cat S33/37/T41
Axin2

Figure S5 continued

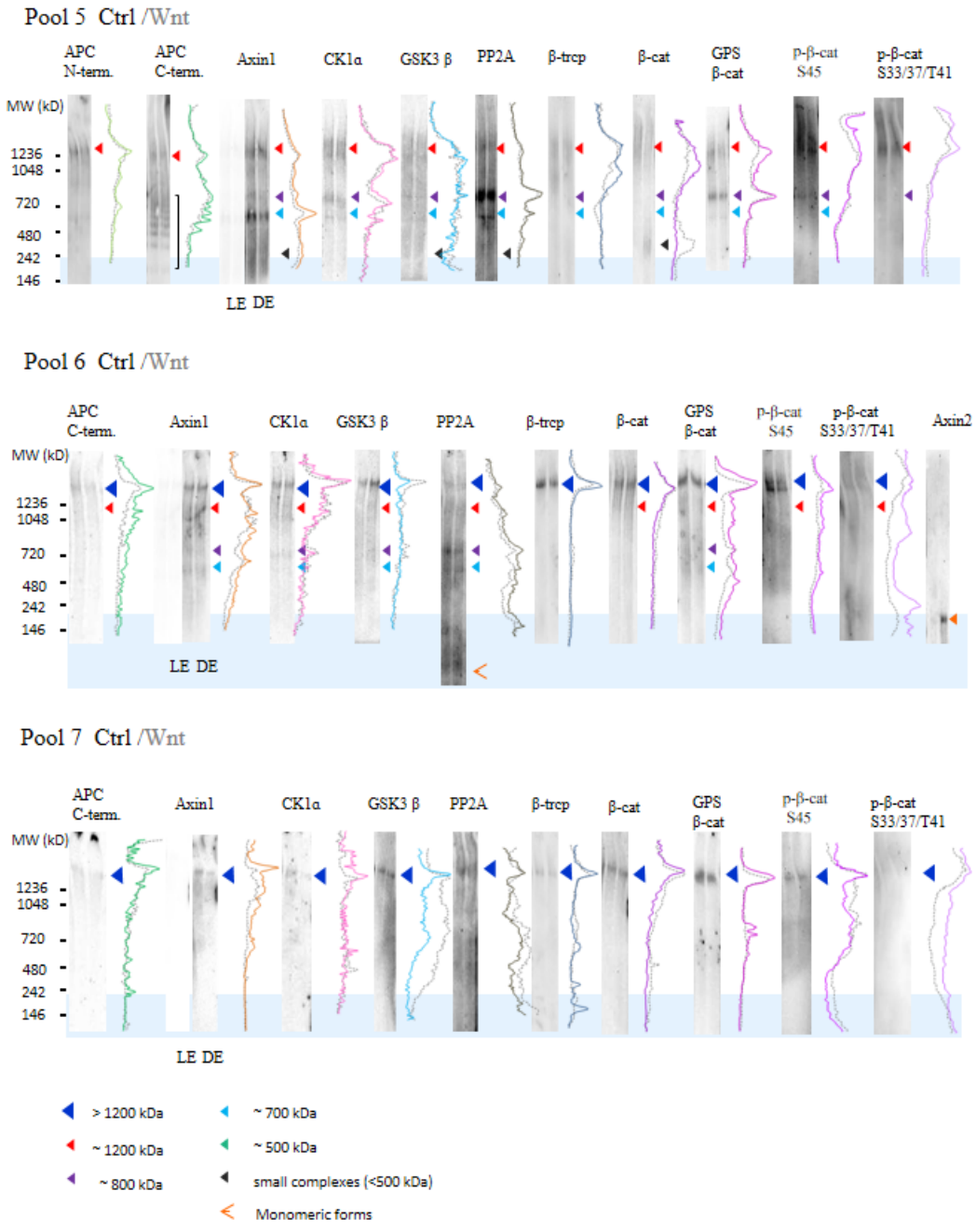

Figure S6. Quantification of the components of the cytosolic complexes.

A) Levels of components of the Axin complex and of the various forms of β-catenin. For each component, the peak intensities in BNGE (see example Figure S5) were quantified as % of the total cytosolic input. Results are averages from 3-5 independent experiments. The approximate size corresponding to each putative complex is indicated with a color code. Two peaks could sometimes be distinguished in the 1100-1200kDa range, which were pooled. Similarly, 2-3 peaks could be detected in the 400-500kDa, which were also pooled for these graphic representations, since individual peaks could not be accurately resolved. Lower molecular species, including free monomers, are not represented in these graphs.

B) Comparison of the amount of each component, measured as relative ratio to Axin, in each putative complex. A color code was used to highlight relative enrichment. Note that some complexes appear particularly enriched in several components, while others seem to have a more restricted composition. For instance, the 850kDa peak in fractions F3-4 has high APC levels, moderate amounts of GSK3, but little CK1α and only low levels of PP2A, β-TrCP, and phosphorylated β-catenin. On the contrary, the highest peaks (>1300kDa) of fractions F11-13 have high levels of all components. The same is true for the 850kDa peak of F9-10, while the adjacent peak of F7-8 specifically lacks β-TrCP and the p33/37/41 form of β-catenin. Note also that all the β-catenin forms, total, non-phosphorylated and phosphorylated, are mostly enriched in the large complexes (850kDa and above).

C) Comparison between phosphorylated to non-phosphorylated β-catenin (ratio of relative levels, not to be mistaken with an absolute ratio, since these different forms cannot be directly compared), and comparison with the *in vitro* kinase activity. Both for p45 and p33/37/41, the ratio calculated globally per SG fraction showed a rather good correlation with the corresponding *in vitro* activity, suggesting that it may be used as an indirect criterion to estimate the relative activity of Axin complexes. Based on this assumption, the most active p45 priming complex would correspond to the 900kDa peak, while p33/37/41 phosphorylation may be performed by smaller complexes in F3-4, as well as by intermediate complexes in F5-F6 and F7-F8.

Figure S6

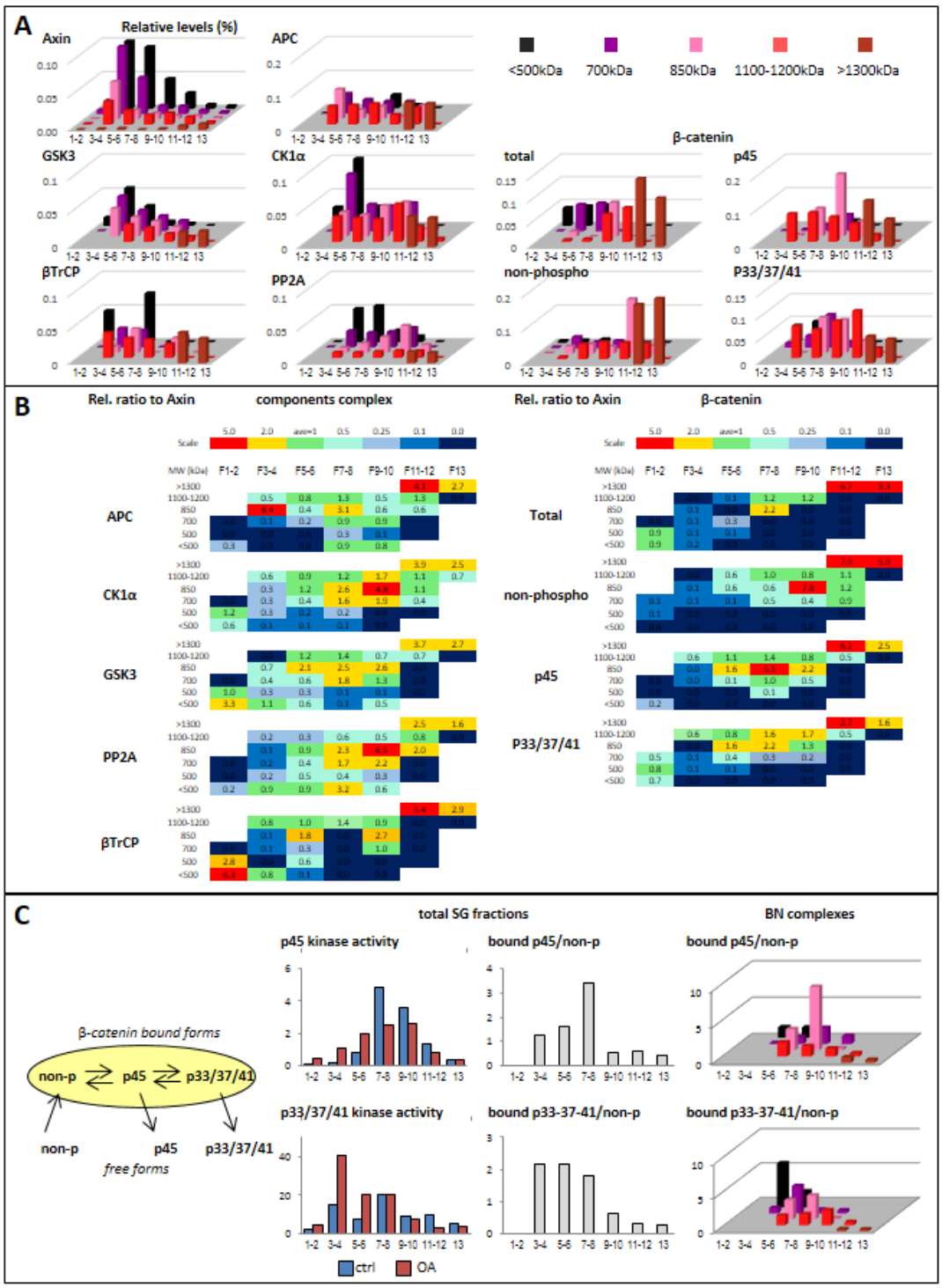
A
Relative levels (%)
Axin
APC
<500kDa
700kDa
850kDa
1100-1200kDa
>1300kDa
β-catenin
GSK3
CK1α
total
p45
βTrCP
PP2A
non-phospho
P33/37/41
1-2 3-4 5-6 7-8 9-10 11-12 13
B
Rel. ratio to Axin
components complex
Rel. ratio to Axin
β-catenin
Scale
MW (kDa)
F1-2 F3-4 F5-6 F7-8 F9-10 F11-12 F13
APC
CK1α
GSK3
PP2A
βTrCP
Total
non-phospho
p45
P33/37/41
C
total SG fractions
BN complexes
β-catenin bound forms
non-p
p45
p33/37/41
free forms
p45 kinase activity
bound p45/non-p
bound p45/non-p
p33/37/41 kinase activity
bound p33-37-41/non-p
bound p33-37-41/non-p
ctrl
OA

Figure S7. Effect of Wnt stimulation on cytosolic Axin complexes.

Axin levels were used to monitor changes in abundance of the various complexes. Error bars, SD. * indicate $p<0.05$, Student's *t*-test (3-4 experiments). Only one significant change was observed, i.e. a global decrease in most of the complexes present in F3-4 and F5-6, which correlated well with the decreased *in vitro* kinase activity observed in the presence of OA.

Figure S7

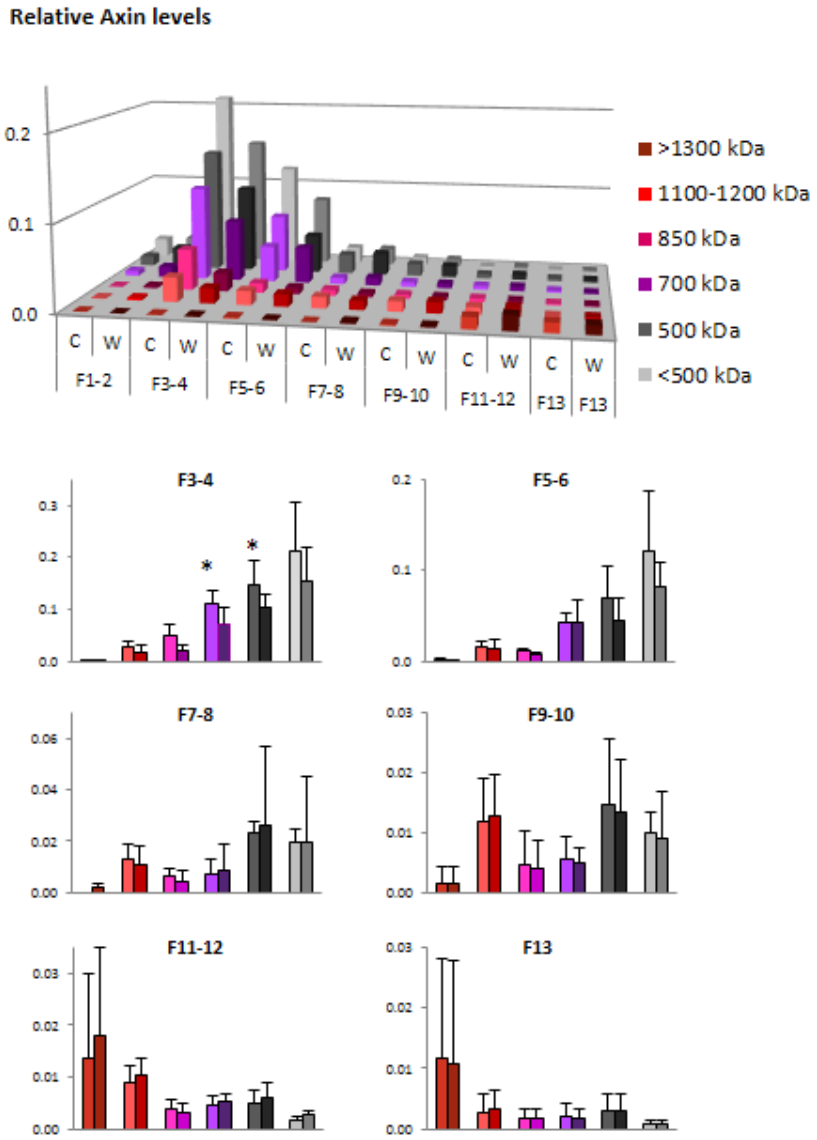
Relative Axin levels
0.2
0.1
0.0
C W C W C W C W C W C W C W
F1-2 F3-4 F5-6 F7-8 F9-10 F11-12 F13 F13
>1300 kDa
1100-1200 kDa
850 kDa
700 kDa
500 kDa
<500 kDa
F3-4
F5-6
F7-8
F9-10
F11-12
F13
*
*

Figure S8. Immunoprecipitation of cytosolic complexes.

Cytosolic components were immunoprecipitated as indicated (APC, Axin and β-catenin). All components could be precipitated with any of them. No significant change was observed between control and Wnt-stimulation conditions, except for increased interaction of β-catenin, which can be simply explained by the large increase in input levels, and a decrease is Axin-APC interaction, also consistent with decreased Axin levels.

Figure S8

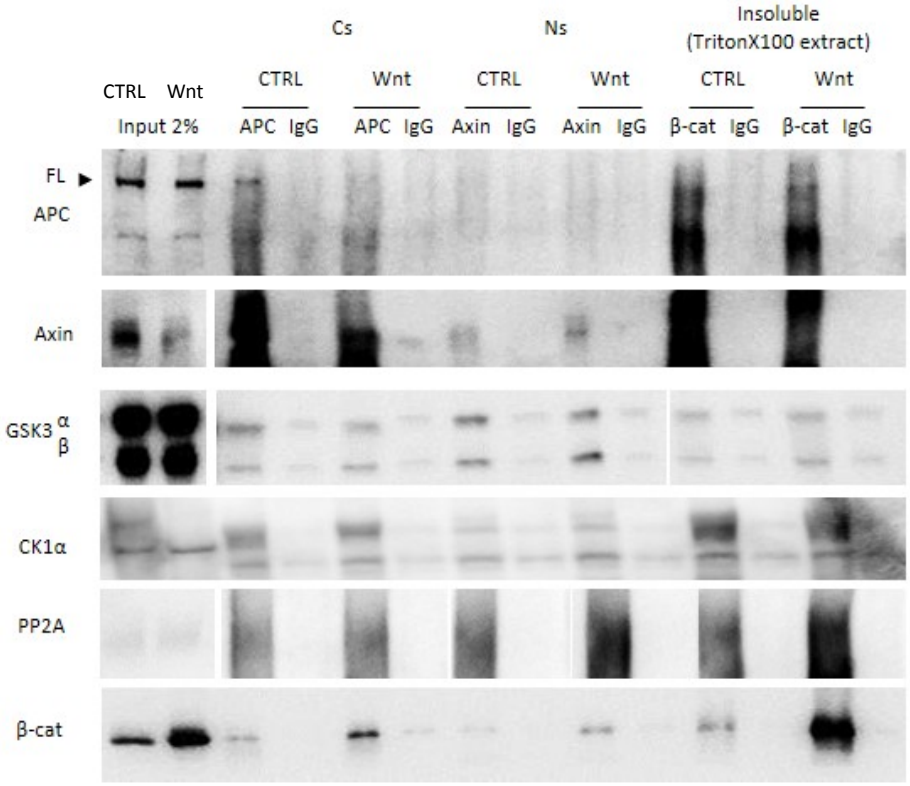
Cs
Ns
Insoluble
(TritonX100 extract)
CTRL
Wnt
CTRL
Wnt
CTRL
Wnt
CTRL
Wnt
Input 2%
APC
IgG
APC
IgG
Axin
IgG
Axin
IgG
β-cat
IgG
β-cat
IgG
FL ▶
APC
Axin
GSK3 α
β
CK1α
PP2A
β-cat

Figure S9. Separation of insoluble components on sucrose gradient.

In samples from control cells, Axin, APC (full length and large fragments) and CK1ε showed a peak around fraction F9. β-TrCP also accumulated in this fraction, and GSK3 signal showed there a shoulder. Little CK1α nor PP2A were detected there. Wnt stimulation led to partial decrease of some components of this peak (Axin, GSK3, APC), with apparent concomitant increase in the lighter fractions.

Figure S9

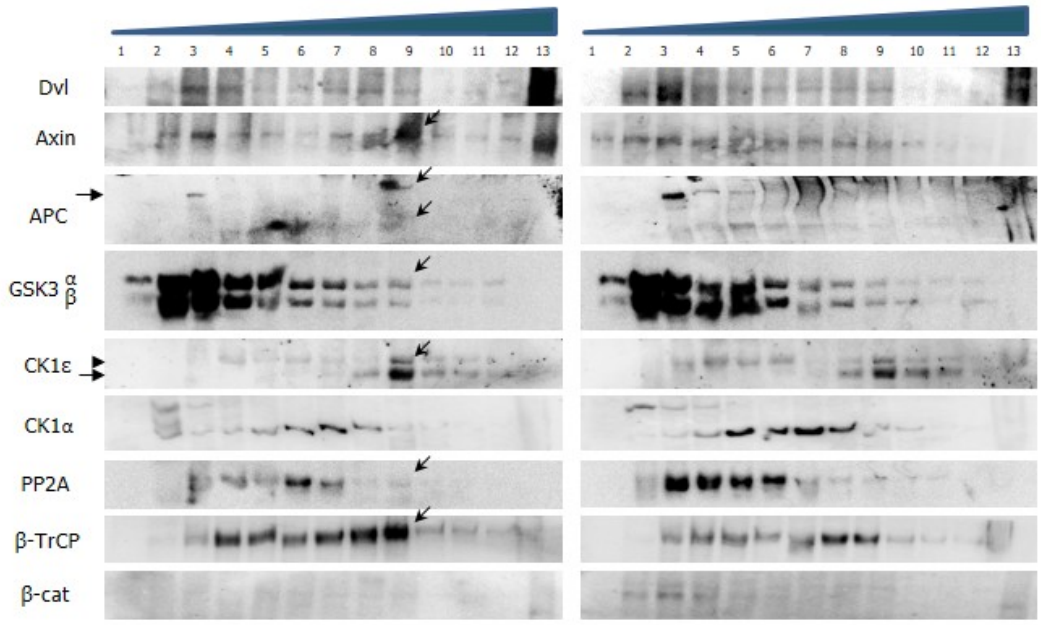
1 2 3 4 5 6 7 8 9 10 11 12 13
1 2 3 4 5 6 7 8 9 10 11 12 13
Dvl
Axin
APC
GSK3 α β
CK1ε
CK1α
PP2A
β-TrCP
β-cat

Figure S10. Quantification of β-catenin forms in native gels from membrane fractions (see Figure 10).

Figure S10

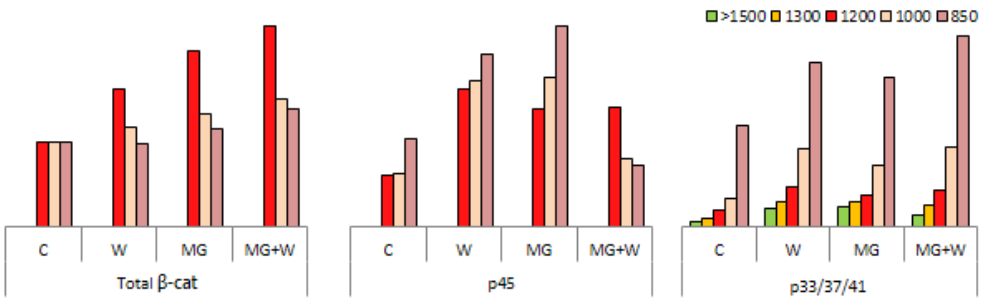
>1500
1300
1200
1000
850
C
W
MG
MG+W
Total β-cat
C
W
MG
MG+W
p45
C
W
MG
MG+W
p33/37/41

CHAPTER IV

Thesis Discussion

The Wnt signaling pathway is highly conserved among various species, and plays essential roles in cell shape, cell movement, cell adhesion, cell proliferation and differentiation, oncogenesis and development. Deregulated Wnt signaling has been implicated in many human diseases, particularly cancers. However, the actual mechanism regulating the pathway remains unclear. According to the most accepted model, Wnt signals are transmitted through a large cytoplasmic protein complex organized around the scaffold protein Axin, which regulates phosphorylation and stability of the downstream transducer, β-catenin. Despite the huge number of data on the many protein-protein interactions along this pathway, virtually nothing is known about the conditions occurring endogenously. We report here a first comprehensive analysis of the endogenous cytoplasmic components of the Wnt pathway under endogenous conditions. We have identified several endogenous complexes that differ in terms of composition, stability, and subcellular localization. Our data support a model where Wnt stimulation, rather than creating or modifying drastically complexes, modulates the dynamic balance between pre-existing complexes.

One aspect of this work that has been essential to produce this new view of the Wnt pathway has been methodological, including the establishment of new biochemical protocols and the adaptation/optimization of several others. In addition to tailor these techniques for the investigation of the Wnt pathway, an important factor that was taken into consideration is to make these techniques compatible with systematic quantification. In this section, I summarize the essential findings presented in this thesis and discuss how these findings fit with data from other Axin studies.

Establishment of novel analytical methods

A new cell fractionation protocol in mammalian culture cells

We realized quite early on that little had been done to determine where Axin complexes were acting in the cell. This required to be able to separate the various compartments were Axin and other components had been detected by

immunofluorescence. While several reports had used cell fractionation do determine the subcellular localization of several components of the pathway, we were surprised to realize that none of the protocols available was able to separate with an acceptable efficiency the most important sites of regulation of the pathway. First of all, nuclei were systematically contaminated with huge amounts of plasma membrane. Thus the two ends of the pathway were mixed in a single fraction, obviously preventing any interpretation of the results. In addition, nuclear localization is a key parameter in β-catenin function, since its nuclear and cytoplasmic activities are completely different. We thus set to establish a completely new protocol that would cleanly separate these fractions. It was also important that the fractions would be quantitative recovered, in order to be able to directly compare the levels and activities between the different compartments. Finally, fractionation had to be compatible with further biochemical steps, such as additional fractionation (density gradients, chromatography, native gel electrophoresis) or enzymatic assays.

The conception and optimization of this protocol has thus been an important aspect of my work, and the success of this first phase has opened vast possibilities to analyze the Wnt pathway, which I exploited in the subsequent work. The protocol should also be very useful for any other work on signal transduction.

Characterization of β-catenin phosphorylation activity by an in vitro kinase assay

Besides the absence of the localization of the components of the complex, direct information on the phosphorylation of β-catenin was also missing from the previous studies. In most studies, the activity of the complex was evaluated based on total levels of soluble β-catenin and/or of its phosphorylated forms. However, the assumption that these steady state levels reflect the actual phosphorylation activity is clearly conceptually unfounded. Quite surprisingly, the only attempts to measure regulation of GSK3 activity in the context of Wnt signaling used irrelevant substrates (Stambolic 1996, Taelman 2010). As for CK1 activity, it had never been evaluated. Therefore, our introduction of a kinase assay, specific and sensitive enough to monitor the endogenous activity toward β-catenin is a significant step toward a more accurate study of the pathway (Gusev, 2012, Wang *et al.,* 2014). The assay has been powerful

to dissect the process, also thanks to the availability of antibodies specific for the two steps of the reaction, and our use of a mutant substrate mimicking the primed form, thus isolating GSK3 activity from CK1 priming.

Use of native gel electrophoresis to study the Axin complexes.

Native gel electrophoresis is one of the oldest biochemical techniques, yet it is nowadays very rarely used. Yet we found that it is a very sensitive method to analyze Axin complexes. One of its major advantages is that the complexes are minimally diluted compared to chromatographic methods, thus increasing the chances to maintain complexes intact. It also allows simultaneous detection of many samples, thus quantitative comparisons are feasible. Another key advantage compared to immunoprecipitation, is that different complexes can be identified. Furthermore, the relative abundance of these complexes and the relative enrichment of each component can be determined. The caveat is that comigration may not necessarily prove association within the same protein complex. However, the patterns were in our case so strikingly similar, and the changes under various conditions, in particular Wnt treatment, were so consistent that there is little doubt that we were indeed observing true complexes.

I would like to mention our innovative use of this technique to examine the *in vitro* kinase reaction and demonstrate that the substrate β-catenin could be released, thus solve a long standing question in the field. We have also applied the method to analyze the composition of membrane-associated complexes, another topic that has not been yet addressed.

Properties and regulation of the endogenous Axin complexes

Based on yeast two-hybrid screenings and immunoprecipitations, it had been established that Axin can interact with most of the major components of the pathway, APC, β-catenin, CK1, GSK3, PP2A, LRP5/6 and Dvl (Behrens 1998, Ikeda 1998,

Kishida 1998, Fagotto 1999, Kishida 1999, Kishida 2001, Mao 2001, Zhang 2002). However, little was known about the actual composition of the complexes, and on the contribution of each component to the Axin complex relative to other complexes and functions. Furthermore, composition and activity had never been directly compared. This study has tried to address these questions. I will highlight those that were successfully addressed and mention some of the remaining issues.

Classical enzymatic complex or "destruction factory"?

The term "destruction complex" suggests indeed that the Axin complex causes β-catenin degradation. This represents however an extrapolation based on the fact that the Axin complex is responsible for the phosphorylation reaction that targets β-catenin for ubiqutination and on its ability to bind the ubiquitin ligase β-TrCP. A definitive demonstration that the whole process occurs within one complex is still missing. We have here confirmed the existence of very large complexes the composition of which is consistent with full processing, from priming to ubiquitination, although we have not yet monitored this last step. We have however detected other complexes that do not contain β-TrCP, and yet have strong phosphorylation activity, arguing that the two reactions are not necessarily coupled. We have validated this assumption by demonstrating that a large fraction of phosphorylated β-catenin is released and recovered as a free form. The observation that the proportion of free protein was higher for the fully phosphorylated form than for the primed form is well consistent with the notion that both steps can be performed consecutively, without release of the intermediate substrate. The fact that one nevertheless detects a significant amount of free p45-β-catenin fits well with our detection of partial complexes, which contain one or the other kinase. Comparison of the cytosolic Axin complexes has shown that Wnt targets those from the light fractions much more than the dense and large ones, which are those which contain β-TrCP. This observation is not consistent with Wnt acting by blocking transfer of β-catenin to β-TrCP (Li, Ng *et al.,* 2012). This mechanism may occur, but cannot account alone for the entire Wnt regulation.

The new picture that we have obtained is quite interesting, as it is much more nuanced and integrative: we find that many different complexes co-exist, and we

believe that they probably constantly exchange components. β-catenin may thus be either processed in different ways, either step by step, or all at once, with some complexes performing only one of the steps, or two, or all.

Where is β-catenin processed?

We detected efficient phosphorylation in all compartments, In L-cells, most of the final phosphorylation takes place in the cytoplasm, but priming is quite similarly active in all fractions. One perhaps surprising location is the insoluble fraction, which is interesting for several reasons: It is regulated (decreased/dissociated) upon Wnt stimulation; it is uniquely characterize in terms of composition by its enrichment in CK1ε, while the soluble complexes have proportionally more of CK1α; the corresponding subcellular compartment remains mysterious, as the complex does not cosediment either with the actin cytoskeleton, not with microtubule/centrosomal markers, two of the obvious systems know to interact with the Wnt pathway's components (Fumoto *et al* 2009). We also think that this insoluble complex must be generally quite important, since we found it to be by far the most active fraction in SW480 cells, a cancer cell line (Wang *et al.,* 2014). Further characterization of this fraction is thus an important future question, which is however technically challenging, precisely due to the insolubility of the material. A first step would be to determine by other ways, such as immunofluorescence, markers that would co-localize and thus could suggest the potential nature of this compartment.

Note also that the nucleosol has a surprisingly high activity, a feature that we have not investigated in detail in this study, but which should certainly be taken into serious consideration to understand regulation of the pathway.

Axin complexes at the plasma membrane

One of the major issues is the mode of inactivation of the complex. Evidence indicates that the Wnt receptors do not send a diffusible signal to regulate cytosolic Axin complexes, but rather regulate them directly: Axin can localize to the plasma membrane (Fagotto *et al.,* 1999) and can bind LRP5/6 (Bilic *et al.,* 1997) and potentially Frizzled via Dvl (Gonzalez-Sancho *et al.,* 2004). Recruitment to LRP5/6 is stimulated by LRP5/6 phosphorylation, which is a Wnt-dependent reaction (Bilic *et*

al., 1997). Which form of Axin or Axin complex gets recruited, and what is its fate are points that are far from clear. Our experiments have for the first time yielded a picture of this step. They show that indeed whole complexes are recruited, and that these complexes still display phosphorylation activity. Quite unexpectedly, the recruitment does not appear to be Wnt-specific: a significant amount of complexes are associated to LRP5/6 even in unstimulated cells, and proteasomal inhibition is sufficient to increase this pool as efficiently as Wnt treatment. In fact, even LRP5/6 phosphorylation can be stimulated by proteasomal inhibition, consistent with an intimate interdependence between Axin-LRP5/6 interaction, LRP5/6 and Axin stability. Taken together, our data do not support models where recruitment to the membrane would block the enzymatic activity of the complex (Kim *et al.,* 2013), but are more consistent with destabilization of Axin itself (Yamamoto 1999, Willert 1999). This would readily explain the significant decrease in Axin levels, and in levels of Axin complexes, both in the cytosol and in the insoluble fraction.

One caveat that cannot be easily circumvented is precisely the destabilization of Axin: if LRP5/6 receptors act indeed as "catalysts" for Axin targeting to the proteasome, the nature of the membrane association is intrinsically transient, and the snapshot image obtained in our experiments (and in all published observation) does not necessarily reflects changes in rate of recruitment and release that may result from Wnt stimulation. In fact, total Axin levels found in the membrane fraction only slightly and transiently increase during Wnt activation. Note however that the increase in rate of Axin destabilization is not huge, and is thus not incompatible with a relatively mild increase in the rate of binding to LRP5/6. What remains to be determined is whether additional changes in the complexes recruited by the receptors may affect Axin stability, including the degree of LRP5/6 phosphorylation or differences in composition of the complexes.

Concluding remarks

Implication for Wnt signaling pathway

Our knowledge of Wnt signaling pathway has broadened incredibly over the past decades. However, it also raises a lot of new questions and a systematic study on Axin and Axin-based complexes is still missing; therefore, hypothesis inferred from these data are controversial, some even on the contradictory.

Our study not only provided valuable tools on investigating precise subcellular signaling and directly monitoring phosphorylation activity rather than β-catenin and phospho-β-catenin levels in cell extracts, but also represented the first comprehensive analysis of the Wnt pathway under endogenous conditions. We have identified the simultaneous existence of multiple Axin-based complexes that differ in terms of composition, stability, and subcellular localization. We have also analyzed the changes induced by Wnt activation. Our data support a model where Wnt stimulation, rather than creating or modifying drastically complexes, modulates the dynamic balance between pre-existing complexes.

Implication for cancer therapy

Ideal anti-cancer drugs should be targeted to specific molecular pathways rather than using cytotoxic chemicals to induce general cell death. Uncontrolled activation of the Wnt pathway has been implicated in several types of cancers, including hepatocellular cancer (Polakis 2007), colorectal cancer (Clements *et al.,* 2003), leukemia (Abrahamsson *et al.,* 2009), wilm's tumor (Ruteshouser *et al.,* 2008), breast cancer (Bjorklund *et al.,* 2009). One well-studied example is colon cancer, where most of the tumors harbor mutations of APC, which appear to impair the function of the degradation complex (Polakis 2007, Morin 1997). Therefore, discovery of Wnt component inhibitors presents a potential opportunity for Wnt-correlated cancers. Axin itself has been regarded as a tumor suppressor, by regulating β-catenin turnover or inducing apoptosis through activating the JNK/SAPK signalling pathway and enhancing phosphorylation of p53 (Neo 2000, Rui 2004). So far, one of the approaches to boost β-catenin down regulation by Axin was to inhibit Tankyrase,

which should result in Axin stabilization (Chen 2009, Lu 2009, Huang 2009). The rationale of this approach was largely based on the belief that Axin is a limiting factor. Our results indicate that this may not be a very efficient method, since we find that Axin is in fact abundant, and furthermore only a small part is effectively active in β-catenin regulation. It is thus unclear that the increased stability of Axin that can be realistically achieved would be sufficient to buffer deregulation of the complex due to APC mutations. Our results provide a preliminary knowledge of the various Axin complexes, and may lead eventually to the characterization of unique features of the most active complexes, and on factors that may favour their formation or stability.

Reference

Abrahamsson AE, Geron I, Gotlib J, Dao KH, Barroga CF, Newton IG, Giles FJ, Durocher J, Creusot RS, Karimi M, *et al.,* 2009. Glycogen synthase kinase 3b missplicing contributes to leukemia stem cell generation. Proc Natl Acad Sci 106: 3925–3929.

Bilic, J. (2007). "Wnt induces LRP6 signalosomes and promotes dishevelled-dependent LRP6 phosphorylation." Science **316**: 1619-1622.

Bjorklund P, Svedlund J, Olsson AK, Akerstrom G,Westin G. 2009. The internally truncated LRP5 receptor presents a therapeutic target in breast cancer. PLoS ONE 4: e4243

Cadigan, K. M. and M. Peifer (2009). "Wnt Signaling from Development to Disease: Insights from Model Systems." Cold Spring Harbor Perspectives in Biology **1**(2).

Chen B, Dodge ME, Tang W, Lu J, Ma Z, Fan C-W, Wei S, Hao W, Kilgore J, Williams NS, *et al.,* 2009. Small molecule- mediated disruption of Wnt-dependent signaling in tissue regeneration and cancer. Nat Chem Biol **5**: 100-107.

Clements WM, Lowy AM, Groden J. 2003. Adenomatous polyposis coli/β-catenin interaction and downstream targets: Altered gene expression in gastrointestinal tumors. Clin Colorectal Cancer 3: 113-120.

Cliffe, A., *et al.,* (2003). "A role of Dishevelled in relocating Axin to the plasma membrane during Wingless signaling." Curr Biol **13**: 960-966.

Cong, F. and H. Varmus (2004). "Nuclear-cytoplasmic shuttling of Axin regulates subcellular localization of beta-catenin." Proc Natl Acad Sci USA **101**: 2882-2887.

Fagotto, F. (1999). "Domains of axin involved in protein-protein interactions, wnt pathway inhibition, and intracellular localization." J. Cell Biol. **145**: 741-756.

Fagotto, F., *et al.,* (1998). "Nuclear localization signal-independent and importin/karyopherin-independent nuclear import of [beta]-catenin." Curr. Biol. **8**: 181-190.

Fanto, M., *et al.,* (2000). "Nuclear signaling by Rac and Rho GTPases is required in the establishment of epithelial planar polarity in the Drosophila eye." Curr Biol **10**(16): 979-988.

Farr, I. G., *et al.,* (2000). "Interaction among GSK-3, GBP, Axin, and APC in Xenopus axis specification." J Cell Biol **148**: 691-702.

Fumoto K, Kadono M, Izumi N, Kikuchi A. Axin localizes to the centrosome and is involved in microtubule nucleation. EMBO Rep. 2009 Jun;10(6):606-13. doi: 10.1038/embor.2009.45.

Guo, X., *et al.,* (2008). "Axin and GSK3- control Smad3 protein stability and modulate TGF- signaling." Genes Dev **22**(1): 106-120.

González-Sancho JM, Brennan KR, Castelo-Soccio LA, Brown AM. Wnt proteins induce dishevelled phosphorylation via an LRP5/6- independent mechanism, irrespective of their ability to stabilize beta-catenin. Mol Cell Biol. 2004 Jun;24(11):4757-68.

Ha, N. C., *et al.,* (2004). "Mechanism of phosphorylation-dependent binding of APC to [beta]-catenin and its role in [beta]-catenin degradation." Mol Cell **15**: 511-521.

Hernández, A. R., *et al.,* (2012). "Kinetic Responses of β-Catenin Specify the Sites of Wnt Control." Science **338**(6112): 1337-1340.

Hinoi, T., *et al.,* (2000). "Complex formation of adenomatous polyposis coli gene product and axin facilitates glycogen synthase kinase-3 beta-dependent phosphorylation of beta-catenin and down-regulates beta-catenin." J Biol Chem **275**(44): 34399-34406.

Huang, S. M., *et al.,* (2009). "Tankyrase inhibition stabilizes axin and antagonizes Wnt signalling." Nature **461**(7264): 614-620.

Ikeda, S., *et al.,* (1998). "Axin, a negative regulator of the Wnt signaling pathway, forms a complex with GSK-3beta and beta-catenin and promotes GSK-3beta-dependent phosphorylation of beta-catenin." EMBO J **17**: 1371-1384.

Itoh, K., *et al.,* (2000). "Interaction of dishevelled and Xenopus axin-related protein is required for wnt signal transduction." Mol Cell Biol **20**: 2228-2238.

Kim Sung-Eun, *et al.,* (2013). ” Wnt Stabilization of β-Catenin Reveals Principles for Morphogen Receptor-Scaffold Assemblies.” Science **340** (6134), 867.

Kishida, S. (1999). "DIX domains of Dvl and axin are necessary for protein interactions and their ability to regulate [beta]-catenin stability." Mol. Cell. Biol. **19**: 4414-4422.

Lee, E., *et al.,* (2003). "The roles of APC and Axin derived from experimental and theoretical analysis of the Wnt pathway." PLoS Biol **1**: E10.

Li, L., *et al.,* (1999). "Axin and Frat-1 interact with Dvl and GSK, bridging Dvl to GSK in Wnt-mediated regulation of LEF-1." EMBO J **18**: 4233-4240.

Li, V., *et al.,* (2012). "Wnt signaling inhibits proteasomal [beta]-catenin degradation within a compositionally intact Axin1 complex." Cell.

Liu, X., *et al.,* (2005). "Rapid, Wnt-induced changes in GSK3[beta] associations that regulate [beta]-catenin stabilization are mediated by G[alpha] proteins." Curr. Biol. **15**: 1989-1997.

Logan, C. Y. and R. Nusse (2004). "The Wnt signaling pathway in development and disease." Annu. Rev. Cell Dev. Biol. **20**: 781-810.

J. Lu, Z. Ma, J.C. Hsieh, C.W. Fan, B. Chen, J.C. Longgood, N.S. Williams, J.F. Amatruda, L. Lum, C. Chen. Structure-activity relationship studies of small-molecule inhibitors of Wnt response. Bioorg. Med. Chem. Lett., **19** (2009), pp. 3825–3827

Luo, W. and S. C. Lin (2004). "Axin: a master scaffold for multiple signaling pathways." Neurosignals **13**(3): 99-113.

Luo, W., *et al.,* (2005). "Axin contains three separable domains that confer intramolecular, homodimeric, and heterodimeric interactions involved in distinct functions." J Biol Chem **280**(6): 5054-5060.

MacDonald, B. T., *et al.,* (2009). "Wnt/beta-catenin signaling: components, mechanisms, and diseases." Dev Cell **17**: 9-26.

Maher, M. T., *et al.,* (2009). "Activity of the beta-catenin phosphodestruction complex at cell-cell contacts is enhanced by cadherin-based adhesion." J Cell Biol **186**(2): 219-228.

Morin PJ, Vogelstein B, Kinzler KW. 1996. Apoptosis and APC in colorectal tumorigenesis. Proc Natl Acad Sci **93**: 7950–7954.

Neo, S.Y., Zhang, Y., Yaw, L.P, Li, P., and Lin, S.-C. Axin-induced apoptosis depends on the extent of its JNK activation and its ability to down-regulate beta-catenin levels. Biochem. Biophys. Res. Comm. **272**:144-150, 2000.

Peifer, M., *et al.,* (1993). "A model system for cell adhesion and signal transduction in Drosophila." Development **Suppl**: 163-176.

Polakis P. 2007. The many ways of Wnt in cancer. Curr Opin Genet Dev **17**: 45–51.

Roberts, D. M., *et al.,* (2012). "Defining components of the [beta]-catenin destruction complex and exploring its regulation and mechanisms of action during development." PLoS ONE **7**: e31284.

Roberts, D. M., *et al.,* (2012). "Regulation of Wnt signaling by the tumor suppressor adenomatous polyposis coli does not require the ability to enter the nucleus or a particular cytoplasmic localization." Mol Biol Cell **23**(11): 2041-2056.

Roberts, D. M., *et al.,* (2011). "Deconstructing the sscatenin destruction complex: mechanistic roles for the tumor suppressor APC in regulating Wnt signaling." Mol Biol Cell **22**(11): 1845-1863.

Rubinfeld, B., *et al.,* (2001). "Axin-dependent phosphorylation of the adenomatous polyposis coli protein mediated by casein kinase 1[epsiv]." J. Biol. Chem. **276**: 39037-39045.

Ruteshouser EC, Robinson SM, Huff V. 2008.Wilms tumor genetics: Mutations in WT1, WTX, and CTNNB1 account for only about one-third of tumors. Genes Chromosomes Cancer 47: 461-470.

Rui Y, Xu Z, Lin S, Li Q, Rui H, *et al.,* (2004) Axin stimulates p53 functions by activation of HIPK2 kinase through multimeric complex formation. EMBO J 23: 4583–4594.

Saito-Diaz, K., *et al.,* (2013). "The way Wnt works: components and mechanism." Growth Factors **31**(1): 1-31.

Stamos, J. L. and W. I. Weis (2013). "The β-Catenin Destruction Complex." Cold Spring Harbor Perspectives in Biology **5**(1).

Taelman, V. F. (2010). "Wnt signaling requires sequestration of glycogen synthase kinase 3 inside multivesicular endosomes." Cell **143**: 1136-1148.

Tolwinski, N. S., *et al.,* (2003). "Wg/Wnt signal can be transmitted through arrow/LRP5,6 and Axin independently of Zw3/GSK3beta activity." Dev Cell **4**(3): 407-418.

Tolwinski, N. S. and E. Wieschaus (2001). "Armadillo nuclear import is regulated by cytoplasmic anchor Axin and nuclear anchor dTCF/Pan." Development **128**(11): 2107-2117.

van Amerongen, R. and A. Berns (2005). "Re-evaluating the role of Frat in

Wnt-signal transduction." Cell Cycle **4**: 1065-1072.

van Amerongen, R., *et al.,* (2005). "Frat is dispensable for canonical Wnt signaling in mammals." Genes Dev **19**: 425-430.

Wiechens, N., *et al.,* (2004). "Nucleo-cytoplasmic shuttling of Axin, a negative regulator of the Wnt-beta-catenin pathway." J Biol Chem **279**: 5263-5267.

Willert, K., *et al.,* (1999). "Wnt-induced dephosphorylation of axin releases [beta]-catenin from the axin complex." Genes Dev. **13**: 1768-1773.

Wu, G., *et al.,* (2009). "Inhibition of GSK3 phosphorylation of β-catenin via phosphorylated PPPSPXS motifs of Wnt coreceptor LRP6." PLoS ONE **4**: e4926.

Xing, Y., *et al.,* (2003). "Crystal structure of a [beta]-catenin//Axin complex suggests a mechanism for the [beta]-catenin Destruction complex." Genes Dev **17**: 2753-2764.

Yamamoto, H., *et al.,* (2001). "Inhibition of the Wnt signaling pathway by the PR61 subunit of protein phosphatase 2A." J Biol Chem **276**(29): 26875-26882.

Yamamoto, H., *et al.,* (1999). "Phosphorylation of axin, a Wnt signal negative regulator, by glycogen synthase kinase-3beta regulates its stability." J Biol Chem **274**: 10681-10684.

Yost, C., *et al.,* (1998). "GBP, an inhibitor of GSK-3, is implicated in Xenopus development and oncogenesis." Cell **93**: 1031-1041.

Zeng, L., *et al.,* (1997). "The mouse Fused locus encodes Axin, an inhibitor of the Wnt signaling pathway that regulates embryonic axis formation." Cell **90**: 181-192.

Zeng, X. (2008). "Initiation of Wnt signaling: control of Wnt coreceptor Lrp6 phosphorylation/activation via Frizzled, Dishevelled and Axin functions." Development **135**: 367-375.